On the phases of strongly coupled gauge theories from holography.

Rafferty, James M

On the Phases of Strongly Coupled Gauge Theories from Holography

James M. Rafferty

Submitted to Swansea University in fulfillment of the
requirements for the degree of *Doctor of Philosophy*
2011

Abstract

In this thesis we extract properties of strongly coupled quantum field theories using holography. Firstly, we compute the real time two point correlation functions of $\mathcal{N} = 4$ supersymmetric Yang-Mills theory on $dS_3 \times S^1$ with antiperiodic boundary conditions for fermions on the circle. When the circle radius is large, the dual geometry is the topological AdS_5 black hole. Here it is possible to solve the wave equations dual to the scalar glueball and R-charge current operators and therefore the correlation functions can be calculated exactly in the limit of large N and strong coupling. Below the critical radius for the circle the topological black hole decays to the AdS bubble of nothing. Here we compute the glueball correlation function in the WKB approximation and find poles on the real axis, indicating stable bound states. The tunnelling from the topological black hole to the bubble is interpreted as a hadronization transition.

In the second part we investigate three holographic theories with an imaginary chemical potential: $\mathcal{N} = 4$ supersymmetric Yang-Mills coupled to fundamental flavours in the probe approximation, the same theory with flavours confined to a codimension k defect and the Sakai-Sugimoto model. There is an infinite series of Roberge-Weiss transitions at high temperature in each of these models and a phase transition which occurs as a result of the presence of flavours in the high temperature phase. We show the latter phase transition is first order for all three models and hence it meets the Roberge-Weiss lines at triple points. We also compute the pressure due to flavours and find for both models dual to type IIB supergravity solutions it scales in a way expected from dimensional analysis. The Sakai-Sugimoto model exhibits unusual scaling. We show the models we consider are analytic in μ^2 when μ^2 is small.

Declaration

This work has not previously been accepted in substance for any degree and is not being concurrently submitted in candidature for any degree.

Signed ..... (candidate)
Date .....1/11/2011.....

This thesis is the result of my own investigations, except where otherwise stated. Where correction services have been used, the extent and nature of the correction is clearly marked in a footnote(s).
Other sources are acknowledged by footnotes giving explicit references. A bibliography is appended.

Signed ..... (candidate)
Date .....1/11/2011.....

I hereby give consent for my thesis, if accepted to be available for photocopying and for inter-library loan, and for the title and summary to be made available to outside organisations.

Signed ..... (candidate)
Date .....1/11/2011.....

"Reality is that which, when you stop believing in it, doesn't go away."

- *Philip K. Dick*

Contents

Acknowledgements

Special thanks must go to two people in particular. The first is my supervisor, S. Prem Kumar, whose many hours of patient and careful explanations have in large part made this work possible. The second is my wife, Ruth Rafferty, whose tolerance of many late nights and early mornings has been unwaivering. Further thanks go to the Gert Aarts and Jimmy Hutasoit who I have had the pleasure of collaborating with.

My family have been a great source of support and encouragement. I would like to thank the Raffertys: Michael, Dawn and Eva and the Illingsworths: Mansel, Sylvia and James. Special thanks go to Abigail Rafferty. The people with whom I have shared an office have made the time at work extremely enjoyable. They are Omar Al-Hartomy, Jérôme Gaillard, Jonathan Lloyd, Jamie Nemeth, Robbie Rickman, Mark Round and Ross Stanley.

Finally I thank the STFC for their financial support.

List of Figures

Chapter 1

Introduction

1.1 Quantum Field Theory

Since the early part of the 20^{th} century, many very successful theories of particle physics have been formulated in the framework of quantum field theory [1]. In quantum field theories the fundamental degrees of freedom are *fields* which are represented mathematically by functions over spacetime coordinates. These functions can be either real or complex numbered functions and may either have a single component (a scalar field), multiple spacetime components (a vector field) or multiple components in an internal space (a spinor field). A particle interpretation of a field theory is achieved when the theory is quantised, and importantly the number of particles in a particular system is not fixed so quantum field theories have seen great success in modelling the interactions of particles where particles are created and destroyed.

An important object in a quantum field theory is the *partition function*

$$\mathcal{Z}[\phi] = \int [d\phi]\, e^{iS[\phi]} \tag{1.1}$$

note that ϕ is a field and S is the action of the system. The action can be written schematically as

$$S = \int d^d x \left(\mathcal{L}_{\text{free}} + \mathcal{L}_{\text{int}}\right) \tag{1.2}$$

here d is the number of spacetime dimensions. $\mathcal{L}_{\text{free}}$ is the part of the action that contains kinetic and mass terms for the fields (if they are non zero) but contains no terms that lead to interactions, either between different fields or between a field with itself (self interactions). Supposing there is only one field in the theory, $\mathcal{L}_{\text{int}}$ contains the remaining terms in the action that lead to interactions and can be written as

$$\mathcal{L}_{\text{int}} = g_1\phi^3 + g_2\phi^4 + \dots \tag{1.3}$$

where g_i are the *coupling constants* of the theory. Gauge field theories or simply *gauge theories* are quantum field theories with extra internal symmetries. The hugely successful standard model of particle physics is an example of a gauge theory. Consider a gauge theory with one coupling constant - if it is small, i.e. the theory is at *weak coupling*, then we can use *perturbation theory* to extract useful information from it. One may show that an expansion in the coupling constant is equivalent to using Feynman diagrams and expanding in the number of loops, so diagrams involving more loops are suppressed relative to those with less loops. There are many examples of important quantities that can be computed using perturbation theory, one example of which is the quantum electrodynamics prediction of the anomalous magnetic moment of the electron that agrees with experiment with an accuracy of eight significant figures [1]. Unfortunately, there is nothing in nature that restricts the coupling of a particular quantum field theory to be small so that perturbation theory will be a good technique to employ in performing calculations. In fact quantum chromodynamics (QCD), the theory of quarks and gluons, is strongly coupled at low energies so to study the theory in this regime we must employ other techniques. One method that has been used extensively in the study of QCD is to use computers to perform numerical simulations. This approach is known as lattice gauge theory (See for example [2–4] and citations therein) and has seen much success in predicting properties of mesons and baryons. While lattice gauge theory is at present the only known nonperturbative approach to QCD, it does not provide us with a way to study non dynamical systems or the theory on time dependent

backgrounds. Another approach that has been used in recent times to study theories at strong coupling and potentially gain an analytical insight into strongly coupled theories that appear in nature like QCD is holography. In the next section we briefly describe string theory with a view to using it to study field theories at strong coupling holographically.

1.2 String Theory

Originally proposed as a theory to describe the strong interaction [5, 6], it was shown that the theory of a quantum string is in fact a consistent theory of quantum gravity [7, 8]. In string theory the fundamental objects are no longer point particles, but extended one dimensional structures. These strings may be open, i.e. they have end points where boundary conditions must be applied, or closed, where the string forms a loop with no end points. The action of the string is known as the Nambu-Goto action [9, 10].

$$S = T_s \int d\tau d\sigma \sqrt{\det \gamma_{ab}} \tag{1.4}$$

T_s is the string tension and γ_{ab} is the induced metric on the worldsheet and is given by

$$\gamma_{ab} = \frac{\partial X^\mu}{\partial \sigma^a} \frac{\partial X^\nu}{\partial \sigma^b} g_{\mu\nu} \tag{1.5}$$

which is the pullback of the background metric $g_{\mu\nu}$ and X^μ gives the mapping from the background to the string worldsheet.

When one quantises the theory it is found that different vibrational modes have different spins and therefore can be interpreted as the different particles that we observe. Consider a closed string where there are both left and right moving modes. The spectrum will contain both a left and a right moving gauge field, the product of which will have spin 2 and therefore is a graviton. The graviton is only massless if the number of spacetime dimensions is a particular number called the critical dimension. In the theories we will consider which are superstring theories, the critical dimension is 10 while for the bosonic string the critical dimension is 26. Superstring theories are

important because including supersymmetry in a string theory is the only known way to formulate a theory without tachyonic modes. To make a string theory supersymmetric a two component real fermion is added to the action. Furthermore, the spectrum of the string will generically contain supersymmetry breaking states, and in order to remove such states we must use a a technique discovered by Gliozzi, Scherk and Olive known as the GSO projection [11]. The GSO projection acts as a chiral projection on the spacetime fermions of the closed string theory. If, for both the left and the right movers the same chirality is projected then the resulting string theory is type IIA. Conversely, if opposite chirality is projected for the left and right movers the string theory is type IIB. In this thesis we will consider only type II string theories, which is a subset of five the known superstring theories.

When we consider a string theory that contains both open and closed strings, it is possible that the open strings may be constrained to end on a lower dimensional hyperplane than the full dimensionality of the space. These planes are known as Dirichlet membranes or simply *D-branes* [12,13]. We will generally consider a low energy limit of the string theories we discuss such that the length of the strings become small and they may be considered point particles. In this limit, the string theory is replaced by a supersymmetric theory of gravity or a theory of *supergravity*, and when one does this these D-branes persist as solitonic solutions of the action. The oscillations of the open strings that end on the D-branes are the source of the massless gauge multiplets that appear in the string theory and therefore, one can think of the D-branes as electric and magnetic sources for the various potentials that are present. The spectrum of the closed string that appears in both of the type II string theories is as follows. There is the metric $g_{\mu\nu}$, a scalar called the dilaton Φ and an antisymmetric two form $B_{\mu\nu}$. Together these fields are known as Neveu-Schwarz fields. The GSO projection leads to differences in the spectrum for each of the type II string theories. In type IIA where the the chiral projections are the same we have a one form and a three form potential, while in type IIB the chiral projections are opposite the resulting potentials are a zero form (a scalar known as the axion), a two form and a four form. These fields are known as Ramond-Ramond fields. These potentials

appear in the supergravity action via their field strengths, which are the antisymmetrised derivatives (denoted by d) of the potentials[1]

$$F_{i+1} = \mathrm{d}C_i \tag{1.6}$$

Since the D-branes source the potentials in this way it can be shown that type IIA supergravity contains D-branes of even dimensionality while type IIB contains D-branes of odd dimensionality. The action of a D-brane is given by the Dirac-Born-Infeld (DBI) action, which says physically that the world volume of the brane is minimized. Extra terms arise because D-branes are sources for field strengths. The full action for a Dp in type IIB supergravity brane is

$$S_{\mathrm{D}p} = -T_{\mathrm{D}p} \int d^{p+1}\xi e^{-\Phi} \sqrt{-\det\left(\gamma_{ab} + B_{ab} + 2\pi\alpha' F_{ab}\right)} \tag{1.7}$$

$T_{\mathrm{D}p}$ is the tension of the brane, ξ are the coordinates on the brane, γ_{ab} is the induced metric of the brane, defined in the same way as for the string previously (equation (1.5)), B is is the Neveu-Schwarz two form and F is an antisymmetric two form that is sourced by the brane. α' is a quantity that is related to the string length and can also be related to the tension of strings and branes. D-branes may also couple to tensor potentials through Chern Simons like terms, we will describe an example of such a term below.

From differential geometry [14] we know that a manifold can accommodate a form with rank less than or equal to the dimensionality of the manifold. We may generate higher rank forms from the ones we have already described using *Hodge duality* (denoted by a $*$). We will not discuss Hodge duality in detail here, but an important property is that the rank of the new field strength is the number of spacetime dimensions minus the rank of the old field strength, for example, the F_3 in type IIB is related to an $F_7 = *F_3$. It is clear that type IIB contains a five form field strength $F_5 = \mathrm{d}C_4$, which must

[1]This shorthand is useful because the number of terms in F_{i+1} increases rapidly as i rises. For example, $F_2 = F_{\mu\nu} = \partial_\mu A_\nu - \partial_\nu A_\mu$ but $F_3 = F_{\mu\nu\rho} = \partial_\mu A_{\nu\rho} - \partial_\mu A_{\rho\nu} + \partial_\nu A_{\rho\mu} - \partial_\nu A_{\mu\rho} + \partial_\rho A_{\mu\nu} - \partial_\rho A_{\nu\mu}$

be treated with care[2]. When one performs this transformation on the $\tilde{F}_5$ one gets a rank 5 field strength back, therefore the $\tilde{F}_5$ is said to be self dual and satisfies

$$\tilde{F}_5 = *\tilde{F}_5 \tag{1.8}$$

When one writes the action of type IIB supergravity this self duality of the $\tilde{F}_5$ must be added by hand as a constraint.

Both of the type II theories contain $\mathcal{N} = 2$ supersymmetry[3]. One may also include open strings into type II theories which breaks supersymmetry to $\mathcal{N} = 1$. Strings can interact if one allows the worldsheet to have non trivial topology. The topology changes are measured by the action of the dilaton Φ, so the quantity e^{Φ} plays the role of the coupling of the theory. Taking the open and closed string sectors together, the combined Yang-Mills coupling is related to the dilaton by $g^2_{\mathrm{YM}} = e^{\Phi}$. With this in mind, one can see that if the dilaton is given by a constant then the Yang-Mills coupling related to the dilaton will also be a constant, i.e. the coupling will not run and the theory will be conformal. As we will see in the next section, the field theory side of the first known gauge/gravity correspondence is a conformal field theory.

Since D-branes are sources for Ramond-Ramond forms in type II string theories, we expect a theory that contains a tensor potential will also contain D-branes. In the following chapter we will use a consistent truncation of type IIB where the only non zero fields are the metric, the dilaton and the Ramond-Ramond 5 form field strength and in these circumstances we would expect the theory to contain D3 branes. A D3 brane sweeps out a 4 dimensional world volume and hence we expect it to couple to the rank 4 tensor potential that when we take the exterior derivative leads to the rank 5 field strength we have in the theory.

Since string theory is a theory of quantum gravity it is not surprising

[2]The F_5 appears in the type IIB action (given in equation (2.1)) as a linear combination of an exterior derivative of a four form potential and some other fields in the action. It is this overall five form field strength that is self dual, and it is denoted $\tilde{F}_5$. This combination, along with the other terms in the type IIB action is defined in (2.5)

[3]This refers to the 10 dimensional theory. When we go on to discuss the boundary theory the number of supercharges (16) will lead an $\mathcal{N} = 4$ theory in four dimensions.

that it should contain both classical gravity and gauge theories. What is interesting and useful is that it is possible to relate some theories of gravity to gauge theories and use this as a calculational tool to study gauge theories at strong coupling. In the next section there is a short discussion of properties of one of the field theories that we will study using the various holographic correspondences.

1.3 $\mathcal{N} = 4$ super Yang-Mills theory

One of the most striking developments in high energy particle physics in recent years has been the proposed correspondence between a string theory on a space with a boundary and a gauge theory defined on the boundary [15]. The original [16] and most well understood example of this gauge gravity correspondence is that of type IIB superstring theory on $AdS_5 \times S^5$ which is dual to $\mathcal{N} = 4$ supersymmetric Yang-Mills theory on the boundary of the space. $\mathcal{N} = 4$ super Yang-Mills theory is a maximally supersymmetric theory in $3 + 1$ dimensions whose field content is as follows; there is a gauge field A_μ with gauge group $SU(N)$. There are four Weyl fermions and six real scalar fields and since these fields form the supersymmetric completion of the theory, they are all in the adjoint representation of $SU(N)$ along with the gauge field. In addition to the gauge symmetry there is an additional global R symmetry group which is $SU(4)$.

It has been shown that the beta function of $\mathcal{N} = 4$ super Yang-Mills vanishes to all orders in perturbation theory, and indeed nonperturbatively, so in addition to the symmetries described above the theory has conformal symmetry [17–19]. The conformal symmetry group $SO(4, 2)$ is exactly the symmetry group of five dimensional anti de Sitter space. Also as described above, the R symmetry group is $SU(4)$ which is isomorphic to $SO(6)$. This is the symmetry group of a five sphere so the symmetries of the gauge theory arise quite naturally on the gravity side. In the following section and chapter we describe the AdS/CFT correspondence and its derivation.

1.4 The AdS/CFT Correspondence

The AdS/CFT correspondence has been fertile ground for research into field theory and is to date the only known way to perform analytic calculations at strong coupling. In the years since Maldacena's discovery of the duality between type IIB supergravity and $\mathcal{N} = 4$ super Yang-Mills at strong coupling, research has proceeded on numerous fronts. Firstly, much effort has been made to understand the original AdS/CFT correspondence. For example, there is a concrete mathematical formalism for computing quantities in the gauge theory by performing a calculation in the string theory (the so called operator-field correspondence) [20, 21] and it is understood how to perform calculations involving thermal field theories by introducing a temperature into the gravity theory [22–24]. Furthermore, it is understood how to incorporate fundamental degrees of freedom into the gauge theory in addition to those in the adjoint representation [25] and one may include a chemical potential [26–28] for the various conserved charges present in the the gauge theory, and more generally the conductivity tensor [29–32]. The phase diagram of the $\mathcal{N} = 4$ theory can be mapped out at strong coupling quite extensively using AdS/CFT.

The second avenue of investigation of dualities between a string theory set up and a gauge theory has been to try to find a holographic dual to a gauge theory that is closer to the ones found in nature, i.e. has less supersymmetry and the correct degrees of freedom. We will not delve very deeply into this direction of research, however we will discuss a duality discovered by Sakai and Sugimoto [33] whose great success was it was the first known holographic theory to realise chiral symmetry breaking. For other holographic duals see for example [34–36].

In the the following chapter we will describe in detail the correspondence between type IIB superstring theory on $AdS_5 \times S^5$ dual to $\mathcal{N} = 4$ super Yang-Mills including a non zero temperature and flavour degrees of freedom. We will discuss including a chemical potential in a latter chapter.

Chapter 2

Gauge / Gravity Duality

2.1 Type IIB String Theory and $\mathcal{N} = 4$ Super Yang-Mills

The original and best understood example of a duality between a gauge theory and a supergravity theory is the relationship between type IIB supergravity and $\mathcal{N} = 4$ supersymmetric Yang-Mills theory. Consider the action of Type IIB supergravity [37–39]

$$S_{\text{IIB}} = S_{\text{NS}} + S_{\text{RR}} + S_{\text{CS}} \tag{2.1}$$

$$S_{\text{NS}} = \frac{1}{2\kappa_{10}^2}\int d^{10}x\sqrt{g}e^{-2\Phi}\left(R + 4\partial_\mu\Phi\partial^\mu\Phi - \frac{1}{2}\left|H_3\right|^2\right) \tag{2.2}$$

$$S_{\text{RR}} = -\frac{1}{4\kappa_{10}^2}\int d^{10}x\sqrt{g}\left(\left|F_1\right|^2 + \left|\tilde{F}_3\right|^2 + \frac{1}{2}\left|\tilde{F}_5\right|^2\right) \tag{2.3}$$

$$S_{\text{CS}} = -\frac{1}{4\kappa_{10}^2}\int C_4 \wedge H_3 \wedge F_3 \tag{2.4}$$

where

$$\begin{gathered} F_1 = \mathrm{d}C, \quad F_3 = \mathrm{d}C_2, \quad F_5 = \mathrm{d}C_4, \quad H_3 = \mathrm{d}B_2 \\ \tilde{F}_3 = F_3 + C \wedge H_3, \quad \tilde{F}_5 = F_5 - \frac{1}{2}C_2 \wedge H_3 + \frac{1}{2}B_2 \wedge F_3 \end{gathered} \tag{2.5}$$

C, C_2 and C_4 are the Ramond-Ramond zero, two and four form potentials respectively. B_2 is the Neveu-Schwarz two form, Φ is the dilaton and g is the metric. We also have the self duality condition on the $\tilde{F}_5$

$$\tilde{F}_5 = *\tilde{F}_5 \tag{2.6}$$

Making the consistent truncation so only the dilaton, the metric and the Ramond Ramond 5 form are non zero the action becomes

$$S_{\text{IIB}} = \frac{1}{2\kappa_{10}^2}\int d^{10}x\sqrt{g}\left[e^{-2\Phi}\left(R + 4\partial_\mu\Phi\partial^\mu\Phi\right) - \frac{1}{4}F_5^2\right] \tag{2.7}$$

Varying the action with respect to each of the fields will give the equations of motion of the system. A solution to these equations is

$$ds^2 = \left(1+\frac{R^4}{r^4}\right)^{-1/2}\delta_{ij}dx^i dx^j + \left(1+\frac{R^4}{r^4}\right)^{1/2}\left(dr^2 + r^2 d\Omega_5^2\right) \tag{2.8}$$

$$\Phi = \text{constant} \tag{2.9}$$

$$F_5 = A(r)dx_0 \wedge dx_1 \wedge dx_2 \wedge dx_3 + B(r)\text{vol}\left(\mathrm{S}^5\right) \tag{2.10}$$

Where i, j run from 0 to 3, $A(r)$ and $B(r)$ are some functions that are not independent but are related in some way that will not be important and $\text{vol}\left(\mathrm{S}^5\right)$ is the volume form of the S^5. Consider the metric (2.8) in the limit that $r \to \infty$. It reduces to

$$ds^2 = \delta_{ij}dx^i dx^j + \left(dr^2 + r^2 d\Omega_5^2\right) \tag{2.11}$$

which is simply 10 dimensional Euclidean space. In the limit $r \to 0$ the coefficient function that appears in front of the two parts of (2.8) becomes

$$\left(1+\frac{R^4}{r^4}\right)^{1/2} \to \frac{R^2}{r^2} \tag{2.12}$$

and hence we have

$$ds^2 = \left[\frac{r^2}{R^2}\delta_{ij}dx^i dx^j + \frac{R^2}{r^2}dr^2\right] + R^2 d\Omega_5^2 \tag{2.13}$$

The terms in square brackets are the metric of 5 dimensional AdS space and the remaining terms form an S^5, hence in this limit the solution is $AdS_5 \times S^5$. It is clear now that the parameter R has an interpretation as the radius of curvature of both the AdS space and the S^5. If we identify the parameter $R^4 = g_s N \alpha'^2$ with g_s the string coupling and α' proportional to the string length squared, a relation that comes from the non linear sigma model for the type IIB superstring in AdS space, then make the coordinate transformation $r = \alpha' u$ the metric (2.8) becomes

$$ds^2 = \left(1 + \frac{g_s N}{\alpha'^2 u^4}\right)^{-1/2} \delta_{ij} dx^i dx^j + \alpha'^2 \left(1 + \frac{g_s N}{\alpha'^2 u^4}\right)^{1/2} \left(du^2 + u^2 d\Omega_5^2\right) \quad (2.14)$$

We can see that taking $\alpha' \to 0$ and keeping u fixed is the same as taking $r \to 0$ and therefore (2.14) becomes.

$$ds^2 = \alpha' \left[\frac{u^2}{\sqrt{g_s N}} \delta_{ij} dx^i dx^j + \frac{\sqrt{g_s N}}{u^2} du^2\right] + \alpha' \sqrt{g_s N} d\Omega_5^2 \quad (2.15)$$

Since α' is proportional to the string length squared it is clear that this is equivalent to taking the supergravity limit so that the the leading order part of the metric is $AdS_5 \times S^5$.

As remarked in the previous chapter, type IIB supergravity with a rank 4 tensor potential turned on contains D3 branes, since the D3 branes act as the source for the rank 4 tensor potential. The Lagrangian for the string theory takes the form

$$\mathcal{L} = \mathcal{L}_{\text{D3 branes and open strings}} + \mathcal{L}_{\text{closed strings in flat space}} + \alpha'^m \mathcal{L}_{\text{interaction}} \quad (2.16)$$

Clearly, taking $\alpha' \to 0$ will have the effect of causing the open and closed string degrees of freedom to cease interacting and hence this limit is also known as the decoupling limit. It is well known that in the supergravity limit the Lagrangian of the open string degrees of freedom for a single D-brane consists of a $U(1)$ $\mathcal{N} = 4$ supersymmetric Yang-Mills theory living on the worldvolume of the D-brane. When we are not in this limit there are corrections to the action of the D-brane consisting of higher derivative

terms that are suppressed by powers of α'. For N D-branes the argument follows through but the gauge group is enlarged to $U(N)$. The $U(N)$ gauge theory contains a free $U(1)$ multiplet and an $SU(N)$ gauge theory, however, in the supergravity theory there are no free modes so the bulk theory is only describing the $SU(N)$ gauge theory part of the D-brane Lagrangian. There is other evidence that strongly implies the gauge group of the field theory is not $U(N)$ but $SU(N)$, in particular, it is understood that there is a topological symmetry associated with the centre of the gauge group. For a $U(N)$ gauge theory this topological symmetry is $U(1)$ while for an $SU(N)$ gauge theory it is $\mathbb{Z}_N$. It has been shown [40] that for type IIB on $\mathrm{AdS}_5 \times \mathrm{S}^5$ there is an extra global $\mathbb{Z}_N$ symmetry so the gauge group is indeed $SU(N)$.

In summary, when we take the decoupling limit of type IIB string theory containing N D3 branes, there are two equally valid descriptions. Firstly, we may consider the back reacted geometry from the presence of the D3 branes and secondly, we may consider the field theory that results from taking the low energy limit of the open strings on the world volume of the D3 branes. Therefore we may write the schematic Lagrangian of the system in the following way

$$\mathcal{L} = \mathcal{L}_{\text{IIB strings on } \mathrm{AdS}_5 \times \mathrm{S}^5} + \mathcal{L}_{\text{closed strings in flat space}} \tag{2.17}$$

$$\mathcal{L} = \mathcal{L}_{\mathcal{N}=4 \text{ SYM}} + \mathcal{L}_{\text{closed strings in flat space}} \tag{2.18}$$

Since the final two terms are clearly the same Maldacena proposed that $\mathcal{N} = 4$ super Yang-Mills is equivalent to type IIB string theory on $\mathrm{AdS}_5 \times \mathrm{S}^5$.

To further motivate the study of the gauge gravity correspondence consider first the regimes of tractability. From previously we have

$$\alpha' = \frac{R^2}{\sqrt{g_s N}} = \frac{R^2}{\sqrt{g_{\mathrm{YM}}^2 N}} = \frac{R^2}{\sqrt{\lambda}} \tag{2.19}$$

The 't Hooft coupling $\lambda = g_{\mathrm{YM}}^2 N$ is the parameter which gives the strength of the gauge theory coupling so when this quantity is small the gauge theory can be treated perturbatively. Recall that R is the radius of curvature of the space and α' is related to the string length. We can see that when λ

is large we are in the supergravity limit, i.e. the parameter $R \gg \alpha'$, but the gauge theory is now strongly coupled and hence is non perturbative. The converse is also true, when the gauge theory is weakly coupled and can be studied using perturbation theory the stringy effects in the string theory are very important. Clearly, this is an extremely useful feature of the duality since when we cannot perform calculations in the gauge theory we can calculate in the supergravity theory where the details are very much more simple and vice versa. This leads to problems in verifying the correspondence, but it is possible to perform certain non perturbative calculations on both sides of the correspondence making use of the large conformal symmetry group. Specifically it has been shown that the Greens functions of chiral primary operators computed on both sides of the correspondence agree (see for example [41, 42]). Currently, the correspondence has not been proven to the standard required by mathematical physics but there is a great deal of evidence in the literature pointing toward it's validity.

2.2 Gauge Gravity Duality and Thermodynamics

The duality between type IIB string theory on $AdS_5 \times S^5$ and $\mathcal{N} = 4$ super Yang-Mills has been formulated for zero temperature, or the extremal case in the language of the gravity theory. In deriving the conjecture, Maldacena worked in Poincaré coordinates, the boundary of which is $\mathbb{R}^3 \times S^1$ and only covers half of AdS space[1]. For the purpose of this discussion we will consider global coordinates where the boundary is $S^3 \times S^1$ because of the work done by Hawking and Page in 1983 [43], which will be described below. In global AdS there are two scales in the problem, the size of the S^3 at the boundary and the temperature while in the Poincaré patch the only scale is the temperature, so we will not see non trivial phase structure there[2].

[1] In this discussion we are working in Euclidean signature.

[2] Note that the AdS/CFT correspondence has not be formulated in global coordinates, but since the two cases are related by a coordinate transformation and we expect physics to be invariant under coordinate transformations, we expect the correspondence to hold

In order to introduce a temperature into the gauge theory on the boundary there are two approaches one could take, and we will see both are valid in certain regimes. Firstly and most simply, we could introduce a thermal bath into the AdS space making thermal AdS. The second way to introduce a non zero temperature is to consider a background that contains a black hole, since black holes have a temperature due to the Hawking process[3] [44]. Note that in both of these scenarios where we introduce a thermal bath into the bulk spacetime it is possible for the system to come to equilibrium because null geodesics get to the boundary in finite time. This is due to the fact that the space we are considering is asymptotically AdS, and it is not the case in asymptotically flat space. When we consider these two geometries in Euclidean signature the imaginary time direction is compact and it's period is related to the inverse temperature of the system. Topologically, thermal AdS_5 is $D_4 \times S^1$ where D_4 is a four ball whose boundary is an S^3 and the imaginary time direction is the S^1. Schwarzschild AdS_5 is $S^3 \times D_2$ where the D_2 is a two ball or disc which contains the imaginary time direction. Importantly, the D_2 must smoothly reduce to zero size at the horizon in order to avoid a conical singularity while there is no such constraint on the imaginary time direction in thermal AdS. In the field theory the order parameter for the transition between the two phases is the expectation value of the phase of the "temporal Wilson" or "Polyakov" loop which we denote by W. Suppose P is some point in the boundary S^3 and C_P is a closed path that goes around the thermal circle. The Polyakov loop is defined by

$$W(P) = \mathrm{Tr}\,\mathrm{Pexp}\left(i \oint_{C_P} A\right) \tag{2.20}$$

In thermal AdS the paths C_P are not on a closed manifold, so $\langle W \rangle$ must vanish while in Schwarzschild AdS the same paths are on a closed manifold since the D_2 shrinks to zero size at the horizon, therefore in the Schwarzschild AdS phase $\langle W \rangle$ will be non zero in general. When $\langle W \rangle$ vanishes the gauge

in global coordinates.

[3]Strictly, this is the big black hole in AdS. The Hawking temperature of the big black hole increases with increasing mass, while the Hawking temperature of the small black hole decreases with increasing mass.

theory is confining, while a non zero value for $\langle W \rangle$ tells us that the gauge theory is in the deconfined phase. This observation implies that thermal AdS and Schwarzschild AdS are dual to the low temperature and high temperature phases respectively [20, 23]. In addition, one may compute the two point correlation functions of the scalar glueball $\mathrm{Tr}F_{\mu\nu}F^{\mu\nu}$ operator and one finds that in the phase dual to thermal AdS the correlator has poles on the real axis, indicating bound states of gluons [21]. In the phase dual to the AdS Schwarzschild black hole there is a series of poles in the lower half plane, indicating unstable states with some finite lifetime [22]. The procedure used to perform calculations of correlation functions in holographic theories will be described in a later section.

Clearly, the field theory is valid at all temperatures so there should be a point where thermal AdS and the black hole in AdS descriptions coincide. Hawking and Page showed that at some critical temperature T_{HP} there is a first order phase transition where thermal AdS tunnels into the black hole solution which is now known as a Hawking-Page transition. This is a rather nice feature of the gauge gravity correspondence since the Hawking-Page transition can be interpreted in the gauge theory as a phase transition between confined and deconfined phases. The first order phase transition was studied on the field theory side for weak coupling in [45].

As remarked previously, $\mathcal{N} = 4$ super Yang-Mills is a conformal theory so one would not expect to get bound states like those that occur in QCD. However, since the gauge theory here is defined on a compact space there is a confining and deconfining interpretation. At low temperature introducing a single free gaugino is not possible since the total flux, and hence the total charge, on a compact space must be zero by Gauss' law. When $T > T_{\mathrm{HP}}$ there are screening effects that make it possible to have free gaugino. Hence, there is a confining and deconfining interpretation that makes the theory similar enough to QCD so that one expects the qualitative behaviour of the theories should at least be similar.

2.3 Quenched Fundamental Flavours

When we consider field theory side of the duality between type IIB supergravity on $AdS_5 \times S^5$ and $\mathcal{N} = 4$ super Yang-Mills, all of the fields present from the low energy limit of open strings on the D3 branes are in the adjoint representation of the gauge group. In order to introduce fields in fundamental representation we must introduce more branes into the supergravity theory. Specifically we add N_f D7 branes[4] into the theory and for simplicity we assume $N_f \ll N$ so that we may neglect their backreaction on $AdS_5 \times S^5$. This was first done in [46]. If the masses of the N_f quarks are equal or equivalently the N_f D7 branes have the same embedding, the field theory now contains an extra $U(N_f)$ symmetry that we interpret in the gauge theory as a flavour symmetry. Open string modes with both ends on the D3 branes correspond to adjoint degrees of freedom in the way described above. Strings with one end on the N_f D7's and one end on the N D3's will carry both flavour and colour charge so they represent quark hypermultiplets. The energy of these strings is proportional to their length at the boundary so in the gauge theory the asymptotic separation of the D7 and D3 branes is related to the quark mass and if the D7's and D3's coincide the quarks are massless. More specifically, the embedding of the D7 branes as a function of the radial coordinate will approach a constant as we take the boundary limit. That constant is related to the quark mass in the gauge theory. Open strings with both ends on the D7's are in the adjoint representation of the flavour symmetry group $U(N_f)$ and therefore naturally represent mesons in the field theory. In the large N and supergravity limit the mesonic string modes decouple from the theory meaning the $U(N_f)$ symmetry is global in the boundary theory.

The D7 brane embedding may or may not break supersymmetry depending on where it lies in the space, we will only consider supersymmetric solutions that retain $\mathcal{N} = 2$ supersymmetry. For a review of flavour in gauge gravity duals see [25]. Consider embedding a D7 brane in thermal AdS. In

[4]D7 branes are used because there is an embedding that retains $\mathcal{N} = 2$ supersymmetry and covers all of the field theory directions. Supersymmetric embeddings of D5 or probe D3 branes only cover a submanifold of the boundary, and consequently the flavour degrees of freedom live on a *defect*. This type of theory will be described in a later section.

	AdS_5					S^5				
	0	1	2	3	4	5	6	7	8	9
D3	×	×	×	×						
D7	×	×	×	×	×	×	×	×		

Table 2.1: The dimensions covered by D3 and D7 branes in type IIB

a supersymmetric embedding the D7 brane extends as shown in table 2.1. Since we assume the backreaction of the D7's are insignificant we may use the Dirac Born Infeld and Chern Simons description of the D7.

$$S_{D7} = -T \int d^8\xi \sqrt{|\det(\gamma_{ab} + B_{ab} + 2\pi\alpha' F_{ab})|} + \frac{(2\pi\alpha')^2}{2} T \int C_4 \wedge F \wedge F \tag{2.21}$$

where γ_{ab} is the induced metric of the D7 brane and was defined in (1.5) and C_4 is the pullback of the four form potential. B_{ab} is the pullback of the NS B field onto the D7 brane and F_{ab} is a worldvolume gauge field on the D7's. Since a supersymmetric embedding for the D7 is where the brane covers $AdS_5 \times S^3$ while the it's position in one of the other directions of the S^5 where the D7 is point like, it is convenient to make a coordinate transformation so that the metric contains and explicit S^3 factor.

$$ds^2 = \frac{r^2}{R^2}\delta_{ij}dx^i dx^j + \frac{R^2}{r^2}\left(d\rho^2 + \rho^2 d\Omega_3^2 + dw_5^2 + dw_6^2\right) \tag{2.22}$$

where $r^2 = \rho^2 + w_5^2 + w_6^2$. Let us consider an example where the $w_5 = w$ direction is a function of the radial direction ρ and the NS B field and the worldvolume gauge field F both vanish. The induced metric of the D7 brane is

$$ds^2_{\mathrm{D7}} = \frac{r^2}{R^2}\delta_{ij}dx^i dx^j + \frac{R^2}{r^2}\left[\left(1 + w'^2\right)d\rho^2 + \rho^2 d\Omega_3^2\right] \tag{2.23}$$

where a prime denotes differentiation with respect to ρ. Computing the DBI action we find

$$S_{\mathrm{D7}} = -T \int d^8\xi \rho^3 \sqrt{1 + w'^2} \tag{2.24}$$

Following the usual Euler Lagrange method the equation of motion is

$$\frac{d}{d\rho}\left(\frac{\rho^3}{\sqrt{1+w'^2}}w'\right)=0 \tag{2.25}$$

Therefore $w(\rho)=0$ is a solution. If this is the case the asymptotic separation between the D7 and D3 branes is zero and the quarks are massless. Solutions where this is not the case and the quark mass is non zero typically have to be found numerically.

As described previously, the mass of the quarks in the boundary theory is related to the asymptotic value of the embedding function as the boundary is approached. The asymptotic behaviour of the embedding function depends on which coordinate system one is working in, but in these coordinates where taking $\rho\to\infty$ is the boundary limit the embedding function there is

$$w=\frac{m_q}{2\pi\alpha'}+\frac{c}{\rho^2}+\ldots \tag{2.26}$$

The leading term is related to the mass of the quarks, while the second term is related to what we call the quark condensate.

With these additional probe branes in the geometry the extra fields in the fundamental representation of the gauge theory are as follows: $\mathcal{N}=2$ is retained in the gauge theory so for $N_f=1$ and in the language of $\mathcal{N}=1$ superfields there are two chiral multiplets Q and $\tilde{Q}$ in the $\overline{N}$ and N representation of $SU(N)$. These multiplets contain a quark and a squark (q,ψ) and an antiquark and an antisquark $(\tilde{q},\tilde{\psi})$ respectively. The superpotential contains the quark mass term and leads to interactions between the quark multiplets and the adjoint chiral multiplets Φ_1,Φ_2 and Φ_3.

$$W=\frac{1}{g_{\mathrm{YM}}^2}\left(\sum_{i=1}^{N_f}\left(\sqrt{2}\,\tilde{Q}_i\,\Phi_3\,Q^i+m_q\,\tilde{Q}_i\,Q^i\right)+\sqrt{2}\,\mathrm{Tr}(\Phi_3\,[\Phi_1,\Phi_2])\right) \tag{2.27}$$

After coupling to the $\mathcal{N}=2$ hypermultiplets, Φ_3 naturally becomes the scalar part of the $\mathcal{N}=2$ vector multiplet, while Φ_1 and Φ_2 together constitute an $\mathcal{N}=2$ adjoint hypermultiplet. In terms of component fields, the mass term

for the quark multiplet induces the following terms in the Lagrangian

$$\mathcal{L} \supset \frac{1}{g_{YM}^2}\left(m_q\tilde{\psi}^i\psi_i + m_q^2 q_i^\dagger q^i + m_q^2\tilde{q}_i^\dagger\tilde{q}^i + \sqrt{2}m_q q_i^\dagger\Phi_3 q^i + \sqrt{2}m_q\tilde{q}_i\Phi_3\tilde{q}^{i\dagger} + \text{h.c.}\right) \tag{2.28}$$

In later sections we will refer to the expectation value of the operator $\Sigma_m = \frac{\partial\mathcal{L}}{\partial m_q}$ as the quark condensate.

The presence of the D7 brane covering $AdS_5 \times S^3$ breaks the global symmetry group of the S^5, which is the R symmetry group in the gauge theory to $SU(2) \times U(1)$. This is exactly the R symmetry group of a theory with $\mathcal{N} = 2$ supersymmetry.

$F_{ab} = \partial_a A_b - \partial_b A_a$ is a $U(1)$ gauge field strength that lives on the D7 branes. It can be shown that it is consistent to set A_a to zero so in the field theory it must be related to parameters that have this property. It has been shown (see for example [26, 47]) that when one turns on a time component of the worldvolume gauge field it is equivalent to turning on a non zero chemical potential for a $U(1)_B$ baryon number symmetry in the gauge theory. This baryon number symmetry is related to the global flavour group by $U(N_f) \approx U(1)_B \times SU(N_f)$.[5] The other components of this $U(1)$ gauge field are related to the conductivity in each of the spatial directions of the field theory, as described in the previous chapter. Note that if we turn on a time component of the worldvolume gauge field and set the other components to zero the Chern Simons term in the D7 brane action will vanish due to the presence of the $F \wedge F$. This is typical of theories where we want to investigate the phase diagram in the (μ, T) plane. The NS B field is related to the expectation value of the phase of the Polyakov loop in the gauge theory. We will describe this in more detail in a later section.

2.4 Other Dualities

Since the discovery of the duality between type IIB string theory on $AdS_5 \times S^5$ and $\mathcal{N} = 4$ super Yang-Mills there has been a large bulk of work involved

[5] For massless quarks the theory has the global symmetry group $U(1)_B \times SU(N_f) \times SU(2)_R \times U(1)_R \times SU(2)_\Phi$.

with finding gravity duals where the field theory is closer to those we observe in nature. In particular, finding a gravity dual to QCD is a highly significant ongoing research programme.

One of the important dualities that is related to QCD was discovered by Sakai and Sugimoto [33]. In order to model QCD at strong coupling holographically the Sakai-Sugimoto model takes a stack of N D4 branes in type IIA supergravity corresponding to the adjoint sector of the field theory and in the large N limit replaces them with a background geometry, as was the case for D3 branes in type IIB supergravity. To incorporate N_f flavours D8 - $\overline{\text{D8}}$ branes are added which we consider in the probe approximation as described in the previous section. The worldvolume of the D4 branes is 5 dimensional and the D8 and $\overline{\text{D8}}$ branes intersect with them in four of their dimensions. The D8 and $\overline{\text{D8}}$ branes are pointlike in the remaining dimension of the D4 branes worldvolume (labelled x_4) and are separated by a distance L. The overlap of the D8 branes with the D4 branes introduces N_f left handed quarks in the fundamental representation while the equivalent overlap of the $\overline{\text{D8}}$ branes with the D4 branes introduces N_f right handed quarks.

To reduce the dimensionality of the boundary from 5 to 4 the x_4 direction is compactified on a circle, so if we consider meson masses below the Kaluza Klein mass scale M_{KK} the boundary gauge theory is effectively 4 dimensional. In addition, imposing antiperiodic boundary conditions for fermions on the compact direction breaks supersymmetry completely making the only light degrees of freedom those of large N QCD. A great successes of the Sakai-Sugimoto model is it is a holographic model that realises chiral symmetry breaking. The geometry resulting from the D4 branes contains a horizon, and the D8 - $\overline{\text{D8}}$ solutions that end at some finite height above that horizon represent a state in the field theory where chiral symmetry is broken. If one increases the temperature with the other parameters of the theory fixed the distance from the horizon to the end point of the D8 - $\overline{\text{D8}}$ branes is reduced. Eventually, the horizon will meet the branes and chiral symmetry is restored. It has been shown in [48, 49] that there are two bulk geometries with similar asymptotics, corresponding to a QCD like theory at low and

high temperatures. For low temperature:

$$ds^2 = \left(\frac{U}{R}\right)^{\frac{3}{2}} \left(dt_E^2 + \delta_{ij}dx^i dx^i + f_{KK}(U)dx_4^2\right) + \left(\frac{R}{U}\right)^{\frac{3}{2}} \left(\frac{dU}{f_{KK}(U)} + U^2 d\Omega_4^2\right) \tag{2.29}$$

with $f_{KK}(U) = 1 - \left(\frac{U_{KK}}{U}\right)^3$. R is the radius of curvature and is related to the string coupling and string length. U_{KK} is the position of the horizon and both are related to the Kaluza Klein mass $M_{KK} = \frac{3}{2}\sqrt{\frac{U_{KK}}{R^3}}$, which is the mass that characterises the scale of the compact direction. For the high temperature deconfined phase we have

$$ds^2 = \left(\frac{U}{R}\right)^{\frac{3}{2}} \left(f_T(U)dt_E^2 + \delta_{ij}dx^i dx^j + dx_4^2\right) + \left(\frac{R}{U}\right)^{\frac{3}{2}} \left(\frac{dU}{f_T(U)} + U^2 d\Omega_4^2\right) \tag{2.30}$$

where $f_T(U) = 1 - \left(\frac{U_T}{U}\right)^3$. Note we have Wick rotated to Euclidean signature, and to avoid a conical singularity at the horizon the Euclidean time direction must be periodically identified, hence there are two compact directions in the geometries and thus one can think of the low / high temperature behaviour as a competition between which circle shrinks to zero size first. Ensuring regularity at the horizon one can deduce that the temperature is given by

$$T = \frac{3}{4\pi}\sqrt{\frac{U_T}{R^3}} \tag{2.31}$$

Quantities in the Sakai-Sugimoto model depend on the temperature, chemical potential and the parameter L which is the asymptotic separation of the D8 - $\overline{\text{D8}}$ branes in the x_4 direction. We will consider this brane set up at strong coupling, i.e. the separation of the D8 - $\overline{\text{D8}}$ branes is much smaller than the coupling, so the effective theory (which is four dimensional when we consider energies below the Kaluza-Klein mass scale) contains terms inducing strongly coupled four fermion interactions with coefficients that depend on L.[6] These operators are irrelevant, so it is not clear exactly how to relate L to the various generated operators when the coupling is large. With this

[6]The gauge theory is five dimensional, so the coupling has dimensions of length. For a discussion of this brane configuration at strong and weak coupling see [50].

in mind, it is clear that the field theory side of the Sakai-Sugimoto model is not simply large N QCD but some other, more complicated field theory. It does have some important features of QCD however, so in studying it we can gain some important insights about QCD at strong coupling.

2.5 Computing Gauge Theory Quantities

In the time since Maldacena proposed that Type IIB supergravity on $AdS_5 \times S^5$ was dual to $\mathcal{N} = 4$ super Yang-Mills theory, much effort has gone into understanding how quantities in one theory relate to quantities in the other. In particular we will be interested in how one may compute quantities in the gauge theory at strong coupling by performing a calculation in the gravity theory. The correspondence was originally formulated in a spacetime with Euclidean signature and a prescription for computing gauge theory correlation functions in this setup was formulated independently by Gubser, Klebanov and Polyakov [21] and Witten [20]. Their thesis was that one can find solutions to the equations of motion of the supergravity theory and relate them in a simple way to the generating functional of the gauge theory:

$$W[\phi_0] = -S_{\text{on shell}}[\phi] \tag{2.32}$$

Here W is the gauge theory generating functional, $S_{\text{on shell}}$ is the on-shell action of the gravity theory, ϕ is some field in the gravity theory and $\phi_0 = \lim_{r \to \text{boundary}} \phi(r)$ is the boundary value of the field ϕ. To obtain the on-shell action of the gravity theory one must solve the equations of motion for the field in question and substitute this into the action. When one has computed the on-shell action it is possible to compute an n point correlation function by taking n functional derivatives with respect to the boundary conditions

$$\langle \mathcal{O}_1 \dots \mathcal{O}_n \rangle = \frac{\delta^n W[\phi_0]}{\delta \phi_0^n} \tag{2.33}$$

Typically, the equations of motion are second order, and therefore there are two independent solutions and two boundary conditions. One may show that

in Euclidean AdS and the Euclidean AdS black hole, the two solutions to the equations of motion are characterised as non normalisable and normalisable in the interior. By demanding regularity of the solution to the equations of motion in the interior, we use the normalisable solution to compute the on-shell action and the non normalisable solution is interpreted as a source for the dual operator. There is no ambiguity and since all correlation functions are known, everything there is to know about the gauge theory is known.

There is a one to one correspondence between canonical fields in the supergravity theory particular single trace, chiral primary operators in the gauge theory. For example:

$$\begin{aligned} \phi &\leftrightarrow \mathrm{Tr}\left(F^a_{\mu\nu}F^{a,\mu\nu}\right) \\ A_\mu &\leftrightarrow J^\mu \\ g_{\mu\nu} &\leftrightarrow T^{\mu\nu} \end{aligned}$$

Where J^μ is the R charge current, A_μ is the gauge field[7] and $T^{\mu\nu}$ is the stress energy tensor. $\mathrm{Tr}\left(F^a_{\mu\nu}F^{a,\mu\nu}\right)$ is commonly referred to as the glueball operator since it corresponds to bound states of gauge bosons in Yang-Mills theory. One can immediately see that the field in the supergravity theory and the corresponding operator in the gauge theory must have the same index structure - a scalar field must correspond to a scalar operator etc. For a complete dictionary relating fields to operators in the AdS/CFT correspondence see for example [51].

In Euclidean signature, this prescription is sufficient to compute gauge theory correlation functions for zero and finite temperature. However, in Lorentzian signature at high temperature one may show that the two solutions to the equations of motion are both normalisable in the bulk so imposing regularity is no longer sufficient to uniquely fix a solution, and hence, the on-shell action. This problem was described in [52]. The ambiguity in the bulk is equivalent to the ambiguity in the two point correlation functions

[7]Although a rank 1 gauge field was not included in the original 10 dimensional action of type IIB supergravity, one can compactify the 10 dimensional $AdS_5 \times S^5$ down to 5 dimensional AdS. The remnant of the S^5 is a rank 1 gauge field with SO(6) symmetry.

that arises in Lorentzian signature weakly coupled quantum field theory - in Euclidean signature there is one correlation function while in Lorentzian signature there is an ambiguity in how to deal with the poles on the real axis, which leads to the various correlation functions in use in quantum field theory. The most commonly used correlation functions are the Feynman, retarded and advanced functions which have particular pole prescriptions. A method to compute two point correlation functions in Lorentzian signature using gauge gravity duality was provided by Son & Starinets in [53].

In order to compute correlation functions in Minkowskian signature from gravity, Son & Starinets suggested that imposing different boundary conditions at the horizon will lead to different correlation functions when one performs a holographic calculation. It was proposed that imposing infalling wave boundary conditions at the horizon will produce the retarded correlation function, while imposing purely outgoing wave boundary conditions at the horizon will yield the advanced correlation function. The prescription was shown to produce the correct correlation functions where they could be computed in other ways and compared, and it has been extensively used to extract real time two point correlation functions for many theories (see for example [54–57]). The method of Son & Starinets is limited however, it can also be shown that it cannot be used to calculate higher point correlation functions. More general prescriptions for computing higher point correlation functions have been subsequently discovered, see for example [58,59]. We will use the Son & Starinets method to compute two point retarded correlation functions in the next chapter.

Chapter 3

Strongly Coupled $\mathcal{N} = 4$ Super Yang-Mills on $dS_3 \times S^1$

3.1 Introductory Remarks

Quantum field theories on a time dependent background are very interesting and important areas of research, but also one where it is traditionally difficult to make progress. The first step to understanding field theories in time dependent backgrounds is clearly to understand how a field theory behaves in curved spacetime [60, 61]. One of the most famous works in this field is that of Hawking [44] which showed that a quantum field in a black hole background will cause the black hole to appear to radiate a thermal bath of particles as viewed by a far away observer. It was shown [62] that in this thermal bath of particles is the result of a horizon appearing in the geometry, for example, de Sitter space is a spacetime that does not contain a black hole but does contain a horizon so it was expected that Hawking radiation should be observed, and the temperature due to this horizon is now known as the Gibbons-Hawking temperature. Of course, research into field theories at weak coupling in curved spacetime is still ongoing. For example, see [63–65] and the references therein.

Since time dependent backgrounds are largely quite well understood in classical gravity, the AdS/CFT correspondence opens up the possibility that

understanding the complicated dynamics of a strongly coupled quantum field theory on a time dependent background may be accessible via a holographic calculation. Understanding these types of theory would be very useful, most notably for applications to cosmology and heavy ion collider physics. In this section we will use the techniques described in the previous chapters to follow the work of [66] the goal of which was to compute real time correlation functions on $dS_3 \times S^1$ dual to the time dependent, locally AdS backgrounds first studied in [67–71].

The authors of [72] studied the double analytic continuations of vacuum solutions such as Schwarzschild and Kerr spacetimes providing examples of smooth, time dependent solutions called "bubbles of nothing" [73–75]. These asymptotically flat solutions were generalized to asymptotically locally AdS spacetimes in [67,68], by considering the double analytic continuations of AdS black holes[1]. The bubbles are obtained by analytically continuing the time coordinate to Euclidean signature $t \to i\chi$ where χ is periodically identified, and a polar angle $\theta \to i\tau$ so effectively we swap one of the spatial directions for the time direction. In addition, the χ circle has supersymmetry breaking boundary conditions for fermions. The resulting bubbles undergo exponential de Sitter expansion in the far future, and contraction in the far past. For the asymptotically locally $AdS_5 \times S^5$ case [68], the boundary of the geometry is $dS_3 \times S^1$. The corresponding dual field theory, $\mathcal{N} = 4$ SYM, is thus formulated on $dS_3 \times S^1$ with antiperiodic boundary conditions for the fermions around the S^1. Each of the two AdS-Schwarzschild black holes (the small and big black holes) yield an AdS bubble of nothing solution, only one of which is stable. The bubble of nothing geometries are vacuum solutions with cosmological horizons [72] and particle creation effects.

It was realized in [69–71] that there is another spacetime with the same AdS asymptotics as the bubble geometries, with $dS_3 \times S^1$ geometry on the boundary. This is the so-called "topological black hole"[2] – a quotient of AdS

[1]For the classifications of solutions obtained by analytically continuing black hole solutions, see [76].

[2]The term "topological AdS black hole" has also been used to refer to black holes with a hyperbolic horizon having a non-trivial topology. In the AdS/CFT context these have been studied in [77–80] and references therein.

space obtained by an identification of global AdS_5 along a boost [81,82]. It is the five dimensional analogue of the BTZ black hole [83,84]. The topological AdS black hole can also be obtained by a Wick rotation of thermal AdS space. Euclidean thermal AdS may decay to the AdS Schwarzschild black hole via the Hawking-Page transition [20, 43] and similarly, the topological AdS black hole may decay via the nucleation of an AdS bubble of nothing. The topological black hole becomes unstable only when the radius of the spatial circle becomes smaller than a critical value, which in the Euclidean thermal setup is when the temperature exceeds a critical value. Precisely such an instability to decay to "nothing" was first noted for flat space times a circle having antiperiodic boundary conditions for fermions [73].

The two different geometries described above are dual to two different phases of strongly coupled, large N gauge theory formulated on $dS_3 \times S^1$. As in the usual thermal interpretation wherein the field theory lives on $S^3 \times S^1$, the two phases are distinguished by the expectation value of the Wilson loop around the S^1. In the bubble of nothing phase, the circle shrinks to zero size in the interior of the geometry and the Wilson loop is non-zero, indicating the spontaneous breaking of the $\mathbb{Z}_N$ symmetry of the gauge theory. The topological black hole phase is $\mathbb{Z}_N$ invariant. Unlike the thermal situation however, the spontaneous breaking of $\mathbb{Z}_N$ invariance is not a deconfinement transition since the circle is a spatial direction and not the thermal circle.

Our primary motivation is to understand how the behaviour of real time correlators in the two geometries reflects the properties and distinguishes the two phases of the $\mathcal{N} = 4$ theory on $dS_3 \times S^1$. Since the de Sitter boundary has its own cosmological horizon accompanied by a Gibbons-Hawking temperature [62], this should also be reflected in the properties of the boundary correlation functions. An interesting feature of both the geometries in question is that infinity is connected, *i.e.* the asymptotic structure of the geometry is unlike the AdS Schwarzschild black hole whose asymptotics consists of two disconnected boundaries. This means the Schwinger-Keldysh approach in [58] is not directly applicable. It would be interesting to understand how to apply that idea and also the recently proposed prescription of [59, 85] in the present context. Instead we simply use the Son-Starinets prescrip-

tion [53,56,86] to compute real time correlators in the topological AdS black hole geometry, by requiring infalling boundary conditions at the horizon of the black hole. In the following sections we will describe in detail the computation of the scalar glueball and conserved R-current correlation functions in the topological black hole geometry. The correlators cannot be computed analytically in the bubble of nothing geometry so provide an analysis of the scalar glueball correlation function using the WKB approximation.

3.2 The Topological AdS Black Hole

The topological black hole in AdS_5 [71,82] is an orbifold of AdS space obtained by the identification of points along the orbit of the Killing vector

$$\xi = \frac{r_\chi}{R}(x_4\partial_5 + x_5\partial_4) \tag{3.1}$$

where r_χ is an arbitrary real number and the AdS space is described as the universal covering of the hypersurface

$$-x_0^2 + x_1^2 + x_2^2 + x_3^2 + x_4^2 - x_5^2 = -R^2 \tag{3.2}$$

R is the AdS radius. In 'Kruskal like' coordinates which cover the whole space the metric is

$$ds^2 = \frac{4R^2}{(1-y^2)^2} dy^\mu dy^\nu \eta_{\mu\nu} + \frac{(1+y^2)^2}{(1-y^2)^2} r_\chi^2 d\chi^2 \tag{3.3}$$

Note that the χ direction is periodic with period 2π, $\mu, \nu \in 0, \ldots, 3$ and the coordinates y^μ are non compact with Lorentzian norm $y^2 = y^\mu y^\nu \eta_{\mu\nu}$ such that $-1 < y^2 < 1$. Note that this spacetime is Anti de Sitter *locally* with the χ direction periodically identified.

$$\chi \sim \chi + 2\pi \tag{3.4}$$

When we take $y^2 \to 1$ we are approaching the boundary of the space, the geometry of which is a three dimensional de Sitter space with radius of curva-

ture R times a circle with radius r_χ, hence the boundary CFT is formulated on $dS_3 \times S^1$.

At $y^2 = 0$ there is a horizon which is given by the three dimensional hypercone

$$y_0^2 = y_1^2 + y_2^2 + y_3^2 \tag{3.5}$$

and there is a singularity at $y^2 = -1$. The singularity arises because timelike geodesics end at $y^2 = -1$ and the norm of the Killing vector ∂_χ, which is the Killing vector that generates the orbifold identification, vanishes there. The global structure of the topological black hole is shown in figure 3.1. It is interesting to note that the topology of this spacetime is $\mathbb{R}^{3,1} \times S^1$ in contrast to that of the AdS Schwarzschild black hole which has the topology $\mathbb{R}^{1,1} \times S^3$. This means that, unlike the infinity of AdS Schwarzschild spacetime which has two disconnected regions, infinity for the topological black hole is a single connected piece. This fact leads to a difficulty in defining a prescription for computing boundary correlation functions in the gauge theory. Normally, we would follow the method provided in [58] to find the generating functional of the gauge theory, but the fact that infinity is connected means we cannot do this. It is possible that one may adapt the method of [59] to compute the full generating functional of the gauge theory, but we leave this for future work and will compute two point Green's functions using the method from [53]. Another useful coordinate system it is possible to recast the metric in are Schwarzschild like coordinates

$$Y^2 = \sum_{i=1}^{3} y_i y_i, \qquad \frac{Y}{y_0} = \coth\left(\frac{t}{R}\right), \qquad \frac{r^2}{R^2} = \frac{4\left(Y^2 - y_0^2\right)}{\left(1 + y_0^2 - Y^2\right)^2} \tag{3.6}$$

These coordinates cover the region $y^0 \geq 0$ or the exterior of the topological black hole. Locally the metric takes the form

$$ds^2 = \frac{R^2}{r^2 + R^2} dr^2 + \left(\frac{r_\chi}{R}\right)^2 \left(r^2 + R^2\right) d\chi^2 + r^2 \left(-\frac{dt^2}{R^2} + \cosh^2\left(\frac{t}{R}\right) d\Omega_2^2\right) \tag{3.7}$$

In these coordinates the horizon is at $r = 0$. Slices of constant r has the geometry of $dS_3 \times S^1$. It is possible to obtain the topological black hole

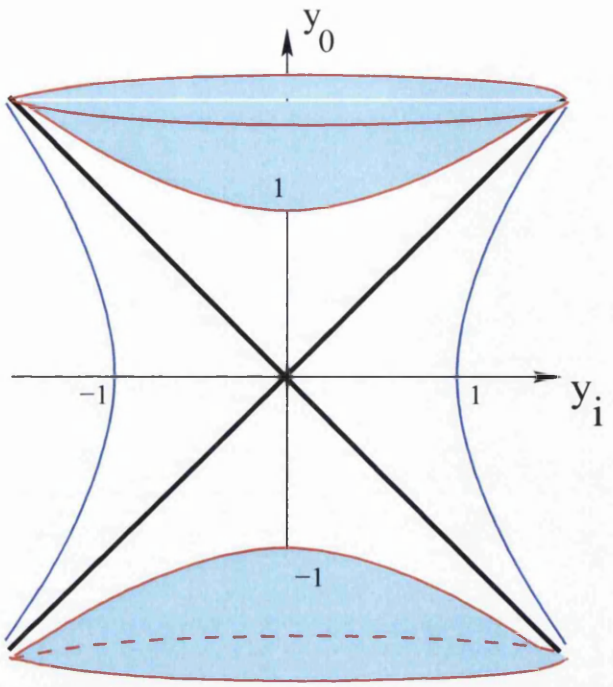

Figure 3.1: The global structure of the topological AdS black hole spacetime. The singularity is the hyperboloid $-y_0^2 + y_i y_i = -1$ and the horizon is at the cone $y_0^2 = y_i y_i$.

metric by the Wick rotation of thermal AdS space. Wick rotating one of the directions in the S^3 of thermal AdS would produce the dS_3 factor, and then the Euclidean time circle would be interpreted as a spatial circle, rather than a thermal circle whose period is related to the temperature. Locally the topological black hole is AdS but globally it differs from AdS because of the periodic identification of the χ direction. Note that at the horizon this spatial circle is finite sized at the horizon and it's radius is r_χ. Indeed, it was argued in [68, 71], the topological black hole in AdS space is automatically a solution to the Type IIB supergravity equations of motion, since it can be obtained via a double Wick rotation (and an identification) of $AdS_5 \times S^5$. The dual field theory is $\mathcal{N} = 4$ supersymmetric Yang-Mills on the boundary of the topological black hole spacetime which is $dS_3 \times S^1$.

3.3 Correlations Functions Dual to the Topological Black Hole

In this section we will compute the real time correlation functions for the glueball and the R-current on $dS_3 \times S^1$ in the phase dual to the topological black hole geometry in the bulk. Since the topological black hole is related to Euclidean thermal AdS by Wick rotation, one could in principle take the correlation functions on $S^3 \times S^1$ and Wick rotate to obtain the correlation function on $dS_3 \times S^1$. However, the Wick rotation required takes the polar angle and changes it into the time direction so a complete knowledge of the angular dependence of the correlators would be required and at finite temperature and strong coupling the full correlators have not been explicitly calculated. For this reason we will use the prescription of Son & Starinets [53] to calculate the correlation functions holographically in the topological black hole background directly, and not use analytic continuation.

3.3.1 Scalar Wave Equation in the Topological Black Hole

Following the outline in section 2.5 we will calculate the particular correlation function by solving the related wave equation in the bulk and evaluating the on shell action. The simplest case in the bulk, the scalar wave equation, is dual to the glueball operator so to find the correlation function we will solve the scalar wave equation in the area of the bulk exterior to the black hole. We will write the metric in the form used by [71]

$$ds^2 = R^2 \left(\frac{d\rho^2}{\rho^2 - 1} + \left(\frac{r_\chi}{R}\right)^2 \rho^2 d\chi^2 + (\rho^2 - 1)\left(-d\tau^2 + \cosh^2\tau d\Omega_2^2\right) \right) \quad (3.8)$$

where we have introduced the dimensionless variables

$$\rho = \sqrt{\left(\frac{r}{R}\right)^2 + 1}, \qquad \tau = \frac{t}{R} \quad (3.9)$$

$\rho \to \infty$ corresponds to the boundary limit, while the horizon is at $\rho = 1$ where the coefficient of $d\tau^2$ vanishes and the coefficient of $d\rho^2$ diverges. The scalar wave equation in general is

$$\left(\frac{1}{\sqrt{-g}}\partial_\mu\left(\sqrt{-g}g^{\mu\nu}\partial_\nu\right) - m^2\right)\phi = 0 \tag{3.10}$$

To solve this equation we will use the method of separation of variables. In this geometry, scalar fields have a natural expansion in terms of spherical harmonics on the $S^2 \times S^1$ spatial slices

$$\phi(\rho, \chi, \tau, \Omega) = \sum_{\ell,m,n} A_{\ell m} Y_{\ell m}(\Omega)\, e^{in\chi} \int \frac{d\nu}{2\pi} \Phi_n(\nu, \rho)\, \mathcal{T}_\ell(\nu, \tau) \tag{3.11}$$

In this expansion $Y_{\ell m}(\Omega)$ are spherical harmonics on the S^2, $e^{in\chi}$ are Fourier modes on the S^1 and $\Phi_n(\nu, \rho)$ contains the dependence on the radial direction which we will discuss below. Plugging this into equation (3.10) one can show the temporal modes $\mathcal{T}_\ell(\nu, \tau)$ satisfy the following equation

$$\frac{1}{\cosh^2\tau}\partial_\tau\left(\cosh^2\tau\partial_\tau\mathcal{T}_\ell(\nu,\tau)\right) + \frac{\ell(\ell+1)}{\cosh^2\tau}\mathcal{T}_\ell(\nu,\tau) = -\left(\nu^2+1\right)\mathcal{T}_\ell(\nu,\tau) \tag{3.12}$$

General solutions to equation (3.12) can be expressed in terms of associated Legendre functions

$$\mathcal{T}_\ell(\nu,\tau) = \frac{1}{\cosh\tau}\left(A_\ell P_\ell^{i\nu}(\tanh\tau) + B_\ell Q_\ell^{i\nu}(\tanh\tau)\right) \tag{3.13}$$

In the usual approach to quantizing free scalar fields in de Sitter space, the integration constants A_ℓ and B_ℓ are determined by the choice of de Sitter vacuum [60, 87, 88] (the so-called α-vacua). However, in the present context, the constants will be specified by picking out infalling wave solutions at the horizon of the topological black hole. These are the holographic boundary conditions relevant for real time correlation functions in the strongly coupled field theory on $dS_3 \times S^1$. Whether α-vacua are defined in theories with couplings is not as yet fully understood, but for a further discussion on this topic in the context of AdS/CFT see [89]. For every $\ell \in \mathbb{Z}$, the equation has

two kinds of solutions that will be relevant for us:

1. normalisable modes labelled by integers $-i\nu = 1, 2, \ldots \ell$.
2. delta-function normalisable modes labelled by a continuous frequency variable $\nu \in \mathbb{R}$.

The inner product is taken at constant ℓ and is given by

$$\langle \mathcal{T}(\nu,\tau), \mathcal{T}(\nu',\tau)\rangle = \int_{-\infty}^{\infty} d\tau \cosh^2\tau\, \mathcal{T}(\nu,\tau)\,\mathcal{T}(\nu',\tau) \tag{3.14}$$

The delta function normalisable modes are chosen such that this integral is equal to $\delta(\nu+\nu')$ while the other modes are normalised to unity. The distinction in the different types of modes is more important for the R-current correlation functions and we will discuss them in more detail in that section.

Consider now the equation for the radial component. To find a solution we will rewrite it as a Schrödinger equation, using Regge-Wheeler type variables

$$u = \frac{1}{2}\log\left(\frac{\rho+1}{\rho-1}\right) \qquad \text{or} \qquad \rho = \coth u \tag{3.15}$$

and

$$\Psi_n = \sqrt{\rho(\rho^2-1)}\Phi_n \tag{3.16}$$

with these coordinate changes the horizon is approached as $u \to \infty$ while the boundary is at $u = 0$. The radial equation is

$$\frac{d^2}{du^2}\Psi_n(\nu,u) + V_n(u)\,\Psi_n(\nu,u) = \nu^2\Psi_n(\nu,u) \tag{3.17}$$

$$V_n(u) = \left((mR)^2 + \frac{15}{4}\right)\frac{1}{\sinh^2 u} + \left(\frac{1}{4}+\bar{n}^2\right)\frac{1}{\cosh^2 u} \tag{3.18}$$

Where we have defined

$$\bar{n} = \frac{Rn}{r_\chi} \tag{3.19}$$

The potential is shown in figure 3.2. It decays exponentially near the horizon, while blowing up near the boundary, which is expected for black holes in AdS

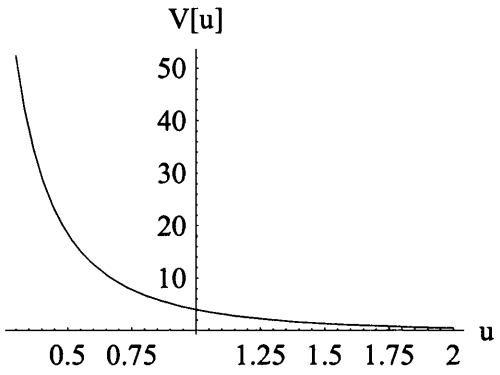

Figure 3.2: The Schrödinger potential for the topological AdS black hole.

space. In the near horizon region where the potential vanishes, the solutions with $\nu > 0$ are travelling waves therefore there is a distinction between incoming and outgoing plane wave solutions and we may apply infalling wave boundary conditions in order to compute the retarded correlation function. For any n and m, the equation has analytically tractable solutions in terms of hypergeometric functions. In this discussion we will restrict attention, for simplicity, to two special cases: i) $n \neq 0$ and $mR = 0$; ii) $n = 0$ and $mR \neq 0$. The solutions to the radial part of the wave equation are given by

$n \neq 0$ and $mR = 0$

$$\begin{aligned}\Phi_n(\nu,\rho) &= C_1\,\rho^{-i\bar{n}}\times \\ &\quad (\rho^2-1)^{-\frac{i\nu}{2}-\frac{1}{2}}\,{}_2F_1\left(-\frac{1}{2}-\frac{i}{2}(\nu+\bar{n}),\ \frac{3}{2}-\frac{i}{2}(\nu+\bar{n});\ 1-i\bar{n};\ \rho^2\right)\\ &+ C_2\,\rho^{i\bar{n}}\times \\ &\quad (\rho^2-1)^{-\frac{i\nu}{2}-\frac{1}{2}}\,{}_2F_1\left(-\frac{1}{2}-\frac{i}{2}(\nu-\bar{n}),\ \frac{3}{2}-\frac{i}{2}(\nu-\bar{n});\ 1+i\bar{n};\ \rho^2\right)\end{aligned} \tag{3.20}$$

$n = 0$ and $mR \neq 0$

$$\Phi_0(\nu,\rho) = C_1 \frac{{}_2F_1\left(\frac{1}{2}(3-\Delta)-\frac{1}{2}i\nu,\ \frac{1}{2}(3-\Delta)+\frac{1}{2}i\nu;\ 3-\Delta;\ -(\rho^2-1)^{-1}\right)}{(\rho^2-1)^{\frac{1}{2}(4-\Delta)}} + C_2 \frac{{}_2F_1\left(\frac{1}{2}(\Delta-1)-\frac{1}{2}i\nu,\ \frac{1}{2}(\Delta-1)+\frac{1}{2}i\nu;\ \Delta-1;\ -(\rho^2-1)^{-1}\right)}{(\rho^2-1)^{\frac{1}{2}\Delta}} \tag{3.21}$$

In the above we have used the shorthand $\Delta = 2+\sqrt{4+(mR)^2}$, which is the dimension of the dual operator in the boundary theory.

3.3.2 The Massless Scalar Glueball Correlator

The field theory, $\mathcal{N}=4$ super Yang-Mills defined on $dS_3 \times S^1$, contains two $SO(6)$ singlet, scalar glueball fields;

$$\mathcal{G}(\vec{x},t) = \mathrm{Tr}F_{\mu\nu}F^{\mu\nu}, \qquad \tilde{\mathcal{G}}(\vec{x},t) = \mathrm{Tr}F_{\mu\nu}\tilde{F}^{\mu\nu} \tag{3.22}$$

These fields are dual to the dilaton and the axion (the RR-scalar) respectively in type IIB theory in the bulk. Both of these fields solve the scalar wave equation and when the equation is massless corresponds to $\Delta = 4$ operators. The retarded propagators for the scalar glueball fields are known on $\mathbb{R}^{3,1}$ at weak coupling for both zero and finite temperature [90]. Since the operator is chiral primary in the $\mathcal{N}=4$ theory, at zero temperature its correlation function on $\mathbb{R}^{3,1}$ receives no quantum corrections and the strong coupling results from supergravity are in exact agreement with those of the free field theory. At finite temperature, however, when supersymmetry is broken, strong and weak coupling results on $\mathbb{R}^{3,1}$ differ [53, 90]. Computations of the glueball correlator also exist in the free $\mathcal{N}=4$ theory at finite temperature and on a spatial S^3, both in the confined and deconfined phases [90]. Their strong coupling counterparts have not been determined.

In this case we are considering the theory on $dS_3 \times S^1$, which leads to three interesting observations. Firstly, we are imposing antiperiodic bound-

ary conditions for fermions on the S^1, so supersymmetry is completely broken. Secondly, the dS_3 on the boundary contains a cosmological horizon with associated Gibbons-Hawking temperature, so it would be interesting to see this emerge from a holographic, strong coupling calculation. Lastly, analogously to the Hawking-Page phase transition from thermal AdS to the (big) AdS Schwarzschild black hole via the Euclidean bounce, when the radius of the boundary S^1 decreases below a critical value, $r_\chi \leq \frac{R}{2\sqrt{2}}$, the topological black hole decays to the small AdS bubble of nothing. We would like to understand how boundary field theory correlators at strong coupling on $dS_3 \times S^1$ change across this transition. The transition from the topological black hole to the Bubble of Nothing is a $\mathbb{Z}_N$ breaking transition. This due to a non-zero expectation value for the Wilson loop around the spatial S^1.

We are primarily interested in real time response and for the sake of simplicity, we will first study only the response functions for glueball fluctuations that are homogeneous on the spatial S^2 slices at the boundary, i.e.

$$G_R(\tau,\tau';n;\ell=0) = \\ -i\int\frac{d\Omega}{4\pi}\frac{d\Omega'}{4\pi}\int\frac{d\chi}{2\pi}\,e^{-in\chi}\,\Theta(\tau-\tau')\,\langle\,[\,\mathcal{G}(\Omega,\chi,\tau),\,\mathcal{G}(\Omega',0,\tau')\,]\,\rangle \qquad (3.23)$$

We will work with the dimensionless variables $\tau = \frac{t}{R}$, $\tau' = \frac{t'}{R}$ and restore appropriate dimensions when necessary. Although we will not generalise to inhomogeneous fluctuations on the spatial sphere for the glueball correlation functions we will when we look at R-current correlators, and we will see that the generalisation is straightforward.

For the moment we focus attention on the s-wave ($\ell = 0$) retarded correlation function of the scalar glueball operator. Also, for the s-waves, the correlator turns out to be a function of $(\tau - \tau')$ so that it is natural to define the temporal Fourier transform of this as,

$$\tilde{G}_R(\nu;n) = \int_{-\infty}^{\infty} d\tau\, e^{-i\nu(\tau-\tau')}\, G_R(\tau,\tau';n;\ell=0) \qquad (3.24)$$

To calculate it at strong coupling and in the large radius regime ($r_\chi \geq \frac{R}{2\sqrt{2}}$),

we solve the dilaton wave equation which is the equation for a massless, minimally coupled scalar field in the background of the topological AdS black hole.

Spatially Homogeneous Case with $n = \ell = 0$

Firstly, consider the simplest case where $n = \ell = 0$. When the mass is also vanishing and the dimension of the dual operator is $\Delta = 4$ the solutions to the radial part of the scalar wave equation are hypergeometric functions.

$$\Phi_0^{(1)}(\nu,\rho) = \frac{\pi}{4}\frac{1+\nu^2}{\cosh\left(\frac{\pi\nu}{2}\right)}\,{}_2F_1\left(-\frac{1+i\nu}{2},-\frac{1-i\nu}{2};1;\frac{\rho^2}{\rho^2-1}\right) \tag{3.25}$$

and

$$\Phi_0^{(2)}(\nu,\rho) = \frac{1}{(\rho^2-1)^2}\,{}_2F_1\left(\frac{3-i\nu}{2},\frac{3+i\nu}{2};3;\frac{1}{\rho^2-1}\right) \tag{3.26}$$

The temporal part of the wave equation is also particularly simple when $\ell = 0$, and has a natural interpretation in terms of positive and negative frequency states.

$$\mathcal{T}^+ = (\nu,\tau)\frac{e^{-i\nu\tau}}{\cosh\tau} \qquad \text{and} \qquad \mathcal{T}^- = (\nu,\tau)\frac{e^{i\nu\tau}}{\cosh\tau} \tag{3.27}$$

In order to find the retarded correlation functions holographically we are required to choose the appropriate linear combination of solutions which is both smooth and is an infalling wave at the horizon, which is approached as $\rho \to 1$. In the near horizon region, the asymptotic form of the solutions is:

$$\Phi_0^{(1)}(\nu,\rho\to 1)\to$$
$$i\left(2\left(\rho-1\right)\right)^{\frac{i-i\nu}{2}} e^{\frac{\pi\nu}{2}}\frac{\Gamma\left(-i\nu\right)\Gamma\left(\frac{3+i\nu}{2}\right)}{\Gamma\left(-\frac{1+i\nu}{2}\right)} + i\left(2\left(\rho-1\right)\right)^{-\frac{1+i\nu}{2}} e^{-\frac{\pi\nu}{2}}\frac{\Gamma\left(i\nu\right)\Gamma\left(\frac{3-i\nu}{2}\right)}{\Gamma\left(-\frac{1-i\nu}{2}\right)} \tag{3.28}$$

and

$$\Phi_0^{(2)}(\nu,\rho\to 1)\to (2(\rho-1))^{-\frac{1-i\nu}{2}}\frac{2\Gamma(-i\nu)}{\Gamma\left(\frac{3-i\nu}{2}\right)^2}+(2(\rho-1))^{\frac{1+i\nu}{2}}\frac{2\Gamma(i\nu)}{\Gamma\left(\frac{3+i\nu}{2}\right)^2} \tag{3.29}$$

We note that these modes diverge like $\frac{1}{\sqrt{\rho-1}}$ as $\rho\to 1$, however they are still normalisable since $\sqrt{-g}\sim(\rho^2-1)^{\frac{5}{2}}$. We must also ensure the solutions are correctly normalised as the boundary is approached. Indeed, we can show

$$\Phi_0^{(1)}(\nu,\rho\to\infty)=1+\ldots,\qquad \Phi_0^{(2)}(\nu,\rho\to\infty)=\frac{1}{\rho^4}+\ldots \tag{3.30}$$

Assuming $\mathcal{T}_0^+$ are positive frequency modes for $\mathrm{Re}(\nu)>0$ the radial part of the solution should be proportional to $(\rho-1)^{-\frac{1+i\nu}{2}}$ at the horizon. With this condition the appropriate linear combination of solutions is

$$\Phi_0(\nu,\rho)=\Phi_0^{(1)}(\nu,\rho)+\frac{i\pi}{32}e^{\frac{\pi\nu}{2}}\frac{(\nu^2+1)^2}{\cosh\left(\frac{\pi\nu}{2}\right)}\Phi_0^{(2)}(\nu,\rho) \tag{3.31}$$

The holographic prescription for computing the real time retarded correlation functions [53,86] requires us to evaluate the boundary terms of the scalar on shell action

$$S=\frac{N^2}{16\pi^2}\int d\tau d\Omega d\chi\; g^{\rho\rho}\sqrt{-g}\,\Phi(\tau,\rho)\,\partial_\rho\Phi(\tau,\rho)\Big|_{\rho\to\infty} \tag{3.32}$$

For the current case under consideration where $n=\ell=0$, the solution for Φ is given by

$$\Phi(\tau,\rho)=\int_{-\infty}^{\infty}\frac{d\nu}{2\pi}\mathcal{T}_0^+(\nu,\tau)\,\Phi_0(\nu,\rho) \tag{3.33}$$

Plugging into the scalar boundary action with the expressions for $\mathcal{T}_0^+(\nu,\rho)$ and the correct linear combination of solutions given in (3.31) we are lead to the unrenormalised retarded correlator in frequency space. Below we include

all contact terms (finite polynomials in the frequency ν.).

$$\begin{aligned}\tilde{G}_R(\nu;0) =& \frac{N^2}{16\pi^2}\left(-\frac{1}{8}(1+\nu^2)^2\left[\psi\left(\frac{3-i\nu}{2}\right)+\psi\left(\frac{3+i\nu}{2}\right)\right]\right.\\ &+\frac{1}{8}(1+\nu^2)^2\left[-i\pi\coth\left(\frac{\pi}{2}(\nu+i)\right)+2\left(\log\rho-\gamma_E+1\right)\right]\\ &\left.+\frac{1}{2}(1+\nu^2)\rho^2\right)\Big|_{\rho\to\infty}\end{aligned} \tag{3.34}$$

Note that the quadratically divergent term in (3.34) comes from a term in the non normalisable solutions near boundary asymptotics proportional to $\frac{1}{\rho^2}$. This would not be present in Poincaré like coordinates, and this piece doesn't contribute any other term to the correlator.

When we subtract the divergent and contact terms we get the renormalised correlation function. At this point we will restore the dimensionful de Sitter radius R by making the replacement $\nu \to \nu R$. The resulting correlator is

$$\tilde{G}_R(\nu;0) = -\frac{N^2}{64\pi^2}\left(\frac{1}{R^2}+\nu^2\right)^2\left[\psi\left(\frac{3-i\nu R}{2}\right)-\frac{2i\nu R}{1+\nu^2R^2}\right] \tag{3.35}$$

The analytic structure of the correlator is shown in figure 3.3 When ν is

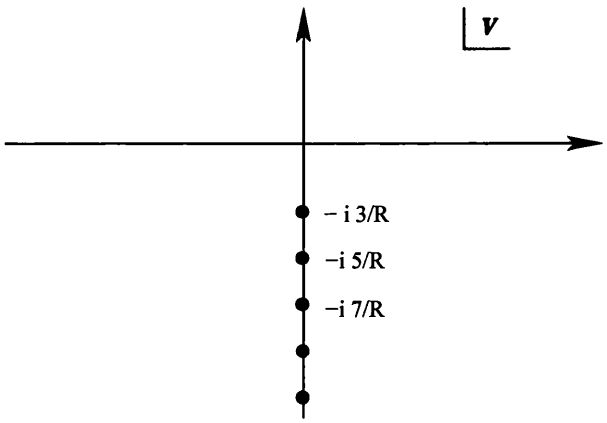

Figure 3.3: The analytic structure in complex frequency plane of the massless, spatially homogeneous ($\ell = n = 0$), retarded Green's function in the $\mathbb{Z}_N$ symmetric phase, corresponding to the topological AdS black hole.

purely real the real and imaginary parts of the correlation function (3.34) match, and the function is analytic in the upper half plane. In the lower half plane there are simple poles at frequencies

$$\nu_k = -\frac{i(3+2k)}{R} \qquad k \in \mathbb{Z} \tag{3.36}$$

It was argued in [53] that the poles of the retarded correlator in a black hole background coincide with the quasinormal frequencies of the black hole. The quasinormal frequencies of the topological black hole in AdS_5 above are quite similar to the corresponding objects in the BTZ black hole.

Non zero Momentum Along the S^1 with $\ell = 0$

Generalising the above calculation to include a discrete non zero momentum equal to $\frac{n}{r_\chi}$ around the S^1 is relatively straightforward. It requires us to write the scalar boundary action using the modes given in (3.20). The steps are identical to the calculation above, but the algebra is more involved. With dimensionful constants restored we find the retarded Green's function is

$$\tilde{G}_R(\nu;n) = -\frac{N^2}{128\pi^2}\left(\left(\nu-\frac{n}{r_\chi}\right)^2+\frac{1}{R^2}\right)\times$$
$$\left[\psi\left(\frac{3}{2}-\frac{iR}{2}\left(\nu-\frac{n}{r_\chi}\right)\right)+\psi\left(\frac{3}{2}-\frac{iR}{2}\left(\nu+\frac{n}{r_\chi}\right)\right)-\frac{2iR\left(\nu-\frac{n}{r_\chi}\right)}{\left(\nu-\frac{n}{r_\chi}\right)^2R^2+1}\right.$$
$$\left.-\frac{2iR\left(\nu+\frac{n}{r_\chi}\right)}{\left(\nu+\frac{n}{r_\chi}\right)^2R^2+1}\right], \qquad n \in \mathbb{Z} \tag{3.37}$$

If we set $n = 0$ in the above we recover (3.35) as we should. The correlation function has poles in the lower half plane located at

$$\nu_k^{\pm} = -\frac{i(3+2k)}{R} \pm \frac{n}{r_\chi}; \qquad k,n \in \mathbb{Z} \tag{3.38}$$

The positions of the poles have the same imaginary part as before, with non zero real part indicating non zero momentum along the S^1. Curiously, the single simple poles at $n = 0$ seem to 'split' into two simple poles when n is non zero. A sensible consistency check on our results is to expand our expression

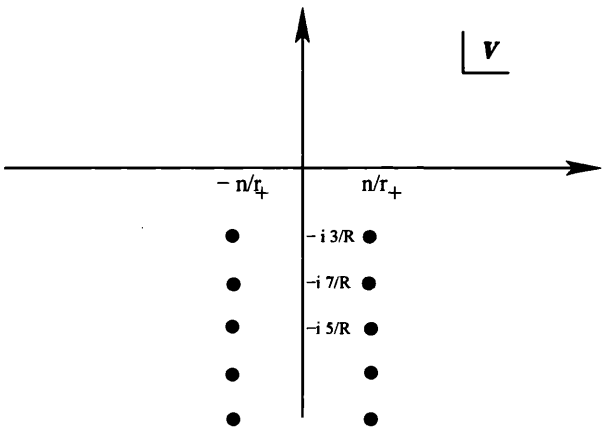

Figure 3.4: The analytic structure of the massless retarded Green's function in the complex frequency plane with non-zero momentum along the spatial circle.

for the correlator in the high frequency limit, which should reproduce the flat space result. The leading behaviour is

$$\tilde{G}_R(\nu;n)\Big|_{\nu R,n\gg 1} \to -\frac{N^2}{128\pi^2}\left(\nu^2-\frac{n^2}{r_\chi^2}\right)^2 \log\left(\nu^2-\frac{n^2}{r_\chi^2}\right) \tag{3.39}$$

which does indeed agree with the scalar glueball correlation function computed in flat space [21].

3.3.3 Thermal Effects and the Gibbons-Hawking Temperature

As remarked upon previously, de Sitter space has a cosmological horizon and therefore has an associated Gibbons-Hawking temperature [62]. With this in mind, we should see thermal properties in the correlation functions we have calculated on the boundary of the topological black hole spacetime, which is $dS_3 \times S^1$. Consider (3.37). When the frequency is real the digamma functions

have a non zero imaginary part.

$$\operatorname{Im} G_R(\nu;n)\Big|_{\nu\in\mathbb{R}} = \frac{N^2}{256\pi}\left(\left(\nu-\frac{n}{r_\chi}\right)^2+\frac{1}{R^2}\right)\left(\left(\nu+\frac{n}{r_\chi}\right)^2+\frac{1}{R^2}\right)\times \left[\coth\left(\frac{\pi R}{2}\left(\nu+\frac{n}{r_\chi}-\frac{i}{R}\right)\right)+\coth\left(\frac{\pi R}{2}\left(\nu+\frac{n}{r_\chi}-\frac{i}{R}\right)\right)\right] \tag{3.40}$$

We have used the relation $\tanh(x) = \coth(x+i\frac{\pi}{2})$ to write the result in a form that will be the most familiar in the context of thermal physics. In flat space for a free field theory at finite temperature the scalar glueball correlator with spatial momentum set to zero and frequency ω is proportional to [90]

$$\tilde{G}_R^{\text{Flat space}}(\omega) = -\frac{N^2}{2\pi^2}\omega^4\psi\left(-\frac{i\omega}{4\pi T}\right) + \text{analytic} \tag{3.41}$$

The spectral function is the imaginary part of the retarded glueball correlator and it is

$$\operatorname{Im}\tilde{G}_R^{\text{Flat space}}(\omega) = -\frac{N^2}{2\pi^2}\omega^4\pi\coth\left(\frac{\omega}{4T}\right) \tag{3.42}$$

While it is not obvious that we can define a spectral representation in de Sitter space (for a more in depth discussion on this topic, see for example [65,91,92]), there is an obvious similarity between the results we have found in de Sitter space (3.40) and the flat space result (3.42). In particular, we can identify the temperature associated with the cosmological horizon in de Sitter space

$$T_H = \frac{1}{2\pi R} \tag{3.43}$$

which is exactly the Gibbons-Hawking temperature. While we have noted the similarities between the imaginary parts of the retard Green's function in flat space and $dS_3 \times S^1$ we note there is also an important difference. The term that appears in place of the frequency or 'energy' of the flat space spectral function in de Sitter space is not the real frequency, but is in fact $\nu - \frac{i}{R}$. The difference appears because of our definition of positive and negative frequency modes in equation (3.27). Choosing modes that would lead to a

real frequency ν in the imaginary part of the retard Green's function the positive frequency modes are red shifted to zero in the far future. To get propagating modes at all times we need to choose $\nu = \omega + \frac{i}{R}$ with $\omega \in \mathbb{R}$.

The results we have computed in the strongly coupled theory for the retarded correlation function of the glueball on de Sitter space seem to match quite closely with what was found in the weakly coupled theory at one loop [93].

3.3.4 The Massive Scalar Glueball Correlator

The holographic calculation of correlation functions in the topological AdS black hole can be easily extended to massive scalars. In the context of the Type IIB theory, such massive states are stringy excitations with masses $m^2 \sim \frac{1}{\alpha'} \gg \frac{1}{R^2}$. A scalar field of mass m in the bulk is dual to a scalar operator $\mathcal{O}_\Delta$ in the field theory with dimension $\Delta = 2 + \sqrt{4 + (mR)^2}$. We will study below the free massive scalar in the bulk geometry to extract information on the analytic structure of correlators of high dimension operators in the field theory, which we have two primary motivations for doing:

1. The works of [94, 95] have demonstrated that propagators of heavy fields, in the geodesic approximation, may be used to probe the bulk geometry behind horizons and perhaps extract information on singularities behind such horizons.

2. One of our main goals is to look for signatures of the transition between a $\mathbb{Z}_N$ symmetric phase and a $\mathbb{Z}_N$ broken phase. In the bulk theory, the latter phase is the small bubble-of-nothing geometry. Correlators in this latter geometry can only be computed using an Eikonal (WKB) approximation involving high frequencies and/or large masses. One reason for this is that it is possible to obtain the the topological black hole geometry and the bubble of nothing geometry by the Wick rotation of thermal AdS and the AdS Schwarzschild black hole respectively.

Although scalar wave equation in the bubble of nothing geometry does not admit exact solutions unless we consider large masses, one can find massive

solutions in the topological black hole background for any mass. Computing the correlator in the massive case means performing the same procedure as for the two cases above, but now using massive solutions to the scalar wave equation given in (3.21). In general we find the correlator is

$$\tilde{G}_R(\nu) = \mathcal{C}_\Delta \frac{\Gamma\left(\frac{1}{2}\left(\Delta - 1 - i\nu R\right)\right)^2 \Gamma\left(3 - \Delta\right)}{\Gamma\left(\frac{1}{2}\left(3 - \Delta - i\nu R\right)\right)^2 \Gamma(\Delta - 1)} \tag{3.44}$$

where the normalization constant $\mathcal{C}_\Delta = 2(\Delta - 2)\epsilon^{2(\Delta-4)}$, with $\epsilon \to 0$ corresponding to the boundary limit. When we take the massless limit of this

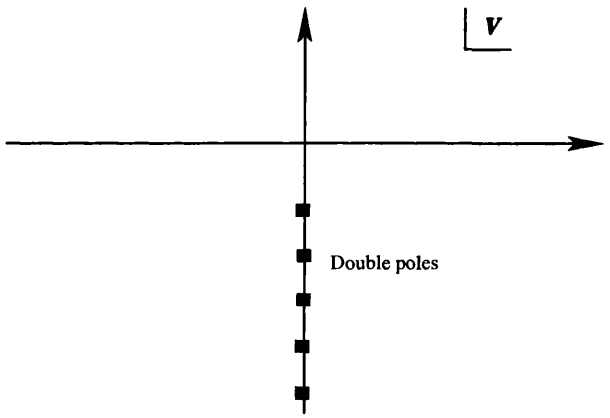

Figure 3.5: The analytic structure of the massive scalar glueball correlator. There are double poles in the lower half plane at zero spatial momentum.

expression $mR \to 0$ we recover the correlator found previously (3.35) after the subtraction of an additional divergent contact term. We note the massive correlator has a different pole structure to the massless case, having an infinite set of double poles at

$$\nu_k = -\frac{i(\Delta - 1 + 2k)}{R}, \qquad k \in \mathbb{Z}. \tag{3.45}$$

The physical meaning of the double poles in the massive retarded correlator is not clear, however we note that double poles have appeared in correlation functions of two dimensional CFT's with non integer conformal dimension, dual to the BTZ black hole [53]. For real frequencies, the massive correlator

also has an imaginary part

$$\text{Im}\,\tilde{G}_R(\nu) = -\mathcal{C}_\Delta \frac{\pi^2}{2}\frac{\Gamma(3-\Delta)}{\Gamma(\Delta-1)}\frac{\sin(\pi\,\Delta)\,\sinh(\pi\nu R)}{\left|\Gamma\left(\frac{1}{2}(3-\Delta-i\nu R)\right)\cos\left(\frac{\pi}{2}(\Delta-i\nu R)\right)\right|^4} \tag{3.46}$$

The thermal origin of this result is not as explicit as it was for the massless scalar. Consider eliminating R in favour of the de Sitter temperature using $T = \frac{1}{2\pi R}$. We have

$$\text{Im}\,\tilde{G}_R(\nu) = -\mathcal{C}_\Delta \frac{\pi^2}{2}\frac{\Gamma(3-\Delta)}{\Gamma(\Delta-1)}\frac{\sin(\pi\Delta)\sinh\left(\frac{\nu}{2T}\right)}{\left|\Gamma\left(\frac{1}{2}\left(3-\Delta-\frac{i\nu}{2\pi T}\right)\right)\cos\left(\frac{1}{2}\pi\left(\Delta-\frac{i\nu}{2\pi T}\right)\right)\right|^4} \tag{3.47}$$

This expression is similar to the equivalent one found for the BTZ black hole. For zero spatial momentum and frequency ω it was found (equation (4.24) of [53]) and it is

$$\text{Im}\,\tilde{G}_R(\omega) \sim -\frac{2\epsilon^{\Delta-2}}{\pi L\Gamma(\Delta-1)^2}\sinh\left(\frac{\omega}{2T}\right)\left|\Gamma\left(\frac{\Delta}{2}-\frac{i\omega}{4\pi T}\right)\right|^4 \tag{3.48}$$

In this expression L is the radius of curvature of the bulk space, T is the temperature, Δ is the dimension of the operator and is greater than 1 and the $\epsilon \to 0$ limit is when the boundary is approached. We will not discuss the BTZ black hole any further, and we only note the similarities between (3.47) and (3.48).

We will not do this explicitly, but we expect turning on a finite momentum around the S^1 to cause the set of double poles to split into simple poles $\frac{2n}{r_x}$ apart, as was the case for the massless correlation function.

Since we are interested in comparing this correlation function with the similar object computed in the bubble of nothing background that can only be found in the large mass and frequency (WKB) approximation, we should look at (3.44) for large mass. Consider $mR \gg 1$ so that $\Delta \approx mR$. In this high frequency, large mass limit it is useful to work with a rescaled frequency;

$$\tilde{\nu} \equiv \frac{\nu}{M}, \qquad \nu R,\ mR \gg 1 \tag{3.49}$$

hence

$$G_R(\tilde{\nu}) \sim \mathcal{C}_\Delta \left(\frac{1-i\tilde{\nu}}{2}\right)^{mR(1-i\tilde{\nu})} \left(-\frac{1+i\tilde{\nu}}{2}\right)^{mR(1+i\tilde{\nu})} \tag{3.50}$$

In the above expression we have omitted an overall phase due to frequency independent coefficients in the large mass limit. Clearly the first term in the expression for the large mass and frequency correlation function causes a branch point at $\tilde{\nu} = i$, which is problematic since this is a nonanalyticity in the upper half plane and we are computing the retarded correlator. Recall the exact correlator (3.44) had no such upper half plane nonanalyticity so this feature must be a result of the approximations we have used. A more careful investigation of the problematic branch cut originating at $\tilde{\nu} = i$ reveals the discontinuity across it is zero in the large mass limit. The origin of the spurious branch cut in the exact correlator is a set of zeroes in the upper half plane that appear to merge together in the high frequency limit. The second branch cut in the lower half plane starting at $\tilde{\nu} = -i$ results from the apparent coalescing of the infinite set of poles in the high frequency limit and therefore is a genuine nonanalyticity. So far we have shown that two

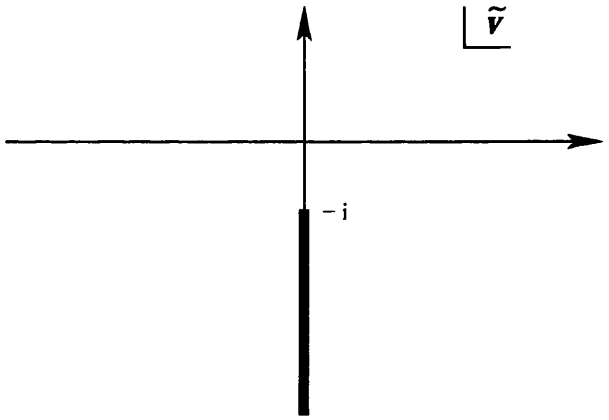

Figure 3.6: The massive scalar correlator in the large mass and frequency limit. There is a branch cut resulting from the apparent merging together of the infinite set of poles shown in figure

point correlation functions for the phase dual to the topological black hole only have nonanalyticities where the imaginary part is strictly less than zero,

i.e. there are no nonanalyticities on the real axis. In the following sections we will compute the two point correlation functions for the R-current in the topological black hole phase and for the scalar glueball in the bubble of nothing phase in the WKB approximation and compare with those found here.

3.3.5 R-current correlation functions

Real time response to perturbations of a conserved charge density can reveal interesting late time physics, such as hydrodynamic or diffusive relaxation. It is now well understood and established [56,86] via holographic calculations in AdS black hole backgrounds, that correlators of conserved global currents exhibit hydrodynamic and diffusion poles. R-charge diffusion in the strongly coupled, high temperature $\mathcal{N} = 4$ plasma was first discovered in [86]. The universal features of strongly coupled plasmas follow from the properties of the stretched horizon of AdS black holes [56]. It is therefore natural to ask whether the horizon in the topological AdS black hole geometry implies hydrodynamic behaviour of correlation functions in the dual field theory. The answer to this question will depend on the relevant time scales involved since the boundary field theory is formulated on an expanding background, namely $dS_3 \times S^1$.

The strong coupling correlators for $SO(6)$ R-currents of $\mathcal{N} = 4$ supersymmetric Yang-Mills theory on $dS_3 \times S^1$ will be obtained holographically from the on-shell action for the $SO(6)_R$ gauge fields in the topological AdS_5 black hole background, by following the prescription of [86]. The Maxwell action for the gauge field is

$$S = -\frac{1}{4g_{SG}^2}\int d^5x\sqrt{-g}g^{\mu\alpha}g^{\nu\beta}F_{\mu\nu}F_{\alpha\beta}, \tag{3.51}$$

varying which gives the following equations of motion

$$\frac{1}{\sqrt{-g}}\partial_\nu\left(\sqrt{-g}g^{\mu\alpha}g^{\nu\beta}F_{\alpha\beta}\right) = 0. \tag{3.52}$$

Here, we have labelled $g_{\rm SG}^2 = \frac{16\pi^2 R}{N^2}$. We find it convenient to use the following form for the metric in the region exterior to the horizon,

$$ds^2 = \frac{R^2}{4z^2(1-z)}dz^2 + \frac{R^2(1-z)}{z}\left[-d\tau^2 + \cosh^2\tau\, d\Omega_2^2\right] + \frac{r_\chi^2}{z}\, d\chi^2. \quad (3.53)$$

Substituting the solution to the equation of motion that corresponds to the boundary value $A_\alpha(z)\big|_{z=0} = A_\alpha^0$ back into the gauge field action will yield a generating functional for the R-charge correlators of the field theory.

Since the field theory lives on the $dS_3 \times S^1$ boundary with spatial $S^2 \times S^1$ spatial slices, it is natural to consider the late time behaviour of long-wavelength fluctuations in the following two cases:

1. The R-charge perturbation is inhomogeneous on the S^1, but homogeneous on the spatial section of dS_3,
2. The fluctuation is homogeneous on the circle, but inhomogeneous on the S^2.

Inhomogeneous perturbation on the S^1

In the first case, we will assume, for simplicity that the R-charge perturbation carries no momentum around the S^2. Furthermore, we use gauge freedom to set the radial component of the gauge potential $A_z = 0$. Hence, from the symmetries of the configuration, there are two remaining bulk gauge fields that are non zero:

$$A_\tau = A_\tau(z,\tau,\chi), \qquad A_\chi = A_\chi(z,\tau,\chi) \quad (3.54)$$

Since the χ-direction is a spatial circle, the two components of the vector potential, A_τ and A_χ, can be conveniently expanded in Fourier modes on the circle. The time dependence can also be re-expressed in terms of a mode expansion. There is a subtlety involved in this however. For A_χ, which is a scalar in dS_3, the mode decomposition is straightforward

$$A_\chi(z,\tau,\chi) = \sum_n \frac{e^{in\chi}}{2\pi}\int_{-\infty}^{\infty}\frac{d\nu}{2\pi}\mathcal{T}_\chi(\nu,\tau)\,\mathcal{G}_n(\nu,z) \quad (3.55)$$

where $n \in \mathbb{Z}$. On the other hand A_τ has its complete time dependence captured by normal modes of two kinds – normalizable and delta-function normalizable. In fact, below we show that there is a single normalizable mode and a continuum of delta-function normalizable states obtained as solutions to a Schrödinger problem. Anticipating this we write

$$A_\tau(z,\tau,\chi) = \sum_n \frac{e^{in\chi}}{2\pi}\left(\int_{-\infty}^{\infty}\frac{d\nu}{2\pi}\,\mathcal{T}_\tau(\nu,\tau)\,\mathcal{F}_n(\nu,z) + \mathcal{T}_\tau^{\mathrm{N}}(\tau)\,\mathcal{F}_n^{\mathrm{N}}(z)\right) \tag{3.56}$$

where $\mathcal{T}_\tau(\nu,\tau)$ and $\mathcal{T}_\tau^{\mathrm{N}}(\tau)$ will be the delta-normalizable and normalizable modes respectively. The mode functions $\mathcal{T}_{\chi,\tau}$ are solutions to

$$\begin{aligned}
&\frac{d}{d\tau}\left(\cosh^{-2}\tau\,\frac{d}{d\tau}\left(\cosh^2\tau\,\mathcal{T}_\tau(\nu,\tau)\right)\right) = -(\nu^2+1)\,\mathcal{T}_\tau(\nu,\tau)\\
&\frac{1}{\cosh^2\tau}\frac{d}{d\tau}\left(\cosh^2\tau\,\mathcal{T}_\tau\right) = -i(\nu+i)\mathcal{T}_\chi
\end{aligned} \tag{3.57}$$

The first of these can be put in the form of a Schrödinger equation, by defining $\mathcal{T}_\tau = \frac{\tilde{\mathcal{T}}}{\cosh\tau}$,

$$-\frac{d^2}{d\tau^2}\tilde{\mathcal{T}} - \frac{2}{\cosh^2\tau}\tilde{\mathcal{T}} = \nu^2\,\tilde{\mathcal{T}} \tag{3.58}$$

It is solved by the associated Legendre function $P_1^{-i\nu}(\tanh\tau)$. For $\nu^2 \geq 0$, there is a continuous infinity of delta-function normalizable states, which yield

$$\mathcal{T}_\tau(\nu,\tau) = \frac{e^{-i\nu\tau}}{\cosh\tau}\left(\frac{\nu - i\tanh\tau}{\nu - i}\right), \qquad \mathcal{T}_\chi(\nu,\tau) = \frac{e^{-i\nu\tau}}{\cosh\tau}, \qquad \nu^2 \geq 0 \tag{3.59}$$

The Schrödinger potential above also has bound states for $\nu^2 < 0$. In fact there is precisely one normalizable bound state with $\nu^2 = -1$, corresponding to the solution

$$\mathcal{T}_\tau^{\mathrm{N}}(\tau) = \frac{1}{\sqrt{2}}\frac{1}{\cosh^2\tau} \tag{3.60}$$

This solution can be directly obtained by evaluating $P_1^{-i\nu}(\tanh\tau)$ at $\nu^2 = -1$ (and appropriately normalized) or can be systematically inferred from the Maxwell equations. The continuum modes for A_χ and A_τ are orthonormal

with respect to the inner product

$$\langle \mathcal{T}_a, \mathcal{T}_a \rangle \equiv \int_{-\infty}^{\infty} d\tau \cosh^2 \tau \; \mathcal{T}_a(\nu,\tau)\mathcal{T}_a(\nu',\tau) = 2\pi\,\delta(\nu+\nu'), \tag{3.61}$$

for $a \in \{\chi, \tau\}$, while the bound state is normalized so that

$$\int_{-\infty}^{\infty} d\tau \; \cosh^2 \tau \; \left(\mathcal{T}_\tau^{\mathrm{N}}\right)^2 = 1 \tag{3.62}$$

In the far future the continuum modes are both given by $\mathcal{T}_a \sim e^{-i\nu\tau}e^{-2\tau}$. Upon analytically continuing to the complex ν plane, for $\nu = i + \omega$, with $\omega \in \mathbb{R}$, they are propagating (purely oscillatory) excitations with frequency ω in the far future. On the other hand the (normalizable) bound state decays exponentially in the far past and future and being real does not contribute to the flux at the horizon of the topological black hole.

Using these modes to eliminate the τ dependence we find three equations that depend only on $\mathcal{F}_n(\nu, z)$ and $\mathcal{G}_n(\nu, z)$:

$$-\frac{1}{R^2}(\nu+i)\,\mathcal{F}_n' + \frac{n(1-z)}{r_\chi^2}\mathcal{G}_n' = 0 \tag{3.63}$$

$$\frac{1}{R^2}\frac{d}{dz}\left((1-z)\mathcal{F}_n'\right) + \frac{n}{r_\chi^2}(\nu-i)\,\mathcal{G}_n - \frac{n^2}{r_\chi^2}\mathcal{F}_n = 0 \tag{3.64}$$

$$4z\frac{d}{dz}\left((1-z)^2\mathcal{G}_n'\right) - n(\nu+i)\mathcal{F}_n + (\nu^2+1)\mathcal{G}_n = 0 \tag{3.65}$$

Here, prime denotes a derivative with respect to z. The radial or z-dependence of the bound state solution, $\mathcal{F}^{\mathrm{N}}(z)$ is found by analytically continuing the profile for generic ν to $\nu = \pm i$. Note that there are three equations for two unknowns so to ensure a non-trivial solution any two equations must imply the third and it is straightforward to check that this is indeed the case. We can then use these equations of motion to derive two independent ones, each

containing only one of the unknown functions:

$$4z(1-z)\mathcal{F}_n''' - 4(3z-1)\mathcal{F}_n'' - 4\mathcal{F}_n' = \left[\bar{n}^2 - \frac{\nu^2+1}{1-z}\right]\mathcal{F}_n' \tag{3.66}$$

$$4z(1-z)\mathcal{G}_n''' - 4(5z-1)\mathcal{G}_n'' - \frac{8(1-2z)}{1-z}\mathcal{G}_n' = \left[\bar{n}^2 - \frac{(\nu^2+1)}{1-z}\right]\mathcal{G}_n' \tag{3.67}$$

where we have used the definition of $\bar{n}$ we made previously (3.19). These equations are immediately solved in terms of hypergeometric functions. Singling out the solutions that satisfy the purely infalling wave boundary condition at the horizon, we find the induced boundary action for the Maxwell fields (see appendix A.1 for details). The R-current correlators can be read off from the finite and non-analytic pieces of this boundary action (6.8), (6.12). We will denote the Fourier harmonics of the R-current along the spatial circle as

$$j_n^\mu(\tau) = \int_0^{2\pi} d\chi\, e^{-in\chi}\, j^\mu(\chi,\tau) \tag{3.68}$$

where we have already restricted attention to the s-wave sector on the spatial two-sphere. For perturbations with non-vanishing momentum along the spatial circle, we define the retarded, real time, Green's functions as

$$G^{\mu\nu}(\tau,\tau';n) = \langle [\, j_n^\mu(\tau),\, j_{-n}^\nu(\tau')]\rangle\, \Theta(\tau-\tau')\,, \qquad \mu,\nu \in \{\chi,\tau\} \tag{3.69}$$

The conserved global currents are in one-to-one correspondence with the boundary values of the 5-d gauge fields. Functionally differentiating the induced boundary action (6.12) with respect to the boundary values of the

gauge fields, we find

$$G^{\tau\tau}(\tau,\tau';n) = \cosh^2\tau\cosh^2\tau'\times$$
$$n^2\left[\int_{-\infty}^{\infty}\frac{d\nu}{2\pi}\mathcal{T}_\tau(\nu,\tau)\mathcal{T}_\tau(-\nu,\tau')\Xi(\nu,n)+\mathcal{T}_\tau^{\mathrm{N}}(\tau)\mathcal{T}_\tau^{\mathrm{N}}(\tau')\Xi(i,n)\right], \tag{3.70}$$

$$G^{\chi\chi}(\tau,\tau';n) = \cosh^2\tau\cosh^2\tau'\int_{-\infty}^{\infty}\frac{d\nu}{2\pi}\mathcal{T}_\chi(\nu,\tau)\mathcal{T}_\chi(-\nu,\tau')\left(\nu^2+1\right)\Xi(\nu,n), \tag{3.71}$$

$$G^{\tau\chi}(\tau,\tau';n) = G^{\chi\tau\,*}(\tau,\tau';n) =$$
$$\cosh^2\tau\cosh^2\tau' n\int_{-\infty}^{\infty}\frac{d\nu}{2\pi}\mathcal{T}_\tau(\nu,\tau)\mathcal{T}_\chi(-\nu,\tau')\left(\nu-i\right)\Xi(\nu,n), \tag{3.72}$$

$$\Xi(\nu,n) = \frac{N^2R}{32\pi^2 r_\chi}\left[\psi\left(\frac{1}{2}+\frac{i}{2}(\bar{n}-\nu)\right)+\psi\left(\frac{1}{2}-\frac{i}{2}(\bar{n}+\nu)\right)\right] \tag{3.73}$$

It is easily established that the above expressions are indeed retarded Green's functions and are non-vanishing only when $\tau > \tau'$. Two essential features ensure that this is the case: The function $\Xi(\nu,n)$ appearing universally in the ν-integrals has only simple poles in the lower half complex plane at

$$\nu = -i(2k+1)\pm\bar{n}\,, \qquad k\in\mathbb{Z} \tag{3.74}$$

There is a second source of non-analyticities in the ν-plane. This lies in the ν-dependent normalization of the mode functions $\mathcal{T}_\tau(\nu,\tau)$ (3.59). The potentially worrisome aspect of this is the appearance of a pole in the upper half plane at $\nu = +i$, which gives a non-vanishing contribution for $\tau < \tau'$. However, the potential problem is eliminated by the term dependent on the discrete, normalizable mode $\mathcal{T}_\tau^N$ in (3.70) which exactly cancels against the contributions from the poles at $\nu = +i$, ensuring that our Green's function is causal. The remaining Green's functions are manifestly free of singularities in the upper half plane.

We thus see that the Son-Starinets recipe for determining real time response functions works in the case of the topological black hole, provided we carefully account for the contributions from both the continuum and discrete

mode functions in dS_3.

It is also clear in the above expressions, that there are no diffusion poles. Instead, from the properties of the digamma function which we have encountered before, the frequency space Green's function which is effectively $\Xi(\nu, n)$, has only simple poles in the complex ν-plane, the lowest of these being at

$$\nu = -i \pm \bar{n} \tag{3.75}$$

Excitations with complex $\nu = \omega - i$, and $\omega \in \mathbb{R}$ will propagate at late times, the perturbations simply evolving as left- and right-moving excitations on the S^1 without dissipating.

The absence of any diffusion or transport like behaviour may be intuitively explained by noticing the similarity of the topological AdS black hole to the BTZ black hole. Setting up an excitation with momentum only on the S^1 is equivalent to saying the variation of the fields along the S^2 is zero. Therefore, aside from the time dependent factors associated to the de Sitter expansion, the metric that is "seen" by the bulk fields is not the full five dimensional metric, but its effective $2+1$ dimensional portion,

$$ds^2 = -R^2(\rho^2 - 1)d\tau^2 + \frac{R^2}{\rho^2 - 1}d\rho^2 + \rho^2 r_\chi^2 d\chi^2 \tag{3.76}$$

Comparing this with the metric for a $2+1$ dimensional BTZ black hole with zero angular momentum

$$ds^2 = -\left(\frac{r^2}{R^2} - M\right)dt^2 + \left(\frac{r^2}{R^2} - M\right)^{-1} dr^2 + r^2 d\phi^2, \tag{3.77}$$

we note the obvious similarity. Therefore we expect the behaviour of fields in the topological black hole background with an inhomogeneous excitation around the S^1, to be similar to the behaviour of the fields in a BTZ black hole background. In other words, they should behave as in a (1+1)-dimensional CFT [53], just as we see from our results above.

Inhomogeneous perturbation on the S^2

We will now examine the real time response to fluctuations carrying momentum along the spatial sections of three dimensional de Sitter space. Each spatial section of dS_3 is a two-sphere which undergoes exponential expansion at late times. For this case, we will focus on a situation where an inhomogeneous R-charge perturbation is set up on the two-sphere with only a dependence on the polar angle θ and time τ. For this configuration, the dual bulk gauge fields are

$$A_\tau = A_\tau(z,\tau,\theta)\,, \qquad A_\theta = A_\theta(z,\tau,\theta)\,, \qquad A_z = A_\chi = 0 \tag{3.78}$$

where A_z is set to zero by the gauge freedom, and A_χ vanishes due to χ-independence of the configuration. By spherical symmetry, the scalar potential A_τ and the vector potential A_θ, each can be expanded in terms of scalar and vector spherical harmonics, respectively

$$A_\tau = \sum_{\ell=0}^{\infty} \mathcal{F}_\ell(z,\tau)\, Y_\ell^0(\theta), \qquad A_\theta = \sum_{\ell=1}^{\infty} \mathcal{G}_\ell(z,\tau)\, \partial_\theta Y_\ell^0(\theta) \tag{3.79}$$

Substituting these into the bulk Maxwell equations, we find

$$4z(1-z)\partial_z\left((1-z)\partial_z\mathcal{G}_\ell\right) - \partial_\tau^2\mathcal{G}_\ell + \partial_\tau\mathcal{F}_\ell = 0 \tag{3.80}$$

$$4z(1-z)\partial_z\left((1-z)\partial_z\mathcal{F}_\ell\right) - \frac{\ell(\ell+1)}{\cosh^2\tau}\left(\mathcal{F}_\ell - \partial_\tau\mathcal{G}_\ell\right) = 0, \tag{3.81}$$

$$\partial_\tau\left(\cosh^2\tau\,\partial_z\mathcal{F}_\ell\right) + \ell(\ell+1)\partial_z\mathcal{G}_\ell = 0. \tag{3.82}$$

From equations (3.81) and (3.82) we obtain a differential equation for $\mathcal{F}'_\ell \equiv \partial_z\mathcal{F}_\ell$

$$4\partial_z\left(z(1-z)\partial_z\left((1-z)\mathcal{F}'_\ell\right)\right) - \frac{\ell(\ell+1)}{\cosh^2\tau}\mathcal{F}'_\ell - \frac{1}{\cosh^2\tau}\partial_\tau^2\left(\cosh^2\tau\,\mathcal{F}'_\ell\right) = 0. \tag{3.83}$$

Now we will separate out the explicit temporal dependence, keeping in mind, as before, the possibility of contributions from both discrete and continuous

modes

$$\mathcal{F}'_\ell(z,\tau) = \int_{-\infty}^{\infty} d\nu\ \mathcal{T}_\ell(\nu,\tau)\ F_\ell(\nu,z) + \sum_m \mathcal{T}^{\rm N}_{\ell m}(\tau)\, F^{\rm N}_{\ell m}(z) \tag{3.84}$$

The mode functions $\mathcal{T}_\ell$ satisfy

$$\left[-\partial_\tau^2 - \frac{\ell(\ell+1)}{\cosh^2\tau}\right]\left(\cosh^2\tau\,\mathcal{T}_\ell\right) = \nu^2\ \left(\cosh^2\tau\,\mathcal{T}_\ell\right) \tag{3.85}$$

which is a Schrödinger equation whose potential clearly will have both bound states and scattering or continuum states. The full set of solutions form an orthonormal, complete set. Indeed, the delta-normalized eigenstates are the Legendre functions

$$\mathcal{T}_\ell(\nu,\tau) = \Gamma(1+i\nu)\,\frac{P_\ell^{-i\nu}(\tanh\tau)}{\cosh^2\tau} \tag{3.86}$$

Those with $\nu^2 > 0$ are scattering states with continuous values of $\nu \in \mathbb{R}$, while the discrete, "bound states" have $-i\nu = 1, 2, \ldots \ell$,

$$\mathcal{T}^{\rm N}_{\ell m} = \sqrt{\frac{m(\ell-m)!}{(\ell+m)!}}\ \frac{P_\ell^m(\tanh\tau)}{\cosh^2\tau}\,, \qquad m = 1, 2, \ldots \ell \tag{3.87}$$

For $\nu^2 > 0$, the late time, $\tau \to \infty$, behaviour of the modes will be significant,

$$\mathcal{T}_\ell(\nu,\tau)\big|_{\tau\gg 1} \to e^{-i\nu\tau}\ e^{-2\tau} \tag{3.88}$$

as these modes are oscillatory. Applying infalling boundary conditions on these modes at the horizon of the topological AdS black hole, (3.83) yields,

$$F_\ell(\nu,z) = C_\ell(\nu)\ (1-z)^{-1-\frac{i\nu}{2}}\ {}_2F_1\left(-\frac{i\nu}{2}, 1-\frac{i\nu}{2}; 1-i\nu; 1-z\right) \tag{3.89}$$

For the discrete series, the radial profile in the bulk, $F^{\rm N}_{\ell m}(z)$ is obtained by evaluating $F_\ell(\nu,z)$ at $\nu = -im$. Putting the above ingredients together, the

general form of the electric field along the radial direction in the bulk is

$$A'_\tau(z,\tau,\theta) = \sum_{\ell=0}^{\infty} Y_\ell^0(\theta) \left(\int_{-\infty}^{\infty} \frac{d\nu}{2\pi} \Gamma(1+i\nu) \frac{P_\ell^{-i\nu}(\tanh\tau)}{\cosh^2\tau} F_\ell(\nu,z) + \right.$$
$$\left. + \sum_{m=1}^{\ell} \sqrt{\frac{m(\ell-m)!}{(\ell+m)!}} \frac{P_\ell^m(\tanh\tau)}{\cosh^2\tau} F_{\ell m}^{\mathrm{N}}(z) \right) \tag{3.90}$$

This also allows us to automatically solve for A'_θ using (3.82) and we get

$$A'_\theta(z,\tau,\theta) = -\sum_{\ell=1}^{\infty} \frac{\partial_\theta Y_\ell^0(\theta)}{\ell(\ell+1)} \left(\int_{-\infty}^{\infty} \frac{d\nu}{2\pi} \Gamma(1+i\nu)\, \partial_\tau P_\ell^{-i\nu}(\tanh\tau)\, F_\ell(\nu,z) + \right.$$
$$\left. + \sum_{m=1}^{\ell} \sqrt{m\frac{(\ell-m)!}{(\ell+m)!}}\, \partial_\tau P_\ell^m(\tanh\tau)\, F_{\ell m}^{\mathrm{N}}(z) \right) \tag{3.91}$$

Now, the bulk gauge field action can be shown to induce a boundary term which will be the generating functional for the boundary R-current correlators. Using the explicit solutions above, the induced boundary action becomes

$$S = \frac{1}{2g_{SG}^2} \int d\tau\, r_\chi \left[\sum_{\ell=0}^{\infty} \mathcal{F}_\ell(z,\tau)\, \mathcal{F}'_\ell(z,\tau) \cosh^2\tau + \right.$$
$$\left. + \sum_{\ell=1}^{\infty} \ell(\ell+1)\, \mathcal{G}_\ell(z,\tau)\, \mathcal{G}'_\ell(z,\tau) \right]_{z=\epsilon\to 0} \tag{3.92}$$

The next step is to express this completely in terms of the boundary values of the gauge potentials $\mathcal{F}_\ell^0(\tau) \equiv \mathcal{F}_\ell(\epsilon,\tau)$ and $\mathcal{G}_\ell^0(\tau) \equiv \mathcal{G}_\ell(\epsilon,\tau)$. Their radial derivatives $\mathcal{F}_\ell{}'$ and $\mathcal{G}'_\ell$ (equivalently A'_τ and A'_θ) at the boundary $z=\epsilon$, are also determined completely by the boundary values of the gauge potentials, $\mathcal{F}_\ell^0(\tau)$ and $\mathcal{G}_\ell^0(\tau)$ as in (6.19).

From the boundary action above, we thus find that the real time, retarded

Green's functions for the R-charge currents j^μ, in the gauge theory are

$$G^{\tau\tau}(\tau,\tau';\ell) = \ell(\ell+1)\left[\int_{-\infty}^{\infty}\frac{d\nu}{2\pi}\frac{\pi\nu}{\sinh\pi\nu}P_\ell^{-i\nu}(\tanh\tau)P_\ell^{i\nu}(\tanh\tau')\,\Upsilon(\nu)+\right.$$
$$\left.+\sum_{m=1}^{\ell}(-1)^m m P_\ell^m(\tanh\tau)P_\ell^{-m}(\tanh\tau')\Upsilon(im)\right], \qquad (3.93)$$

$$G^{\theta\theta}(\tau,\tau';\ell) = \ell(\ell+1)\left[\int_{-\infty}^{\infty}\frac{d\nu}{2\pi}\frac{\pi\nu}{\sinh\pi\nu}\partial_\tau P_\ell^{-i\nu}(\tanh\tau)\,\partial_{\tau'}P_\ell^{i\nu}(\tanh\tau')\Upsilon(\nu)+\right.$$
$$\left.+\sum_{m=1}^{\ell}(-1)^m m\partial_\tau P_\ell^m(\tanh\tau)\partial_{\tau'}P_\ell^{-m}(\tanh\tau')\Upsilon(im)\right], \qquad (3.94)$$

$$G^{\tau\theta}(\tau,\tau';\ell) = \ell(\ell+1)\left[\int_{-\infty}^{\infty}\frac{d\nu}{2\pi}\frac{\pi\nu}{\sinh\pi\nu}P_\ell^{-i\nu}(\tanh\tau)\partial_{\tau'}P_\ell^{i\nu}(\tanh\tau')\Upsilon(\nu)+\right.$$
$$\left.+\sum_{m=1}^{\ell}(-1)^m m P_\ell^m(\tanh\tau)\partial_{\tau'}P_\ell^{-m}(\tanh\tau')\Upsilon(im)\right], \qquad (3.95)$$

$$\Upsilon(\nu) = \frac{N^2 r_\chi}{64\pi^2 R}\left(\psi\left(-\frac{i\nu}{2}\right)-\frac{1}{i\nu}\right) \qquad (3.96)$$

We need to first confirm that these Green functions satisfy basic consistency checks. Specifically, the retarded functions must vanish for $\tau < \tau'$. As in the previous case, this property is not manifest, but follows from the nature of the non-analyticities of $\Upsilon(\nu)$, and the normalized mode functions $\Gamma(1+i\nu)P_\ell^{-i\nu}(\tanh\tau)$, in the complex ν-plane. For real values of ν, the associated Legendre function is [96]

$$\Gamma(1+i\nu)\,P_\ell^{-i\nu}(\tanh\tau) = e^{-i\nu\tau}\,{}_2F_1\left(-\ell,\,\ell+1;\,1+i\nu,\,\frac{(1-\tanh\tau)}{2}\right) \qquad (3.97)$$

For integer ℓ, the hypergeometric function is a finite polynomial in $\tanh\tau$ and a ratio of degree ℓ polynomials of ν. Therefore the exponential frequency dependence means that, for $\tau-\tau' < 0$, the integrals over the frequency ν can be evaluated by closing the contour in the upper half plane. The function $\Upsilon(\nu)$ has no poles in the upper half complex plane. It has simple poles at

$$\nu = 0,\,-2i,\,-4i\ldots \qquad (3.98)$$

The normalized modes, $\Gamma(1+i\nu)P_\ell^{-i\nu}(\tanh\tau)$ have exactly ℓ simple poles in the upper half plane at $\nu = i, 2i \ldots \ell i$. The contributions from these are, however, cancelled by the inclusion of the discrete modes in the retarded Green's function above. Hence our correlators are zero for $\tau < \tau'$.

Late time behaviour

The real time response functions in general contain important information on the long time relaxation of perturbations away from the equilibrium or ground state. In thermal field theory on flat space, the relaxation of such fluctuations of conserved charges proceeds via hydrodynamic or diffusion modes. The response functions at strong coupling then exhibit diffusion poles in frequency space, $G^{\tau\tau} \propto (i\omega - Dk^2)^{-1}$, where ω is the frequency and k, the soft spatial momentum. Due to the explicit time dependence of the background metric, we cannot do a similar frequency space study of the full Green's functions in de Sitter space. Instead, we will analyse their behaviour as functions of time.

In de Sitter space, perturbations labelled by wave number ℓ, get red-shifted so that given sufficient time their physical wavelengths become super-horizon sized. This happens when

$$\frac{\ell\, e^{-\tau}}{R} \sim \frac{1}{R} \tag{3.99}$$

At late enough times, even very high harmonics on the sphere get stretched and eventually exit the horizon. To zoom in on the time evolution of such modes, it is useful to think of $\ell e^{-\tau}$, the physical wave number, as being fixed as $\tau \to \infty$. For example, in this late time approximation we neglect terms like $\ell\, e^{-2\tau}$ in comparison to powers of $\ell\, e^{-\tau}$. This is practically equivalent to going to planar coordinates for de Sitter space and the mode functions behave as

$$P_\ell^{-i\nu}(\tanh\tau)\big|_{\ell e^{-\tau}=\text{fixed}} \to \ell^{-i\nu}\, J_{i\nu}\left(2\ell e^{-\tau}\right) \tag{3.100}$$

It is possible to derive this by replacing the potential $\ell(\ell+1)\mathrm{sech}^2\tau$ in the mode equation (3.85), with $4\,\ell^2\, e^{-2\tau}$. Note that, instead of a fixed physical

wavelength if we focus attention on fixed comoving wavenumber, given by ℓ, all modes simply approach the s-wave at late times,

$$\lim_{\tau\to\infty} \Gamma(1+i\nu)\, P_\ell^{-i\nu}(\tanh\tau)\big|_{\ell \text{ fixed}} \to e^{-i\nu\tau} \tag{3.101}$$

For fixed physical wavelengths, $\ell\, e^{-\tau}$, or equivalently, at the time when a harmonic ℓ crosses the horizon, the real time correlators are given by the exact results with the replacement (3.100). The integral over ν can be easily evaluated using the method of residues, and it turns out that the leading contribution at late times is from the residue at $\nu = 0$. Thus

$$G^{\tau\tau}(\tau,\, 0;\ell),\ \ G^{\tau\theta}(\tau,\, 0;\ell)\ \sim\ J_0(2\,\ell e^{-\tau}) \tag{3.102}$$

and

$$G^{\theta\tau}(\tau, 0;\, \ell),\ \ G^{\theta\theta}(\tau, 0;\, \ell)\ \sim\ \partial_\tau J_0(2\,\ell e^{-\tau}) \tag{3.103}$$

The late time behaviour deduced above is not characteristic of diffusion in de Sitter space. Suppose that the R-charge fluctuation relaxed via diffusion modes, then the covariant conservation of the R-current together with Fick's law would lead to the diffusion equation

$$\partial_\tau j^\tau = D\nabla_\theta\nabla^\theta j^\tau \tag{3.104}$$

in dS_3, D being the diffusion constant. The spherical harmonics of j^τ on the expanding spatial spherical sections would then obey,

$$\partial_\tau j^\tau_\ell = -D\,\frac{\ell(\ell+1)}{\cosh^2\tau}\, j^\tau_\ell \tag{3.105}$$

At late times $\tau \to \infty$ and large enough ℓ, this is solved by

$$j^\tau_\ell \sim \exp\left(\tfrac{1}{2} D\,\ell^2\, e^{-2\tau}\right) \tag{3.106}$$

The large time behaviour of the Green's functions ((3.102) and (3.103))do not match up with expected diffusive relaxation (3.106) on dS_3. A natural reason for this is that the rate of exponential expansion of the spatial section and

the Gibbons-Hawking temperature are both set by $\frac{1}{R}$. Thus the mean free path or the mean free time between collisions is comparable to the expansion time scales so that the system never enters a diffusive regime.

3.4 The AdS Bubble of Nothing

As discussed previously, the topological AdS black hole can decay via a nucleation transition to the small AdS bubble of nothing. This happens when the size of the S^1 is less than a critical value;

$$r_\chi < \frac{R}{2\sqrt{2}} \tag{3.107}$$

This instability only occurs if there are antiperiodic boundary conditions for fermions on the S^1 - if we apply periodic boundary conditions for bosons and fermions on the S^1 the topological black hole is stable and may not decay.

The decay of the false vacuum is computed by the Euclidean bounce which has the same asymptotics as the false vacuum in Euclidean signature [73]. In the present scenario, the Euclidean false vacuum is thermal AdS and the bounce solution is the small AdS Schwarzschild black hole. Suppose the decay occurs at $t = 0$ in Lorentzian signature. When this happens the $t > 0$ part of the spacetime is replaced with the correct analytic continuation of the Euclidean bounce solution. In this case, the appropriate spacetime with $dS_3 \times S^1$ boundary is the analytic continuation of the small AdS Schwarzschild solution, the small AdS bubble of nothing [71]. The metric of the bubble of nothing is

$$ds^2 = f(r) r_\chi^2 \, d\chi^2 + \frac{dr^2}{f(r)} + r^2 \left(-\frac{dt^2}{R^2} + \cosh^2\left(\frac{t}{R}\right) d\Omega_2^2 \right) \tag{3.108}$$

with

$$f(r) = 1 + \frac{r^2}{R^2} - \frac{r_h^2 (R^2 + r_h^2)}{r^2} \tag{3.109}$$

The global structure of the small AdS bubble of nothing is shown in figure.

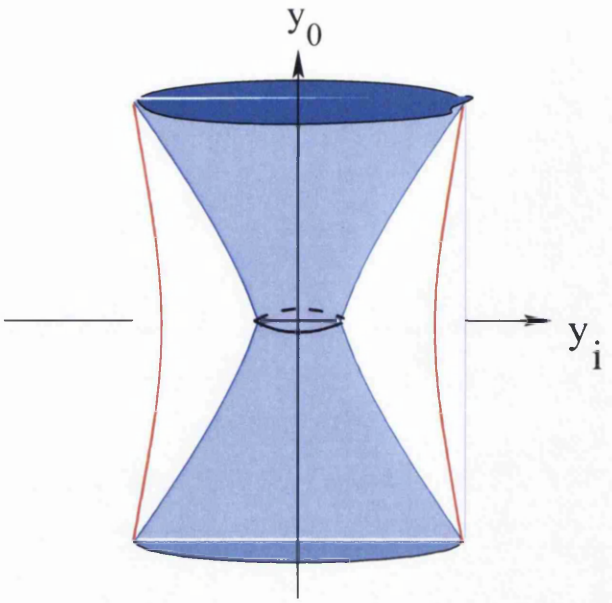

Figure 3.7: The global structure of the small AdS bubble of nothing. The shaded region is the interior of the bubble and is empty.

3.7[3] In these coordinates, supposing the bubble of nothing exists at all times, the bubble occupies the entire spacetime in the far past and is shrinks exponentially. It reaches a minimum size at $t = 0$ and then expands. In the far future it expands exponentially to eventually fill the spacetime again. To avoid a conical singularity in the interior the χ direction must be related to the parameter r_h and we find

$$2\pi r_\chi = \frac{2\pi R^2 r_h}{r_h^2 + R^2} \tag{3.110}$$

Rewriting using the dimensionless coordinates introduced earlier (3.9) the metric becomes

$$ds^2 = R^2 \left[\tilde{f}(\rho) \frac{r_\chi^2}{R^2} d\chi^2 + \frac{\rho^2}{\rho^2 - 1} \frac{d\rho^2}{\tilde{f}(\rho)} + (\rho^2 - 1)(-d\tau^2 + \cosh^2 \tau d\Omega_2^2) \right] \tag{3.111}$$

[3]The y coordinates in figure 3.7 are Kruskal like coordinates similar to those used previously for the topological black hole. For a more detailed exposition on the bubble of nothing see [70]

with

$$\tilde{f}(\rho) = \rho^2 - \frac{\tilde{r}_h^2\,(\tilde{r}_h^2+1)}{\rho^2-1} \tag{3.112}$$

At each slice of constant ρ the geometry is $dS_3 \times S^1$. However, the S^1 shrinks smoothly to zero size at $\rho = \sqrt{\tilde{r}_h^2+1}$ since this circle is exactly the cigar of the Euclidean AdS Schwarzschild black hole. Taking $\rho \to \infty$ corresponds to the boundary limit. Supposing the topological black hole decays to a bubble of nothing at $\tau = 0$ then a bubble appears suddenly, and occupies the space with $\rho^2 \leq 1 + \tilde{r}_h^2$.

3.4.1 WKB for the AdS Bubble of Nothing

Since one may view the AdS bubble of nothing as the analytic continuation of the AdS Schwarzschild black hole it follows that an exact solution of the equations of motion will not be possible. In the light of this we will find the correlation function in this background using the WKB approximation. This approach has been used successfully in studying the correlation functions dual to the AdS Schwarzschild black hole [95].

Consider the scalar wave equation (3.10) in the bubble of nothing background. It is natural to expand the solution to the wave equation in harmonics on $dS_3 \times S^1$ as we did in (3.11). The radial component the satisfies the following equation

$$\frac{d^2\Phi_n}{dx^2} + \left(\frac{1}{x-1} + \frac{1}{x+\tilde{r}_h^2} + \frac{1}{\tilde{r}_h^2-1}\right)\frac{d\Phi_n}{dx} + 4\,(x-1)\,(x+\tilde{r}_h^2)\,(x-\tilde{r}_h^2-1)\times$$
$$\times\left(\nu^2+1-\bar{n}^2\frac{(x-1)^2}{(x+\tilde{r}_h^2)(x-\tilde{r}_h^2-1)} - m^2R^2(x-1)\right)\Phi_n = 0 \tag{3.113}$$

where $x = \rho^2$ and $\bar{n}$ labels the momentum along the S^1 and is defined in equation (3.19). Analytic solutions to this equation are not known although a similar equation was studied in [97] whose goal was to find the mass spectrum of glueballs in the three dimensional effective theory obtained from Euclidean thermal $\mathcal{N} = 4$ super Yang-Mills at strong coupling on $\mathbb{R}^3 \times S^1$ with supersymmetry breaking boundary conditions.

We will use the WKB approximation to find solutions to this equation,

and it is convenient to write it in the form of a Schrödinger equation using the following variables

$$\Phi = \frac{\Psi}{\sqrt{\rho\left(\rho^2-1\right)}}$$
$$u = \frac{\tilde{r}_h}{1+2\tilde{r}_h^2}\cot^{-1}\left(\frac{\rho}{\tilde{r}_h}\right) + \frac{\sqrt{1+\tilde{r}_h^2}}{1+2\tilde{r}_h^2}\coth^{-1}\left(\frac{\rho}{\sqrt{1+\tilde{r}_h^2}}\right) \tag{3.114}$$

These coordinates naturally generalise those used in (3.15) and (3.16) to the bubble of nothing background. The cigar in the geometry smoothly goes to zero size at $\rho = \sqrt{\tilde{r}_h^2+1}$ but in terms of the new coordinates (3.114) this happens when $u \to \infty$. The equation of motion for $\Psi_n(\nu, u)$ is given by

$$\frac{d^2\Psi_n}{du^2} + \tilde{V}_n(\nu,u)\,\Psi_n(\nu,u) = 0 \tag{3.115}$$
$$\tilde{V}_n(\nu,u) = \left((mR)^2 - \frac{\nu^2+1}{\rho^2-1}\right)\left(\rho^2 - 1 - \frac{\tilde{r}_h^2}{\rho^2}\left(\tilde{r}_h^2+1\right)\right) + \\ + \frac{\bar{n}^2\left(\rho^2-1\right)}{\rho^2}\left(15\rho^4 - 10\rho^2 - 1\right) \tag{3.116}$$

Note that ρ is a function of u, which one can obtain by inverting (3.114). The important difference between the Schrödinger potential for the topological black hole and the current one given in (3.116) is the fact that, in addition to being more complicated, it is not possible to write the potential in a way that is independent of the frequency ν. This situation is also in contrast to that of the AdS Schwarzschild black hole studied in [95]. With this in mind, we will attempt to find the zero energy eigenstate of the Schrodinger equation (3.115) for a given mass and frequency. We note that the qualitative behaviour of the potential changes depending on the relative values of the mass and frequency. We show examples of this in figure 3.8. We will set $\bar{n}$ to zero for simplicity and take the high frequency and mass limit.

$$\nu \to \infty, \quad mR \to \infty, \quad \tilde{\nu} = \frac{\nu}{mR} \text{ fixed} \tag{3.117}$$

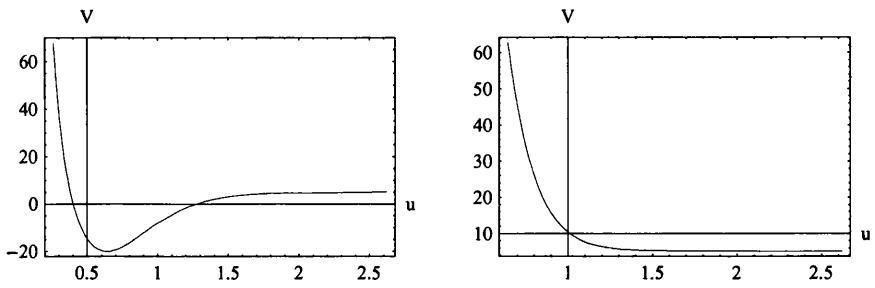

Figure 3.8: Schrödinger potentials for the massive scalar in the bubble of nothing geometry. In both plots $\nu = 7$ and $\tilde{r}_h = 1$. On the left we have the case when the mass $mR = 2$. On the right we have $mR = 7$.

When we do this the leading behaviour of the potential is

$$\tilde{V}_0(\nu, u) \to \mathcal{V}(\tilde{\nu}, u) = (mR)^2 \left(1 - \frac{\tilde{\nu}^2}{\rho^2 - 1}\right)\left(\rho^2 - 1 - \frac{r_h^2}{\rho^2}(\tilde{r}_h^2 + 1)\right) \quad (3.118)$$

The two pairs of brackets in (3.118) leads to two zeroes of the potential. There is one at $\rho = \sqrt{\tilde{r}_h^2 + 1}$ which is the tip of the cigar. Close to this point, $u \sim -\log(\rho - \sqrt{\tilde{r}_h^2 + 1})$ and it follows that $\mathcal{V}(\tilde{\nu}, u)$ decays exponentially as a function of u. The second is where $\rho = \sqrt{\tilde{\nu}^2 + 1}$. Since the spacetime ends at $\rho = \sqrt{1 + \tilde{r}_h^2}$, whether the second zero of the potential actually contributes depends on whether $|\tilde{\nu}|$ is greater than or less than $\tilde{r}_h$. In fact when $|\tilde{\nu}| > \tilde{r}_h$ the potential has two zeroes and the qualitative behaviour is that of the left diagram of figure 3.8. On the other hand, if $|\tilde{\nu}| < \tilde{r}_h$ then the only zero is when the radial coordinate approaches the tip of the cigar, as shown in the right diagram of figure 3.8.(the potential asymptotes to a constant different from zero in the figures; however this constant becomes negligible in the high frequency limit).

WKB approximation for $\tilde{\nu}^2 > \tilde{r}_h^2$

There are two distinct regions in the potential. The first is where the solution behaves like a quantum mechanical tunnelling solution which we label region I, and it covers the region $\sqrt{1 + \tilde{\nu}^2} < \rho < \infty$. The second is where the solution resembles a free particle wavefunction and covers the region

$\sqrt{1+\tilde{r}_h^2} < \rho < \sqrt{1+\tilde{\nu}^2}$ which we call region II. In region I, we write the WKB solutions as

$$\Psi_{\rm WKB}(\tilde{\nu},u) = \frac{1}{\mathcal{V}^{1/4}}\left(A_+ \exp\left(\int_{u_c}^{u}\sqrt{\mathcal{V}}du\right) + A_- \exp\left(-\int_{u_c}^{u}\sqrt{\mathcal{V}}du\right)\right) \tag{3.119}$$

where the classical turning point u_c is defined by

$$\rho(u_c) \equiv \sqrt{\tilde{\nu}^2+1} \tag{3.120}$$

These represent the growing and decaying modes in the near boundary region of the bulk geometry. This can be understood easily as follows.

$$\left.\frac{du}{d\rho}\right|_{\rho\to\infty} \approx -\frac{1}{\rho^2} \Rightarrow \mathcal{V} \approx (mR)^2\,\rho^2 \tag{3.121}$$

from which we can find the near boundary WKB solution (3.119) for Ψ. Along with the relation between (3.114) and the massive scalar field Φ implies

$$\Phi_{\rm WKB}\big|_{\rho\to\infty} \sim \mathcal{A}_1 A_+ \rho^{-2-mR} + \mathcal{A}_2 A_- \rho^{-2+mR} \tag{3.122}$$

$\mathcal{A}_1$ and $\mathcal{A}_2$ are normalisation constants. The two terms in (3.122) are the non normalisable and the normalisable modes of the massive scalar field. The prescription for computing retarded correlation functions requires that we normalise $\Psi_{\rm WKB}$ so that it is 1 at the boundary. In the interior for $\rho \le \sqrt{1+\tilde{\nu}^2}$ the solution enters region II and becomes oscillatory. In region II we have

$$\Psi_{\rm WKB}(\tilde{\nu},u) = \frac{1}{|\mathcal{V}|^{\frac{1}{4}}}\left(B_+ \exp\left(i\int_{u_c}^{u}\sqrt{|\mathcal{V}|}d\rho\right) + B_- \exp\left(-i\int_{u_c}^{u}\sqrt{|\mathcal{V}|}du\right)\right) \tag{3.123}$$

The constants are determined by the WKB matching conditions at the classical turning points of the potential and the normalisation condition on A_- near the boundary. The WKB matching procedure is explained in appendix A.3. The most important result of the matching procedure is that the solu-

tion near the boundary region has a normalisable mode with strength

$$A_+ = -\frac{1}{2}A_- \tan\left(\int_\infty^{u_c} \sqrt{|\mathcal{V}(\tilde{\nu},u)|}du\right) \tag{3.124}$$

The argument in the above expression can, as usual, be identified with the action of a zero energy classical particle trapped in the potential $\mathcal{V}(\tilde{\nu},u)$ between the two turning points u_c and $u \to \infty$ (the latter corresponding to $\rho \to \sqrt{1+\tilde{r}_h^2}$ where the spacetime ends).

It is important to note the difference between the prescriptions being used to compute the correlation functions in the topological black hole geometry and the bubble of nothing geometry. The real time prescription for computing retarded correlation functions in the topological black hole geometry required us to specify infalling wave boundary conditions at the horizon, but in the bubble of nothing the spacetime ends smoothly so we have no freedom to choose what boundary conditions we apply there. Our only choice is to require regularity of the solutions in the interior, which means we must have a solution to the Schrödinger equation (3.115) that approaches a constant exponentially as $u \to \infty$. The correlation function at high frequency is

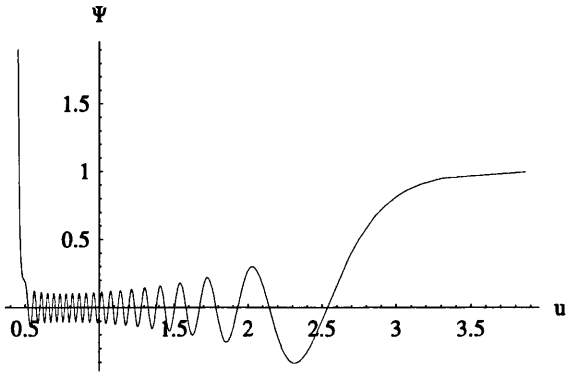

Figure 3.9: The numerical solution to the Schrödinger problem for the AdS bubble of nothing. Here $\nu R = 200$, $mR = 100$ and $\frac{r_h}{R} = 1$. The solution approaches a constant for $u \gg 1$, while the classically forbidden region is $0 < u < u_c \approx 0.49$.

determined (up to contact terms) by the ratio $\frac{A_+}{A_-}$. After substituting the

solution (3.122) into the boundary action we find;

$$\tilde{G}_R(\tilde{\nu}) \approx \lim_{\epsilon\to 0} mR \exp\left(2\int_{u_c}^{\epsilon}\sqrt{\mathcal{V}(\tilde{\nu},u)}du\right)\tan\left(\int_{\infty}^{u_c}\sqrt{|\mathcal{V}(\tilde{\nu},u)|}du\right) \quad (3.125)$$

The exponential prefactor in this expression is the WKB transmission coefficient into the classically forbidden Region I. The physically relevant contribution to the transmission coefficient is the constant, ϵ-independent term in an expansion around the boundary $\epsilon \to 0$. The leading ϵ dependence, which is an overall multiplicative constant proportional to ϵ^{2mR}, can be absorbed into the normalization of the correlation function.

The first observation we can make without actually evaluating (3.125), is that it has an infinite set of poles as a function of $\tilde{\nu}$ on the real axis for $\tilde{\nu}^2 > r_h^2$. These occur whenever

$$\mathcal{S}_{II}(\tilde{\nu}, mR) = \int_{\infty}^{u_c} du\sqrt{|\mathcal{V}(\tilde{\nu},u)|} = (n+\frac{1}{2})\pi, \quad n \in \mathbb{Z} \quad (3.126)$$

That is, the semiclassical action in the propagating region is a half-integral multiple of π. We note that this is the condition for the existence of a bound state wave function, and the poles in the Green's function reflect the appearance of these bound states at certain values of $\tilde{\nu}$ on the real axis. Recall that the corresponding correlators in the topological black hole phase do not have any poles on the real axis, and the only nonanalyticities that appear in the correlation function are the poles in the lower half plane that represent the quasinormal frequencies of the topological black hole.

The poles on the real axis may appear surprising, however they have a natural physical interpretation. The low energy physics of the gauge theory on the boundary of the spacetime is that of $\mathcal{N} = 4$ super Yang-Mills with supersymmetry completely broken on dS_3. Supersymmetry is broken by the antiperiodic boundary conditions for fermions on the S^1 and therefore the fermionic excitations are all massive and there are large radiative corrections to the scalar masses. In the three dimensional effective theory the dynamical scale is expected to be set by the size of the S^1, $\frac{1}{r_\chi}$. When the Gibbons-Hawking temperature $T_H = \frac{1}{2\pi R}$ in dS_3 is smaller than $\frac{1}{r_\chi}$ the gauge theory

is expected to be in the confined phase where the fundamental degrees of freedom are glueballs. The appearance of poles on the real axis in the high frequency retarded correlator is consistent with this physical argument.

The WKB integral in Region II, in the high frequency approximation to the Green's function (3.125) can be expressed in terms of complete elliptic integrals as

$$\mathcal{S}_{II}(\tilde{\nu}, mR) = \frac{mR}{2}\int_{\tilde{\nu}^2+1}^{\tilde{r}_h^2+1} dx \frac{\sqrt{\frac{\tilde{\nu}^2}{x-1}-1}}{\sqrt{(x+\tilde{r}_h^2)(x-\tilde{r}_h^2-1)}} = i\frac{mR}{\sqrt{1+2\tilde{r}_h^2}}\times$$
$$\times\left[|\tilde{\nu}|\left(K\left(\frac{a}{b}\right)-\sqrt{\frac{b}{a}}K\left(\frac{b}{a}\right)\right)+\frac{(1+\tilde{r}_h^2)}{|\tilde{\nu}|}\left(\Pi\left(a\middle|\frac{a}{b}\right)-\sqrt{\frac{b}{a}}\Pi\left(b\middle|\frac{b}{a}\right)\right)\right]$$
$$a=\frac{\tilde{\nu}^2+1+\tilde{r}_h^2}{\tilde{\nu}^2}, \qquad b=\frac{1+2\tilde{r}_h^2}{\tilde{r}_h^2}, \qquad \tilde{\nu}^2>r_h^2 \tag{3.127}$$

From the general characteristics of these elliptic functions and their singularities [98], it can be checked that $\mathcal{S}_{II}(\tilde{\nu}, mR)$ has no singularities on the real axis for $\tilde{\nu}^2 < \tilde{r}_h^2$. Potential logarithmic branch points at $\tilde{\nu}^2 = \tilde{r}_h^2$ and at $\tilde{\nu} = 0$, cancel out between the individual terms above. In fact, for any fixed value of $\tilde{r}_h$, it also follows that, for large $\tilde{\nu}$, the WKB integral increases linearly with $\tilde{\nu}$.

$$\mathcal{S}_{II} \propto |\tilde{\nu}|, \qquad |\tilde{\nu}| \gg 1 \tag{3.128}$$

Hence for $|\tilde{\nu}| \gg \tilde{r}_h$, the propagator (3.125) has approximately equally spaced simple poles on the real axis, whenever $\mathcal{S}_{II} = \left(n+\frac{1}{2}\right)\pi$. Although there are no other sources of singularities from S_{II}, the WKB transmission coefficient in Region I, which also enters the Green's function (3.125) can have branch point singularities on the real axis,

$$\mathcal{S}_I(\tilde{\nu},\, mR) = -\frac{1}{2}mR\int_{1+\tilde{\nu}^2}^{\frac{1}{\epsilon^2}} dx \frac{\sqrt{1-\frac{\tilde{\nu}^2}{x-1}}}{\sqrt{(x+\tilde{r}_h^2)(x-\tilde{r}_h^2-1)}} \tag{3.129}$$

$$= -\frac{mR}{\sqrt{1+2\tilde{r}_h^2}}\left(|\tilde{\nu}|\left(F\left(\csc^{-1}\sqrt{a},\frac{a}{b}\right)-K\left(\frac{a}{b}\right)\right)-\frac{1}{|\tilde{\nu}|}\left(1+\tilde{r}_h^2\right)\Pi\left(a\middle|\frac{a}{b}\right)\right)$$

$$-\frac{mR}{2}\left(\log\left(\frac{2}{\epsilon^2|\tilde{\nu}|\sqrt{1+\tilde{r}_h^2}}\right)+i\pi\right) \tag{3.130}$$

This function is also free of any branch cuts at $\tilde{\nu} = \pm\tilde{r}_h$, as can be checked by directly evaluating the integral at this point. However, the logarithmic growth at large $\tilde{\nu}$ implies a branch point at infinity.

WKB approximation for $\tilde{\nu}^2 < \tilde{r}_h^2$

For low (real) frequencies $\tilde{\nu}^2 < \tilde{r}_h^2$, the nature of the WKB potential changes (The right graph of figure 3.8). Bound states are no longer possible. The zero energy WKB solution is

$$\Psi_{\text{WKB}}(\tilde{\nu},u) = A_+\frac{1}{\mathcal{V}^{\frac{1}{4}}}\exp\left(\int_\infty^u\sqrt{\mathcal{V}}du\right)+A_-\frac{1}{\mathcal{V}^{\frac{1}{4}}}\exp\left(-\int_\infty^u\sqrt{\mathcal{V}}du\right) \tag{3.131}$$

The relation between the two coefficients is determined by matching to the wavefunction at large u, where the potential decays exponentially and the wavefunction is a modified Bessel function (see Appendix A.4). We find that

$$A_+ = iA_- \tag{3.132}$$

The asymptotics of this solution near the boundary at $u = \epsilon$ (6.47) allows to compute the boundary action and the Green's function

$$\tilde{G}_R(\tilde{\nu}) \approx \lim_{\epsilon\to 0} imR\exp(\mathcal{S}_I) = imR\exp\left(2\int_\infty^\epsilon\sqrt{\mathcal{V}(\tilde{\nu},u)}du\right) \tag{3.133}$$

In terms of elliptic functions the explicit form for the WKB action is

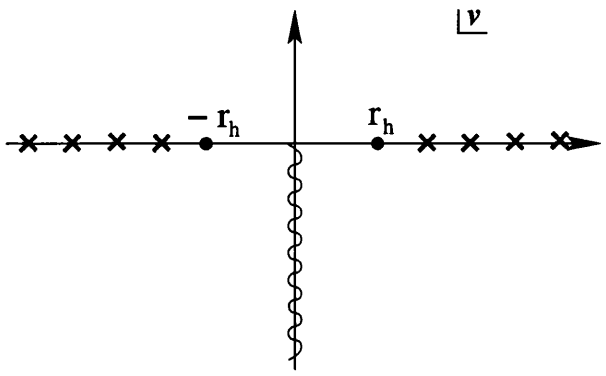

Figure 3.10: The analytic structure of the boundary Green's function in the bubble of nothing phase in the WKB approximation $\nu \to \infty$, $mR \to \infty$ with $\tilde{\nu} = \frac{\nu}{mR}$ fixed. Approximately equally spaced simple poles on the real axis for $\tilde{\nu}^2 > \tilde{r}_h^2$, are accompanied by branch points at $\tilde{\nu} = 0$ and infinity.

$$\mathcal{S}_I = -\frac{mR}{\sqrt{1+2\tilde{r}_h^2}}\left[|\tilde{\nu}|\left(F\left(\csc^{-1}\sqrt{a},\frac{a}{b}\right)-\sqrt{\frac{b}{a}}K\left(\frac{b}{a}\right)\right)+\right.$$
$$\left.-\frac{1}{|\tilde{\nu}|}(1+\tilde{r}_h^2)\sqrt{\frac{b}{a}}\Pi\left(a\middle|\frac{b}{a}\right)\right]-\frac{mR}{2}\left(\log\left(\frac{2}{\epsilon^2|\tilde{\nu}|\sqrt{1+\tilde{r}_h^2}}\right)+i\pi\right) \tag{3.134}$$

and the only singularity of this expression is the branch point singularity at $\tilde{\nu} = 0$ which complements the singularity at $\tilde{\nu} = \infty$ found above.

The analytic structure of the retarded correlation function is shown in figure 3.10. This can be compared with the correlation found for the topological black hole in the high mass and frequency limit, figure 3.6. It should be pointed out that taking the high frequency limit has the effect of making the inverse frequency very much smaller than the de Sitter radius, and therefore the space is effectively very close to flat. Therefore the singularities of the retarded correlation functions may be interpreted in the same way as one would for a flat space correlation function. A feature of the correlator whose origin is not completely clear is the branch point at $\tilde{\nu} = 0$. The branch point at $\tilde{\nu} = -i$ that appears on the high mass and frequency correlator for the topological black hole phase arose as a result of the quasinormal poles appearing to merge. Whether the branch cuts of the bubble of nothing

correlation function (3.134) come from a similar source is as yet unknown.

3.5 Discussion

In this chapter we studied strongly coupled $\mathcal{N} = 4$ supersymmetric Yang-Mills theory on $dS_3 \times S^1$. Specifically, we computed the two point correlation functions of the scalar glueball operator and the R-charge current operator in the $\mathbb{Z}_N$ invariant phase, dual to the topological black hole geometry in the bulk. The retarded scalar glueball correlator has an infinite set of poles in the lower half plane representing the quasinormal modes of the topological black hole, and the imaginary parts of the retarded correlation function are associated with the Gibbons-Hawking temperature due to the cosmological horizon on the boundary. These facts about the correlation functions suggest the $\mathbb{Z}_N$ symmetric phase of the of the boundary field theory corresponds to a deconfined plasma in an exponentially expanding universe.

We also computed the retarded correlation functions for the spatial spherical harmonics of the conserved R-charge currents using the prescription of Son and Starinets. Here we encountered a subtlety, the solution of which was to include the effect of real, normalisable discrete solutions to the temporal mode equations. The resulting correlator also has an infinite set of poles in the lower half plane, but does not seem to have any diffusion poles. The lack of hydrodynamic behaviour is a result of the rate of expansion of the de Sitter universe being of the same order as the Gibbons-Hawking temperature. Furthermore, we calculated the retarded correlation functions of the scalar operators $\mathcal{O}_\Delta$, with dimension $\Delta \gg 1$ in both the $\mathbb{Z}_N$ invariant phase and $\mathbb{Z}_N$ broken phase dual to the topological black hole and the bubble of nothing in the bulk respectively. The correlators in the $\mathbb{Z}_N$ broken phase feature an infinite number of poles on the real frequency axis, in contrast to the $\mathbb{Z}_N$ invariant phase where there are no poles on the real axis. These poles are naturally associated to bound glueball like states which suggests that this phase is a hadronized phase, where the de Sitter temperature is low. Since this geometry contains no horizon the Son-Starinets prescription [53] is not applicable in this phase and we have restricted ourselves to the high

frequency and large mass regime by using WKB approximation.

It would be interesting to understand how to compute the full generating functional of theory in Lorentzian signature so three point and higher correlation functions could be found. This work has shown that, since infinity is connected in the topological black hole and the AdS bubble of nothing geometries, it is unclear how to apply the prescription of Son and Herzog [58] to obtain the generating functional. The avenue with the most potential seems to be using the work of Skenderis and van Rees [59] to compute the generating functional. As yet, this has not been done.

In the time since this work was published there have been efforts to build upon it by other research groups, in particular there has been some interesting work that attempts to model the early universe holographically. See for example [89, 99–103]

Chapter 4

Holographic Roberge-Weiss Transitions

4.1 Introductory Remarks

Understanding how a particular theory behaves when one turns on a chemical potential for the various conserved charges in it is one of the most basic steps that must be taken in truly understanding the theory. Since the discovery of the AdS/CFT correspondence and the many similar dualities that are known, much progress has been made in understanding how chemical potentials affect the phases of these models [26, 27, 47, 104–120]. In this section we will take a slightly different approach in that we will explore the behaviour of three holographic theories in the presence of an *imaginary* chemical potential, following the work of Roberge and Weiss [121] from 1986. The primary motivation for the exploration of thermodynamics in the presence of imaginary chemical potentials comes from QCD. As is well known, the phase structure of QCD at nonzero temperature and quark chemical potential is difficult to determine. When the chemical potential or the temperature is sufficiently large perturbation theory is adequate to describe the theory, however a significant portion of the phase diagram requires a nonperturbative study, and much effort has gone into using lattice gauge theory to study such a theory. However at non zero chemical potential a straightforward application of

lattice QCD runs into problems since the fermion determinant is complex. As such algorithms based on importance sampling can no longer be applied resulting in the infamous sign problem. Various approaches to circumvent the sign problem in QCD at finite density have been developed over the past decade, and a review can be found in [122].

The sign problem is due to the nonhermiticity of the Dirac operator. Let $\not{D}$ denote the massless Dirac operator, satisfying $\gamma_5 \not{D} \gamma_5 = \not{D}^\dagger$. Integrating out the fermion fields then yields the determinant $\det M(\mu) = \det(\not{D} + m + \mu\gamma_0)$. Using γ_5-hermiticity it immediately follows that this determinant is complex,

$$[\det M(\mu)]^* = \det M(-\mu^*), \tag{4.1}$$

unless the chemical potential vanishes or is purely imaginary. This last observation suggests that lattice QCD simulations at imaginary chemical potential $\mu = i\mu_I$ can be performed using standard algorithms. Information about the phase structure at real chemical potential can then be obtained by analytic continuation. Since the partition function is an even function of μ, computations can be performed for imaginary μ ($\mu^2 < 0$) and then analytically continued to real μ ($\mu^2 > 0$). This approach has indeed been used extensively [123–132].

In this section we will compute the phase diagrams in the (μ_I, T) plane of three holographic theories with such an imaginary chemical potential. Firstly we will describe $SU(N)$ $\mathcal{N} = 4$ super Yang-Mills theory coupled to fundamental matter using the D3-D7 setup at strong coupling [46, 133] and the same theory where the flavours are confined to a codimension k defect of the boundary, using a D3 - D$(7-2k)$ set up as studied in [134]. We will also perform a similar calculation for and the Sakai-Sugimoto model [33], which was described in section 2.4.

4.2 General Remarks

4.2.1 Roberge - Weiss Transitions

It is well understood that, in the Euclidean formulation, the phases of a pure $SU(N)$ gauge theory at finite temperature can be distinguished by the expectation value of the Polyakov loop $\langle W \rangle$. At low temperatures the theory is in the confined phase which implies the expectation value of the phase of the Polyakov loop vanishes. This further implies there is a $\mathbb{Z}_N$ symmetry where the Polyakov loop transforms as $W \to e^{\frac{2\pi i r}{N}} W$ with r an integer. For high temperatures this symmetry is spontaneously broken and hence $\langle W \rangle \neq 0$ so the theory becomes deconfined. When one introduces fundamental matter into the theory the $\mathbb{Z}_N$ symmetry is never a symmetry of the theory, however a remnant of the $\mathbb{Z}_N$ symmetry is still present. Introducing an imaginary chemical potential makes this explicit and resolves the ambiguity between confined and deconfined phases of the theory. Consider the partition function for such a theory,

$$Z\left[\mu_I\right] = \mathrm{Tr}\left(e^{-\beta H + i\beta\mu_I N_q}\right) \tag{4.2}$$

N_q is the quark number operator and μ_I is the imaginary chemical potential[1] for quark number. One can see this partition function has a symmetry under the transformation $\mu_I \to \mu_I + \frac{2\pi}{\beta}$ where β is the inverse temperature of the system. Together with the fact that N_q is quantised, this implies $\beta\mu_I \in [-\pi, \pi]$.

The adjoint sector also contains a $\mathbb{Z}_N$ symmetry which introduces a further periodicity into the theory. The imaginary chemical potential couples to fundamental matter in the same way as the time component of an $SU(N)$ gauge field. Hence, the time component of the gauge covariant derivative which acts on matter fields in the fundamental representation associated to this gauge field is modified by the presence of this chemical potential in the following way,

$$\partial_\tau + iA_\tau \to \partial_\tau + iA_\tau - i\mu_I \tag{4.3}$$

[1]Note that we have made the replacement $\mu \to i\mu_I$ so μ_I on it's own is in fact real.

We can remove the dependence of the action on μ_I by rescaling the fields so that the dependence on μ_I is in the boundary conditions around the thermal circle

$$\phi(\vec{x}, \beta) \sim e^{i\mu_I \beta} \phi(\vec{x}, 0) \tag{4.4}$$

where the fermionic and bosonic modes differ by a sign. We may now apply an $SU(N)$ gauge transformation with the group element $U(\vec{x}, \tau)$ with the property that $U(\vec{x}, \beta) = e^{\frac{2\pi i r}{N}} U(\vec{x}, 0)$ and r an integer. The action and path integral measure are left invariant but the boundary conditions around the thermal circle are not, hence

$$\phi(\vec{x}, \beta) \sim e^{i\left(\mu_I \beta + \frac{2\pi r}{N}\right)} \phi(\vec{x}, 0) \tag{4.5}$$

The partition function must be invariant under these transformations, therefore

$$Z[\mu_I] = Z\left[\mu_I + \frac{2\pi r}{\beta N}\right] \tag{4.6}$$

which further implies $\beta\mu_I \in \left[-\frac{\pi}{N}, \frac{\pi}{N}\right]$.

The free energy $F[\mu_I] = -T \log[Z]$ of QCD in perturbation theory, valid at high temperature, was first computed in [121] who found first order phase transitions at constant values of μ_I. These values are

$$\mu_{\mathrm{RW}} = \frac{(2r-1)\pi T}{N_c} \tag{4.7}$$

At low temperatures where the theory is strongly coupled lattice studies suggest $F[\mu_I]$ is smooth as a function of the chemical potential.

4.2.2 Roberge - Weiss transitions at weak coupling

At suitably high temperatures when the gauge theory is in a deconfined phase it is generically possible to compute the effective potential as a function of μ_I perturbatively. In this section we state the important results from weak coupling, but for a full analysis see [121, 135, 136]. The basic idea involves computing an effective potential for the eigenvalues of the the Polyakov loop matrix, $\exp(i \oint A_\tau)$ in the presence of fundamental matter. The effective

potential at one-loop is the sum of a gluonic (adjoint matter) piece that is $\mathbb{Z}_N$ invariant and independent of μ_I, and a flavour (fundamental matter) piece that is not $\mathbb{Z}_N$ invariant and explicitly depends on the imaginary chemical potential.

$$V_{\text{eff}}\left(\{\alpha_i\}\right) = V_A\left(\{\alpha_i\}\right) + V_f\left(\left\{\alpha_i - \frac{\mu_I}{T}\right\}\right) \tag{4.8}$$

Here $e^{i\alpha_j}$, $j = 1, 2, \ldots N$ are the eigenvalues of the Polyakov loop matrix. Generically, at high temperatures, in the absence of fields in the fundamental representation of $SU(N)$, V_A will have N minima, each of which breaks the $\mathbb{Z}_N$ symmetry spontaneously. At these minima $\alpha_i = \frac{2\pi k}{N}$ for $k = 0, 1, 2, \ldots N-1$. Introduction of fundamental matter raises the degeneracy and the minima become local minima with a single global minimum at $\alpha_i = 0$ for vanishing μ_I. Since V_f depends only on the combination $(\alpha_i - \frac{\mu_I}{T})$, the global minimum will move to $\alpha_i = \frac{2\pi r}{N}$ when $\frac{\mu_I}{T} = \frac{2\pi r}{N}$ $(r \in \mathbb{Z})$. We conclude that the different local minima of the effective potential compete as μ_I is varied and there are first order phase transitions between two neighbouring minima whenever $\frac{\mu_I}{T} = \frac{(2r-1)\pi}{N}$ $(r \in \mathbb{Z})$. It has been shown [137] that the perturbative result for the free energy across the Roberge-Weiss transitions is given by

$$F\left[\mu_I\right] = N\frac{T^4}{12}\left(2n_f + \tilde{n}_f\right)\min_{r\in\mathbb{Z}}\left(\frac{2\pi r}{N} - \frac{\mu_I}{T}\right)^2 \tag{4.9}$$

In this equation the gauge group is $SU(N)$ where N is taken to be large. There are n_f massless scalars and $\tilde{n}_f$ massless Weyl fermions in the fundamental representation of $SU(N)$. The free energy is a function with cusps (see figure 4.1) located at odd integer multiples of $\frac{\pi}{N}$.

We note here that at weak coupling only the ratio $\frac{m_q}{T}$ is relevant. Typically however, nonperturbative physics will generate another scale (such as Λ_{QCD} in QCD). In that case the notion of high and low temperatures and masses has an independent meaning and the weak coupling result can be trusted when $T \gg \Lambda_{\text{QCD}}$. In the models we study here, the 't Hooft coupling $\lambda = g_{YM}^2 N$ can be dialled to any fixed value (assuming the number of flavours is small compared to N), and there is no dynamical scale. This means that the ratio $\frac{m_q}{T}$ is the only parameter which can be varied at fixed 't Hooft

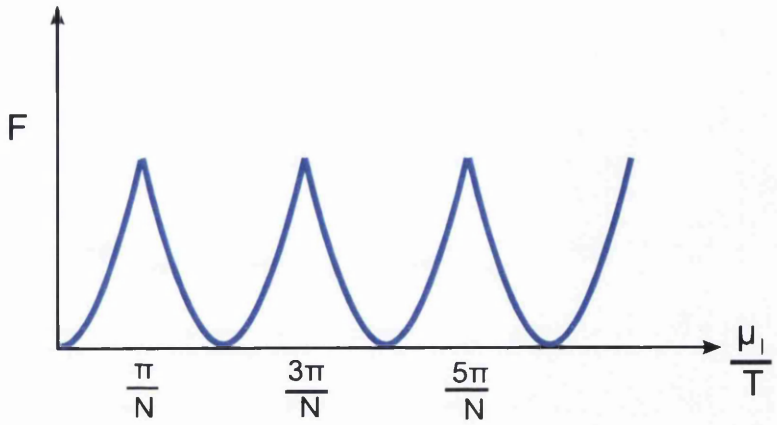

Figure 4.1: The generic behaviour of the free energy across Roberge-Weiss transitions.

coupling and we expect the perturbative analysis to be valid for $\lambda \ll 1$. For large λ, perturbation theory is clearly not valid and we must use the dual gravity picture.

4.2.3 $\mathbb{Z}_N$ breaking in thermal holographic theories

In this section we will consider the effective potential for type IIB supergravity as a function of an imaginary chemical potential. We will see that the periodicity that was found at weak coupling arises quite naturally in the gravity dual to the strongly coupled theory as well. As argued in [40] one may understand the spontaneous breaking of the $\mathbb{Z}_N$ center symmetry at high temperatures as follows . We first note that the disk D_2 in the black hole geometry naturally allows turning on a Neveu-Schwarz potential B with $dB = 0$ and

$$\alpha \equiv \frac{1}{2\pi l_s^2} \int_{D_2} B \tag{4.10}$$

This yields a phase $e^{i\alpha}$ for the Polyakov-Maldacena loop[2] [138,139] computed by wrapping a fundamental string worldsheet on the cigar D_2. Thus α is defined modulo 2π. One then finds that an effective potential for α is induced if we consider terms in the type IIB effective action that depend on the RR 3-form $F_{(3)}$,

$$S_{\rm IIB} \supset \frac{1}{(2\pi)^7 l_s^8}\left(\int d^{10}x\,\sqrt{g}\,\frac{1}{12}F_{(3)}^2 - \int F_{(5)}\wedge F_{(3)}\wedge B\right) \tag{4.11}$$

Integrating over $S^5 \times D_2$, we may obtain the effective theory for the $F_{(3)}$ field on $\mathbb{R}^3$. Since $F_{(3)}$ has only one non zero component F_{123} on $\mathbb{R}^3$ we have

$$S_{\rm eff}[F_{(3)}] = \int d^3x\,\left[\frac{\lambda}{T^3}\frac{1}{2^8\pi^6\,l_s^4}\,(F_{123})^2 - \frac{N\alpha}{4\pi^2 l_s^2}F_{123}\right] \tag{4.12}$$

where we have used the fact that the type IIB background has N units of five-form flux through S^5, $\int_{S^5}\frac{F_5}{(2\pi l_s)^4} = N$. Adapting the arguments arising in the context of $U(1)$ gauge theory in two dimensions to the present situation [40], gauge invariance of quantum states implies the quantization of F_{123}. States are characterized by a constant (quantized) value for the field strength (similarly to constant electric fields in two dimensions) and one finally finds the effective potential for the phase of Polyakov-Maldacena loop to be

$$V_A(\alpha) = 4\pi^2 N^2 T^4\,\frac{1}{\lambda}\min_{r\in\mathbb{Z}}\left(\alpha - \frac{2\pi}{N}r\right)^2 \tag{4.13}$$

The potential is minimized when $\alpha = \frac{2\pi r}{N}$ for $r \in \mathbb{Z}$ and this leads to a spontaneous breaking of the $\mathbb{Z}_N$ symmetry of the $\mathcal{N}=4$ theory in the deconfined, high temperature phase. Note that this effective potential is $\mathcal{O}(N^2)$, as expected for a leading order large-N effect and proportional to T^4, as expected from dimensional analysis. Interestingly, it is also proportional to $\frac{1}{\lambda}$ in the

[2]Strictly speaking, the Wilson loop computed by the wrapped string world-sheet is the supersymmetric version of the standard Polyakov loop and includes the adjoint scalar fields of $\mathcal{N}=4$ SYM in its definition, $\mathcal{U} \equiv \exp i\oint(A_\tau - i\theta^I(\tau)\Phi^I)$. This is an important distinction in principle, but will not influence our discussion below, as the Polyakov-Maldacena loop has the same transformation properties under $\mathbb{Z}_N$ transformations as the standard Polyakov loop order parameter.

strongly coupled theory. We have presented the argument for type IIB supergravity but it is readily generalisable to type IIA, so that the same periodic structure that appears in $\mathcal{N} = 4$ super Yang-Mills will also be present in the Sakai-Sugimoto model. This was done in [120]. The action for type IIA contains the following terms

$$S_{\text{IIA}} \supset \frac{1}{(2\pi)^7 l_s^8}\left(\int d^{10}x\sqrt{g}F_{(4)}^2 - \int F_{(4)} \wedge F_{(4)} \wedge B\right) \tag{4.14}$$

Since the gauge theory is five dimensional, we will find the effective theory for F_{1234} in the four spatial directions. After integrating out the S^4 and the D_2 containing the radial and Euclidean time direction the effective action is

$$S_{\text{eff}}\left[F_{1234}\right] = \int d^3x d\chi \left(\frac{3g_s N}{2^9\pi^6 l_s^5 T^3}\left(F_{1234}\right)^2 - \frac{\alpha N}{(2\pi l_s)^3}F_{1234}\right) \tag{4.15}$$

Similarly to the type IIB case, the factor of N comes from integrating the $F_{(4)}$ over the S^4, and the α is a result of integrating the NS B field over the thermal cigar. As before, the potential is minimised when

$$\alpha = \frac{2\pi r}{N}, \qquad r \in \mathbb{Z} \tag{4.16}$$

4.2.4 The effect of flavours

Now we would like to calculate how the effective potential for α is modified upon introducing fundamental flavours and in the presence of an imaginary chemical potential for quark number. The basic effect of introducing flavour D7-branes was already addressed in [120] and was argued to lift the degeneracy of the N vacua discussed above. The overall dynamics of N_f flavour D7-branes, ignoring the non-Abelian world-volume degrees of freedom in the probe limit ($N_f \ll N$), can be described by the (Euclidean) Dirac-Born-Infeld action

$$S_{Dp} = N_f T_{Dp} \int d^{p+1}\xi e^{-\Phi}\sqrt{\det(\gamma_{ab} + (2\pi\alpha' F_{ab} + B_{ab}))} \tag{4.17}$$

where γ_{ab} and B_{ab} are the pullbacks of the spacetime metric and the Neveu-Schwarz two-form potential on to the brane worldvolume. In addition we have that the dilaton $e^{-\Phi} = 1$ in the background dual to the $\mathcal{N} = 4$ supersymmetric gauge theory. The D7-brane tension can be written in terms of gauge theory parameters λ, N (and R, the AdS radius) as

$$T_{D7} = \frac{1}{g_s \alpha'^4 (2\pi)^7} = \frac{\lambda N}{32\pi^6 R^8} \tag{4.18}$$

In the case of the D3-D7 system, we will take the D7-brane probe to wrap the S^3 in the S^5 at an angle θ and fill the entire AdS_5 space. When we consider defect theories with a codimension k intersection the brane will cover S^{3-k} in the S^5 and $3-k$ spatial directions on the boundary, in addition to the radial and time directions. In the Sakai-Sugimoto model the D8 and $\overline{\text{D8}}$ branes cover all of the directions in the bulk except for the compact fifth dimension on the boundary that we label x_4. For the most part, we will primarily be interested in classical configurations that completely wrap D_2, the cigar in the Euclidean black hole, corresponding to "melted meson" states [116,140]. For these configurations it will be consistent to turn on a field strength F_{ab} along the world-volume.

4.2.5 Imaginary chemical potential

In the boundary field theory formulated on Minkowski space, a chemical potential for a global $U(1)$ symmetry can be thought of as follows: We imagine that the global symmetry is gauged and then turn on a constant background value for the time component of the gauge field, while setting other components to zero. $A_t(\rho)$ is the t component of a $U(1)$ gauge field and ρ is a radial coordinate. The gauge field strength is $F = F_{\mu\nu} dx^\mu \wedge dx^\nu$ and the only non zero component is $F_{tr} dr \wedge dt$. When we work in Euclidean signature the gauge field must be completely real in order that the chemical potential is purely imaginary since when we Wick rotate the time direction the field strength becomes $iF_{\tau r} dr \wedge d\tau$.

The gauge field associated to the overall $U(1)$ factor describing the center-

of-mass dynamics of the probe D7-branes, is dual to $U(1)_B$. In the Euclidean theory, the imaginary chemical potential μ_I corresponds to a constant real boundary value for the gauge field A_τ on the world-volume of the D7-brane,

$$\mu_I = -T \int_0^\beta d\tau \int_{r_H}^\infty d\rho \, F_{\tau\rho} = \lim_{\rho\to\infty} A_\tau(\rho) \tag{4.19}$$

Here we choose by gauge freedom to set $A_\rho = 0$ and we require that $A_\tau(r_H) = 0$ in order to avoid a singularity at the tip of the cigar. We are implicitly assuming that the D7 brane wraps the black hole cigar D_2 completely. The case where it turns back before getting to the horizon will be discussed separately.

4.2.6 Periodicity in μ_I

The periodicity in μ_I discussed earlier is naturally built into the supergravity dual because the D-brane action only depends on the combination $B+2\pi\alpha' F$. This means that the classical solutions to the DBI equations of motion will be characterized by the combination

$$\alpha - \frac{\mu_I}{T} = \int_{D_2} \left(F + \frac{B}{2\pi\alpha'} \right) \tag{4.20}$$

A shift of μ_I by $2\pi T$ can be absorbed by $\alpha \to \alpha + 2\pi$. Hence μ_I is only defined modulo $2\pi T$ as expected from general considerations.

As at weak coupling, there is a further periodicity visible in the finite temperature theory at strong coupling. The shift $\mu_I \to \mu_I + \frac{2\pi T}{N}$ can be compensated by a corresponding shift of α by the same amount, leaving the physics unchanged since the "glue" sector of the theory (i.e. the fields in the adjoint sector, dual to the N D3 or D4 branes in the type IIB models and Sakai-Sugimoto model respectively) is invariant under such shifts of α (from Eq.(4.13)). Note that this "periodicity" involves a jump from one $\mathbb{Z}_N$ vacuum to another. Therefore, this system should be expected to display the infinite sequence of Roberge-Weiss transitions as the effective potential will be a sum of two pieces, one of which is $\mathbb{Z}_N$ invariant, while the other piece, induced by the fundamental flavours, depends only on the combination

$\alpha - \frac{\mu_I}{T}$.

4.3 $\mathcal{N} = 4$ super Yang-Mills coupled to $\mathcal{N} = 2$ fundamental matter

When the gauge theory is at finite temperature and is in the deconfined phase, the corresponding geometry is the Schwarzschild black hole in $AdS_5 \times S^5$ (with flat horizon). Wick rotating to Euclidean signature, the spacetime metric is

$$ds^2 = \left(f(r) d\tau^2 + \frac{dr^2}{f(r)} + \frac{r^2}{R^2} d\vec{x}^2 + R^2 \, d\Omega_5^2 \right) \tag{4.21}$$

where

$$f(r) = \frac{1}{R^2} \left(r^2 - \frac{r_H^4}{r^2} \right), \quad r_H = \pi T R^2, \quad R^4 = 4\pi (g_s N) \alpha'^2 = g_{YM}^2 N \, \alpha'^2 \tag{4.22}$$

and R is the AdS radius. In the Euclidean picture the geometry ends smoothly at $r = r_H$, provided we make the periodic thermal identification $\tau \simeq \tau + \frac{1}{T}$. Topologically, the Euclidean black hole spacetime is $\mathbb{R}^3 \times D_2 \times S^5$.

The flavour D7-branes must wrap an $S^3 \subset S^5$ while filling the AdS_5 directions [46, 111, 133]. The embedding of the D7-brane is characterized by the "slipping angle" which determines the size of the three-sphere wrapped by the D7-brane. The slipping angle θ is defined by the following parametrization of the S^5 metric

$$d\Omega_5^2 = d\theta^2 + \sin^2\theta \, d\phi^2 + \cos^2\theta \, d\Omega_3^2, \qquad 0 \leq \theta \leq \frac{\pi}{2} \tag{4.23}$$

It is more convenient to rewrite the background metric in a Fefferman-Graham type coordinate system [141, 142]. We use the conventions of [140],

to write the black hole metric in the form

$$ds^2 = \frac{1}{2}\frac{\rho^2}{R^2}\left(\frac{h^2}{\tilde{h}}\,d\tau^2 + \tilde{h}\,d\vec{x}^2\right) + \frac{R^2}{\rho^2}\,(d\rho^2 + \rho^2\,d\Omega_5^2) \qquad (4.24)$$
$$h(\rho) \equiv 1 - \frac{r_H^4}{\rho^4}\,, \qquad \tilde{h}(\rho) \equiv 1 + \frac{r_H^4}{\rho^4}$$

This form of the metric is obtained after the coordinate change $r^2 = \frac{1}{2}\left(\rho^2 + \frac{r_H^4}{\rho^2}\right)$, and we take the metric of the five-sphere as in Eq.(4.23). The slipping angle θ will be dual to the quark mass operator Σ_m, and depend only on the radial coordinate of AdS space, as discussed in chapter 2.

$$\theta = \theta(\rho) \qquad (4.25)$$

This parametrization is convenient for making contact with the weak coupling D-brane picture. Focussing on the six directions transverse to the D3-branes, we write

$$d\rho^2 + \rho^2 d\Omega_5^2 \;=\; d\rho_2^2 + \rho_2^2\,d\phi^2 + d\rho_1^2 + \rho_1^2\,d\Omega_3^2 \qquad (4.26)$$

with

$$\rho_1 = \rho\cos\theta\,, \qquad \rho_2 = \rho\sin\theta \qquad (4.27)$$

The $x_8 - x_9$ plane can now be identified with the (ρ_2, ϕ) plane. We choose the D7-brane to be at $\phi = 0$, *i.e.* the x_8 axis. The asymptotic value of the D3-D7 separation, given by ρ_2 for large ρ, yields the hypermultiplet mass m_q.

4.3.1 Solving the DBI equations of motion

The action for the D7-brane probe configuration described above is

$$S_{D7} = 2\pi^2 N_f T_{D7} \int \beta\, d^3x \times$$
$$\times \int_{r_H}^{\infty} d\rho \frac{\rho^3}{4}\, h\,\tilde{h}\,\cos^3\theta \sqrt{1 + \rho^2\theta'(\rho)^2 + 2(2\pi\alpha' F_{\tau\rho} + B_{\tau\rho})^2 \frac{\tilde{h}}{h^2}} \qquad (4.28)$$

We note that if we set the B field to zero and Wick rotate $F \to iF$, this is the same action used in [140]. The qualitative nature of the family of solutions is, however, different to that encountered in [47,117,140] for real baryon number chemical potential. Specifically, for a real chemical potential, the term under the square root in Eq.(4.28) would be of the form $\sqrt{1+\rho^2\theta'^2 - \frac{2(2\pi\alpha' F)^2\tilde{h}}{h^2}}$, yielding solutions with different behaviour to the ones we will find below.

From the solutions to the DBI equations of motion following from Eq.(4.28), we will reconstruct the dependence of the effective potential on $\alpha - \frac{\mu_I}{T}$, for generic quark masses.

We work in the gauge $A_\rho = 0$, so that $F_{\tau\rho} = -\partial_\rho A_\tau$. Since the action (4.28) does not depend explicitly on A_τ, the conjugate momentum is conserved. In the usual situation with real chemical potentials, the variable conjugate to A_τ is the quark density. We will continue to refer to this conjugate variable as the "charge density" d, in the situation with an imaginary chemical potential,

$$\begin{aligned} d &\equiv -\frac{\partial \mathcal{L}_{\rm D7}}{\partial A'_\tau} \\ &= 2\pi^2 N_f T_{D7}(2\pi\alpha')\,\frac{\rho^3}{2}\frac{\tilde{h}^2}{h}\cos^3\theta\,\frac{2\pi\alpha' F_{\tau\rho}+B_{\tau\rho}}{\sqrt{1+\rho^2\theta'^2+2(2\pi\alpha' F_{\tau\rho}+B_{\tau\rho})^2\frac{\tilde{h}}{h^2}}} \end{aligned} \tag{4.29}$$

This is a constant of motion. It is useful to define the dimensionless combination

$$\tilde{d} \equiv d\,(2\pi\alpha')^{-1}\left(2\pi^2 N_f T_{D7}\, r_H^3\right)^{-1} = \frac{8}{\sqrt{\lambda}\,N_f\,N}\frac{d}{T^3}. \tag{4.30}$$

The solutions can be characterized by this dimensionless density which, as we will see below, is restricted to take values less than unity. Solving algebraically for the combination $(2\pi\alpha' F + B)$, using the above equations we obtain

$$B_{\tau\rho} + 2\pi\alpha' F_{\tau\rho} = \tilde{d}\,\frac{2h\sqrt{1+\rho^2\theta'(\rho)^2}}{\sqrt{\tilde{h}\left(\tilde{h}^3\frac{\rho^6}{r_H^6}\cos^6\theta - 8\tilde{d}^2\right)}}. \tag{4.31}$$

For solutions that reach the horizon of the black hole (*i.e.* which wrap the

cigar D_2), we deduce from the above expression that

$$|\tilde{d}| \leq \cos^3\theta\big|_{\rho=r_H}. \tag{4.32}$$

The explicit relation between the density $\tilde{d}$ and the chemical potential μ_I follows from integrating Eq.(4.31)

$$\alpha - \frac{\mu_I}{T} = \sqrt{\lambda}\,\tilde{d}\int_1^\infty dy \frac{(1-y^{-4})\sqrt{1+y^2\theta'(y)^2}}{\sqrt{(1+y^{-4})\left((1+y^{-4})^3y^6\cos^6\theta - 8\tilde{d}^2\right)}}. \tag{4.33}$$

Here, the dimensionless variable $y = \frac{\rho}{r_H}$.

The D7-brane configurations that reach the horizon are referred to as "black hole embeddings". Analysis of the spectral functions of various fluctuations around such solutions reveals a continuous, gapless spectrum [143,144] leading to the interpretation that these describe a phase where the "mesonic" fluctuations have melted in the high temperature plasma.

The action

Evaluated on the solution for $B+2\pi\alpha' F$, the unrenormalised D7-brane action is

$$\begin{aligned} S_{D7} &= \lambda N_f N \frac{T^3}{64}\int d^3x \times \\ &\times \int_1^\infty dy\, y^6(1-y^{-4})(1+y^{-4})^{\frac{5}{2}} \frac{\cos^6\theta\sqrt{1+y^2\theta'(y)^2}}{\sqrt{(1+y^{-4})^3y^6\cos^6\theta - 8\tilde{d}^2}}. \end{aligned} \tag{4.34}$$

Note that this action cannot be varied to obtain the correct equations of motion for $\theta(y)$. The equation of motion for θ follows as usual by varying (4.28) or by using a different action where we trade A_τ for $F_{\tau\rho}$ as the independent variable, the equation for the latter being algebraic. This is achieved by the Legendre transform,

$$S_{D7} \to S_{D7}^{LT} = S_{D7} - d\int \beta\, d^3x \int d\rho \left(F_{\tau\rho} + \frac{B_{\tau\rho}}{2\pi\alpha'}\right). \tag{4.35}$$

The resulting Legendre transformed action can be evaluated on the solution for F, to yield

$$S_{D7}^{LT} = \lambda N_f N \frac{T^3}{64} \int d^3x \times \\ \times \int_1^\infty dy\, y^3\, h\tilde{h}\, \sqrt{1+y^2\theta'(y)^2} \left(1 - \frac{8\,\tilde{d}^2}{\tilde{h}^3\, y^6\, \cos^6\theta}\right)^{1/2} \cos^3\theta \qquad (4.36)$$

One may make the replacement $\tilde{d} \to i\tilde{d}$ and show that the corresponding expressions for real densities and real chemical potentials are recovered.

4.3.2 $m_q = 0$: constant solutions

It is straightforward to see that the DBI action admits constant solutions with $\theta = 0$ for a range of densities $\tilde{d}$. Since the constant solutions extend all the way to the horizon, they describe a phase of melted mesons. They also correspond to having vanishing masses for the fundamental hypermultiplets. In general, the large ρ asymptotics of $\theta(\rho)$ are given by

$$\theta(\rho) = \frac{\theta_{(0)}}{\rho} + \frac{\theta_{(2)}}{\rho^3} + \ldots \qquad (4.37)$$

where the coefficients $\theta_{(0)}$ and $\theta_{(2)}$ are related to the quark mass and condensate respectively. According to the AdS/CFT dictionary, this boundary behaviour signals the fact that θ is dual to a dimension 3 operator, namely, the quark bilinear. From the earlier description of the D3-D7 system and from Eq.(4.26), the asymptotic value of $\rho \sin\theta$ is the D3-D7 separation, which is the quark mass *i.e.*, $\theta_{(0)} = 2\pi\alpha' m_q$. The coefficient of the subleading term, $\theta_{(2)}$, determines the VEV of the same operator which is the quark condensate $\langle\Sigma_m\rangle = \langle\tilde{\psi}_i\psi_i\rangle + \ldots$

It follows then that the solution with $\theta = 0$ has $m_q = 0$, $\langle\tilde{\Sigma}_m\rangle = 0$. When the slipping angle θ is vanishing, the D7-brane wraps the equatorial S^3 inside the five-sphere in the geometry. For this solution, the contribution of the flavours to the effective potential for α can be computed analytically[3]. From

[3]The same expressions were obtained in [47] for the zero mass 'black hole embedding'

Eq.(4.33) we find

$$\frac{1}{\sqrt{\lambda}}\left(\alpha - \frac{\mu_I}{T}\right) = \frac{\tilde{d}}{2}\int_1^\infty d\hat{y}\frac{1}{\sqrt{\hat{y}^6 - \tilde{d}^2}} = \frac{\tilde{d}}{12}|\tilde{d}|^{-2/3} B_{\tilde{d}^2}\left(\frac{1}{3},\frac{1}{2}\right) \quad (4.38)$$

where $B_z(a,b)$ is the incomplete beta function and the integration variable $\hat{y}$ is related to y as $\hat{y}^2 = \frac{1}{2}(y^2 + y^{-2})$. The action is formally divergent and requires renormalisation which is achieved by a simple subtraction for the constant solutions,

$$\begin{aligned} S_{D7}^{\text{ren}} &= \lambda N_f N \frac{T^3}{16}\int d^3x \int_1^\infty d\hat{y}\left(\frac{\hat{y}^6}{\sqrt{\hat{y}^6 - d^2}} - \hat{y}^3\right) \quad (4.39)\\ &= \lambda N_f N \frac{T^3}{96}\int d^3x \left[|\tilde{d}|^{4/3} B_{\tilde{d}^2}\left(-\frac{2}{3},\frac{1}{2}\right) + \frac{3}{2}\right] \end{aligned}$$

The effective potential induced by the flavours can be found by eliminating $\tilde{d}$ from equations (4.38) and (4.39). It is important to note that since α is a phase defined modulo 2π, and likewise, the imaginary chemical potential μ_I is also a periodic variable, the combination $\alpha - \frac{\mu_I}{T}$ is bounded. In the strong

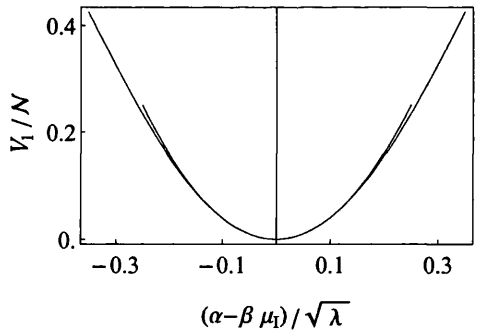

Figure 4.2: The potential for α from the flavours, as a function of $\frac{1}{\sqrt{\lambda}}(\alpha - \frac{\mu_I}{T})$. The curve in green is the full potential implied by the DBI action. The curve in blue is the quadratic piece that is consistent to keep in the $\lambda \to \infty$ limit. The normalization constant $\mathcal{N} = \frac{N_f N T^3 \lambda}{16}$.

solutions for real baryonic chemical potential.

coupling limit $\lambda \gg 1$, we must therefore have that

$$\tilde{d} = \frac{4}{\sqrt{\lambda}}\left(\alpha - \frac{\mu_I}{T}\right) + \mathcal{O}\left(\frac{1}{\lambda}\right) \tag{4.40}$$

by inverting Eq.(4.38). Since $|\tilde{d}| \ll 1$ at strong coupling, we can expand the action (4.39) for small $\tilde{d}$ to obtain the contribution to the effective potential from the flavours,

$$V_f = N_f N T^4 \left(\alpha - \frac{\mu_I}{T}\right)^2 + \mathcal{O}\left(\frac{1}{\sqrt{\lambda}}\right), \qquad \alpha, \frac{\mu_I}{T} \in [-\pi, \pi] \tag{4.41}$$

which is independent of λ at the leading order in the strong coupling limit. The full effective potential at strong 't Hooft coupling with $N_f \ll N$ in the deconfined phase is then

$$V_{\text{eff}} = V_A + V_f = \min_{r \in \mathbb{Z}} 4\pi^2 N^2 \frac{T^4}{\lambda}\left(\alpha - \frac{2\pi r}{N}\right)^2 + N_f N T^4 \left(\alpha - \frac{\mu_I}{T}\right)^2. \tag{4.42}$$

From this effective potential it is obvious that the degeneracy of the $\mathbb{Z}_N$ vacua has been lifted by the massless fundamental flavour fields. Curiously, while the flavour contribution is $\mathcal{O}(\frac{1}{N})$ suppressed compared to the leading term in the large N limit, it is unsuppressed by powers of the 't Hooft coupling λ in the strong coupling limit. The order of limits is, of course, unambiguous in the present context since N is taken to infinity first, keeping the 't Hooft coupling fixed and large.

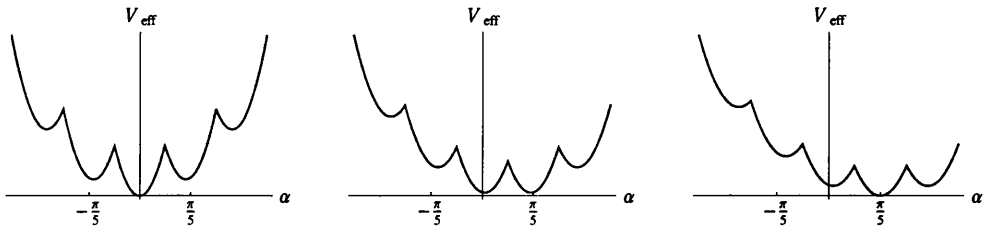

Figure 4.3: The full effective potential as a function of α from the flavours for three different values of $\frac{\mu_I}{T}$. As $\frac{\mu_I}{T}$ is increased from left to right, the local minima of the effective potential compete, resulting in a first order phase transition.

There are N local minima, but a unique global minimum at $\alpha = 0$ when $\mu_I = 0$. As μ_I is increased smoothly from zero and approaches $\mu_I = \frac{\pi}{N}$, two neighbouring minima become degenerate and any further increase in μ_I results in a first order phase transition from the $\alpha = 0$ vacuum to the vacuum with $\alpha = \frac{2\pi}{N}$ (see Fig.(4.3)) as described previously.

Free Energy

As the phase transitions at $\frac{\mu_I}{T} = (2r-1)\frac{\pi}{N}$ for $r \in \mathbb{Z}$ are first order, it is useful to compute the free energy as a function of the imaginary chemical potential μ_I. The free energy (the grand potential) density can be calculated by minimizing the effective potential Eq.(4.42) with respect to α for all μ_I and we find

$$\begin{aligned} F[\mu_I]\Big|_{\lambda\gg 1} &= N_f N T^4 \left(1+\frac{\lambda}{4\pi^2}\frac{N_f}{N}\right)^{-1} \min_{r\in\mathbb{Z}} \left(\frac{\mu_I}{T}-\frac{2\pi r}{N}\right)^2 \\ &\simeq N_f N T^4 \min_{r\in\mathbb{Z}} \left(\frac{\mu_I}{T}-\frac{2\pi r}{N}\right)^2 \end{aligned}$$

While the quadratic behaviour is simply a consequence of large N, it is interesting to compare the coefficient with the result at weak coupling and zero hypermultiplet mass Eq.(4.9). Since we have $2N_f$ complex scalars and $2N_f$ Weyl fermions, the free energy at weak coupling (and $m_q = 0$) is

$$F[\mu_I]\Big|_{\lambda\ll 1} = \frac{1}{2} N N_f T^4 \min_{r\in\mathbb{Z}} \left(\frac{\mu_I}{T}-\frac{2\pi r}{N}\right)^2 \tag{4.43}$$

We observe that the strong and weak coupling results differ by a factor of 2.

4.3.3 $m_q \neq 0$ non-constant solutions

Solutions with non zero quark mass also happen to be non constant and these need to be understood numerically. For smooth solutions that get to the horizon from the boundary, we require that the $S^3 \subset S^5$ wrapped by the D7-brane remains non vanishing along the solution. As is well known, there are two classes of non constant D7 brane solutions: those that get all the

way to the horizon (the so called "black-hole embeddings"), and those that end smoothly before they get to the horizon. For both classes of solutions, the quark mass and the condensate can be read off from the asymptotic behaviour (4.37) near the boundary of AdS_5. Specifically, in terms of the dimensionless variable $y = \frac{\rho}{r_H}$, the boundary behaviour of the slipping angle is

$$\theta(y) = \frac{2}{\sqrt{\lambda}} \left(\frac{m_q}{T}\right) \frac{1}{y} + \frac{\theta_{(2)}}{\pi^3 T^3 R^6} \frac{1}{y^3} + \dots \tag{4.44}$$

Note that it is only the ratio $\frac{m_q}{T}$ which is relevant here, since the theory without hypermultiplets is the conformal $\mathcal{N} = 4$ theory without an intrinsic scale. We thus define the natural dimensionless ratio that characterizes these solutions,

$$\frac{M}{T} \equiv \frac{2m_q}{\sqrt{\lambda}T} \tag{4.45}$$

where the mass scale $M = \frac{2m_q}{\sqrt{\lambda}}$ is the characteristic scale of meson bound states at zero temperature (and strong coupling) [145].

The Euclidean action for these solutions requires careful renormalisation via subtractions to yield finite results. The correct procedure of holographic renormalisation has been developed for probe Dp-branes in AdS spacetime [118, 142]. The result of this procedure in the present context is that the renormalized action is defined as an integral over y from $y = 1$ (the IR) to $y = \Lambda$ (a UV cutoff) along with counterterms defined locally at $y = \Lambda$,

$$S_{D7}^{\text{ren}} = S_{D7}\big|_{\Lambda} - \lambda N_f N \frac{T^3}{64} \left(\frac{1}{4}\Lambda^4 - \frac{1}{2}\Lambda^4\theta(\Lambda)^2 + \frac{5}{12}\Lambda^4\theta(\Lambda)^4\right) \tag{4.46}$$

The first two counterterms are divergent while the third is a finite subtraction. Further counterterms are necessary if the boundary is not flat.

Black Hole Embeddings

Solutions extending all the way to the black hole horizon, referred to previously as black-hole embeddings, of the D7-brane, satisfy $\theta'(y = 1) = 0$ and $0 \leq \theta(y = 1) < \frac{\pi}{2}$. Thus for these embeddings, the S^3 remains blown-up all along the solution, while the S^1 (the thermal circle) shrinks at the horizon, so

the D7-brane caps off smoothly. By varying $\theta(y = 1)$ we can explore different values of the hypermultiplet mass $\frac{M}{T}$. These Euclidean solutions can exist only if

$$|\tilde{d}| \leq \cos^3\theta\big|_{y=1} \tag{4.47}$$

The black hole embeddings describe a high temperature phase where mesons have melted.

For a fixed density $\tilde{d}$, solutions with different hypermultiplet masses can be found by dialling $\theta(y = 1)$ provided the condition (4.47) is satisfied. As in the massless case analysed above, we will obtain (numerically) the effective potential as a function of $\frac{1}{\sqrt{\lambda}}(\alpha - \frac{\mu_I}{T})$. We summarize the properties of the solutions below.

- The solutions for finite density $0 < |\tilde{d}| \leq 1$, are all of the type described above and are qualitatively similar to black-hole embeddings found earlier for vanishing baryonic chemical potential [111,116]. They are qualitatively distinct from the configurations with real chemical potential [26,47,117,140]. We elaborate on this below.

- For any given density $|\tilde{d}|$ (between 0 and 1) there is a fixed value of $\frac{M}{T}$, above which solutions cease to exist. The allowed range of masses decreases with increasing $|\tilde{d}|$ (Figure 4.4). When the density $\tilde{d}$ approaches

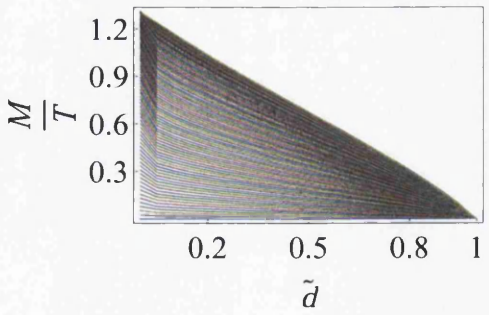

Figure 4.4: The values of $\frac{M}{T}$ and the density variable $\tilde{d}$ (conjugate to imaginary μ) for which the black hole embeddings or melted meson solutions exist.

unity, all allowed solutions bunch up near the zero mass constant solution. This is illustrated in Figure 4.5 where we plot solutions in the

$\rho_1 - \rho_2$ plane ($\rho_2 = \rho \sin\theta$ and $\rho_1 = \rho\cos\theta$). In contrast to this picture, for a real chemical potential, it was observed (e.g. in [47, 140]) that black hole embeddings can exist at all possible values of the ratio $\frac{M}{T}$. For large values of the mass (or low temperatures), these solutions could be viewed as a probe D7-brane with strings (quarks) attached which drop into the black hole horizon. The absence of these kinds of solutions substantially alters the phase diagram for imaginary chemical potential.

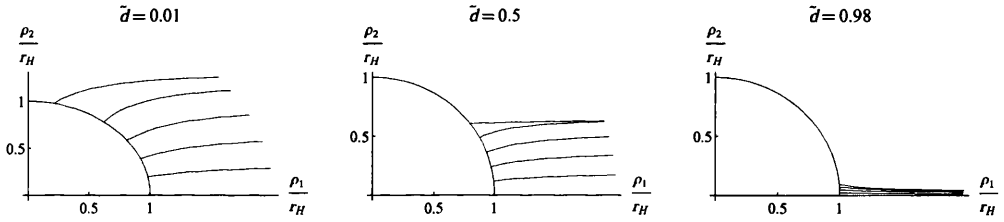

Figure 4.5: D7-brane solutions extending to the horizon for $\tilde{d} = 0.01$, 0.5 and 0.98. For each density we have plotted a family of solutions with increasing masses up to the maximum value allowed for that density. The asymptotic distance from the ρ_1 axis gives the ratio $\frac{M}{T}$. The black hole horizon is the blue curve $\rho_1^2 + \rho_2^2 = r_H^2$.

- The largest value of the ratio $\frac{M}{T} = \frac{2m_q}{\sqrt{\lambda}T}$ for which the black hole embedding exists is ≈ 1.30 and this occurs when $\tilde{d} = 0$ and is the critical embedding solution (Figure 4.9).

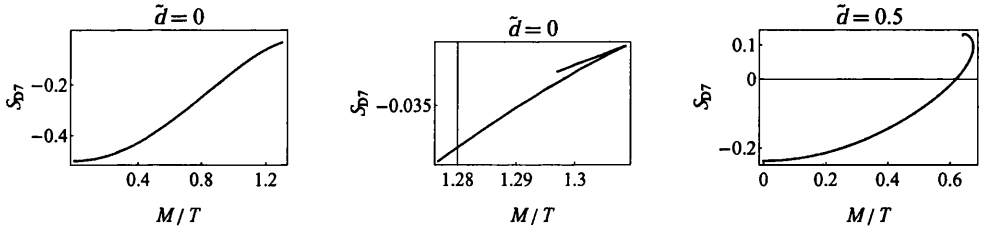

Figure 4.6: The action as a function of $\frac{M}{T}$ for $\tilde{d} = 0$ and $\tilde{d} = 0.5$.

- By evaluating the action and the expectation value of the quark condensate operator $\langle \Sigma_m \rangle$, for a given density $\tilde{d}$, we may see that for large

enough masses, there exist two classical solutions with the same mass but different values for the action and condensate (Figure 4.6). This feature, well-known at zero density, also appears for non zero densities conjugate to an imaginary chemical potential. The solution with the lower action is then taken to be the physical one.

The Effective Potential

The contribution to the effective potential for the phase of the Polyakov-Maldacena loop α, can be found numerically (Figure 4.7). However, we

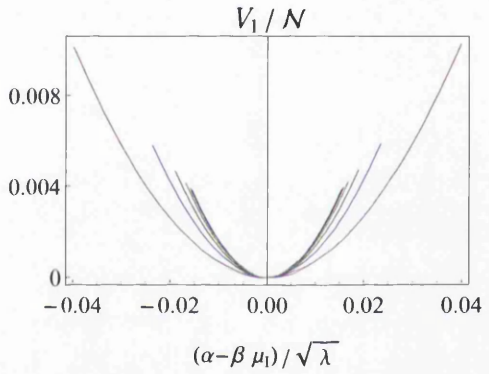

Figure 4.7: The effective potential from flavours for increasing values of m_q, for $\frac{M}{T} = 0$, 0.24, 0.48, 0.72, 0.96 and 1.2. The potential tends to flatten out as $\frac{M}{T}$ approaches the critical value of 1.3.

can already be fairly precise about the form of this contribution due to Eq. (4.33): since α and $\frac{\mu_I}{T}$ are bounded, we must have that $|\tilde{d}| \sim \mathcal{O}\left(\frac{1}{\sqrt{\lambda}}\right) \ll 1$. Notice that this scaling of $\tilde{d}$, actually implies that the dimensionful density $d \sim N_f N T^3$, which is a natural scaling for N_f quark flavours. In taking $\tilde{d} \sim \mathcal{O}\left(\frac{1}{\sqrt{\lambda}}\right)$, we are also assuming that the integral in Eq. (4.33) is well-behaved as $\tilde{d} \to 0$ and we can check numerically that this is the case for all hypermultiplet masses in the range $0 \leq \frac{M}{T} \lesssim 1.30$ corresponding to the black hole embedding solutions. In addition since the D7-brane action is a function of $\tilde{d}^2$, for small $\tilde{d}$, it can be expanded in powers of $\tilde{d}^2$. In the large λ limit, the quadratic piece alone dominates and therefore we find that the

effective potential is of the form

$$\begin{aligned} V_{\text{eff}} &= V_A + V_f \\ &= \min_{r\in\mathbb{Z}} 4\pi^2 N^2 \frac{T^4}{\lambda}\left(\alpha - \frac{2\pi r}{N}\right)^2 + N_f N T^4 f\left(\frac{M}{T}\right)\left(\alpha - \frac{\mu_I}{T}\right)^2 . \end{aligned} \tag{4.48}$$

Here M is the mass scale $\frac{2m_q}{\sqrt{\lambda}}$ and f is a dimensionless function of $\frac{M}{T}$. The coefficient $f\left(\frac{M}{T}\right)$ is unity when $m_q = 0$ and decreases monotonically with increasing mass, eventually approaching ≈ 0.2 as $\frac{M}{T}$ is dialled to its maximum value of approximately 1.3 (Figure 4.8). We should emphasize that in

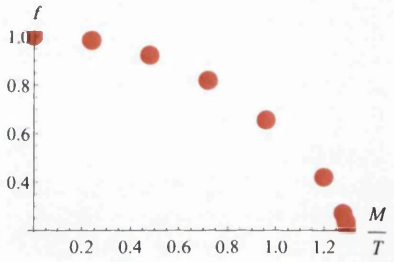

Figure 4.8: The dimensionless coefficient f in the quadratic effective potential V_f due to hypermultiplets.

deriving the effective potential above, in the large λ and large N limit, we only needed to use solutions with small $\tilde{d}$, strictly only those in the vicinity of $\tilde{d} \sim \mathcal{O}\left(\frac{1}{\sqrt{\lambda}}\right)$. When we turn to the low temperature regime below, we will see that this is actually crucial for ensuring a consistent picture of the transition between high and low temperatures.

To summarize, for all values of the parameter $\frac{M}{T}$ for which black hole embeddings of the D7-brane exist, with an imaginary chemical potential, first order Roberge-Weiss transitions will occur at $\frac{\mu_I}{T} = (2r-1)\frac{\pi}{N}$, $r \in \mathbb{Z}$. This means that, for fixed hypermultiplet mass m_q, the RW transition will occur for temperatures $T \gtrsim \frac{2m_q}{(1.3\sqrt{\lambda})}$. We will determine the value of this temperature, representing the RW endpoint, more precisely below.

The monotonic decrease in $f\left(\frac{M}{T}\right)$ with decreasing temperature (or increasing mass m_q) is in accord with intuition from weak coupling. The quadratic potential for α can be interpreted as a thermal contribution to

the mass of the mode α from the flavours. That this thermal correction should decrease as the flavours are made heavier (eventually decoupling for infinite mass), appears intuitively to be consistent. At weak coupling, it would be natural to identify the mass of the mode α with the Debye mass (inverse electric screening length). It is unclear whether any such interpretation should be possible at strong coupling. Finally, we can again write the free energy as a function of μ_I, (taking $\frac{\lambda N_f}{N} \ll 1$),

$$F[\mu_I] = N_f N T^4 f\left(\frac{m_q}{2\sqrt{\lambda}T}\right) \min_{r\in\mathbb{Z}} \left(\alpha - \frac{\mu_I}{T}\right)^2 \tag{4.49}$$

Given our numerical results for f, we can say that near $m_q = 0$, $f \approx 1 - f''(0)\frac{m_q^2}{8\lambda T^2}$.

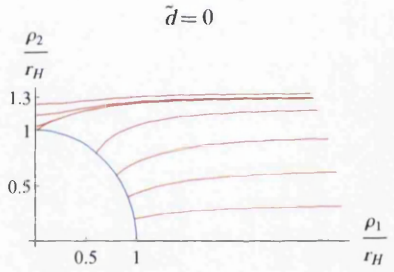

Figure 4.9: The well known transition at zero density, from black hole embeddings (falling into the black hole) to Minkowski embedding probe D7-branes placed away from the horizon.

Low temperatures/Large masses, $M \gtrsim 1.3$

The critical black hole embedding of the D7-brane has the property that the slipping angle θ of the solution approaches $\frac{\pi}{2}$ at the horizon and the corresponding S^3 wrapped by the probe brane shrinks. Hence, the only solutions with masses higher than $\frac{M}{T} \approx 1.3$ are those where the S^3 wrapped by the D7-brane shrinks before the D7-brane gets to the horizon. For these embeddings the thermal S^1 remains non-vanishing while the S^3 shrinks smoothly before the brane gets to the horizon. Since the S^3 shrinks at the tip of such

a solution, we are forced to have $\tilde{d} = 0$ due to Eq.(4.47) and hence

$$F_{\tau\rho} + 2\pi\alpha' B_{\tau\rho} = 0 \tag{4.50}$$

The D7-brane action has no dependence on either α or μ_I. Hence there is no potential induced by flavours for the phase α of the Polyakov-Maldacena loop: $V_f\left(\alpha - \frac{\mu_I}{T}\right)$ vanishes identically and the physics is completely smooth as a function μ_I. Note that despite the fact that the field strength F is fixed by B, we can always add a constant to the world-volume gauge potential A_τ, which will not change the field strength, and can be interpreted as a chemical potential μ_I in the boundary field theory. Hence, in the grand canonical ensemble, at low temperatures ($T \ll M$), for every μ_I the only solution possible is the $\tilde{d} = 0$ Minkowski embedding representing unmelted mesons. The situation is quite distinct from the case of real chemical potential [26] wherein, at fixed low temperatures, there is a transition from Minkowski embedding solutions to the spiky black hole embeddings as the chemical potential is increased.

The solutions with $\tilde{d} = 0$ are the same as those originally obtained in [111, 114, 116]. The transition from the black hole embeddings to the second class of solutions involves a topology change: the first category of solutions exhibits a shrinking S^1 and a finite S^3, while the second has the S^3 shrinking in the interior. The transition between these is well-known and is a first order phase transition as may be inferred from plotting the action as a function of $\frac{M}{T}$ (Figure 4.10) for the solution with $\tilde{d} = 0$. The phase transition between the two classes of solutions is a "meson-melting" transition. At low enough temperatures (or large enough hypermultiplet mass), the only allowed D7-brane embeddings are the unmelted mesons with zero density $\tilde{d} = 0$. The spectrum of fluctuations about this solution exhibits a mass gap and a discrete spectrum [145] at zero temperature. The mass gap in the meson spectrum is

$$M_{\text{gap}} = \frac{4\pi m_q}{\sqrt{\lambda}} = 2\pi M \tag{4.51}$$

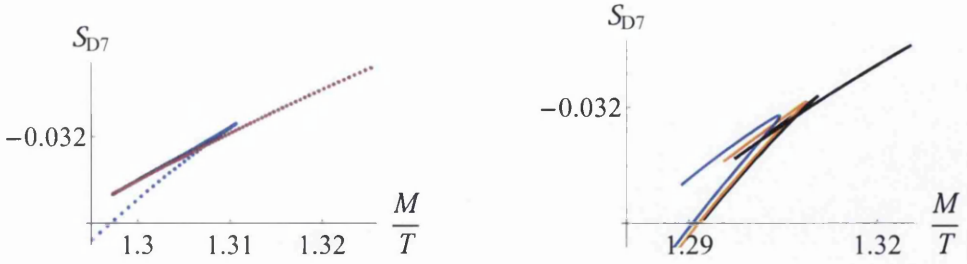

Figure 4.10: Left: The action for $\tilde{d} = 0$, D7-brane embeddings. As the ratio $\frac{M}{T}$ is increased, just before the black hole embedding (melted meson) ceases to exist, there is a transition to the family of so-called "Minkowski embeddings" corresponding to unmelted mesons. Right: In the second figure we see that the action (grand potential) for black hole embeddings with $\tilde{d} > 0$, (0.004 (orange) and 0.008 (blue)), is always larger than the action for the $\tilde{d} = 0$ solutions (black). There is no Minkowski embedding solution with $\tilde{d} \neq 0$.

We also see that as the density $\tilde{d}$ is increased from zero, for small enough densities $\tilde{d} \ll 1$, the black hole embeddings with $\tilde{d} \neq 0$ coexist with the zero density $\tilde{d} = 0$ Minkowski embedding solution for a range of temperatures (Figure 4.10). This will be important for determining the phase diagram and the shape of the phase boundaries in the grand canonical ensemble. With increasing density, there is a critical value of $\tilde{d}$, ($\gtrsim 10^{-2}$) beyond which the curves for black hole embeddings (as in Figure 4.10) cease to intersect the Minkowski solution at $\tilde{d} = 0$. They turn back and terminate at progressively smaller values of $\frac{M}{T}$ (Figure 4.6). The presence of such configurations in the grand canonical ensemble could make the low temperature region of the phase diagram inaccessible. However, it should be clear from the preceding discussions that these configurations are essentially removed as a consequence of the Roberge-Weiss transition. The RW transitions occur at values of $\left(\alpha - \frac{\mu_I}{T}\right)$ that are parametrically suppressed by $\frac{1}{N}$ corresponding to parametrically small values of $\tilde{d}$. The configurations with such low densities will always be of the kind depicted in Figure 4.10.

4.3.4 Phase diagram

The above analysis of the dominant configurations at different densities and temperatures now allows us to determine the phase diagram of the theory as a function of the temperature/meson mass scale ratio $\frac{T}{M}$ and the imaginary chemical potential μ_I. We have already established that at low temperature the physics is independent of μ_I and α, the phase of the Polyakov loop, and is dominated by the unmelted meson (Minkowski embeddings) configurations with vanishing density $\tilde{d} = 0$. In addition, we have seen that at high temperature the dominant configurations are the black hole embeddings representing melted mesons with $\tilde{d} \neq 0$. For these configurations the system experiences a first order Roberge-Weiss phase transition at $\frac{\mu_I}{T} = \frac{(2r-1)\pi}{N}$ $(r \in \mathbb{Z})$, characterized by a discrete jump in the phase of the Polyakov loop. Specifically, α jumps from $\frac{2\pi(r-1)}{N}$ to $\frac{2\pi r}{N}$.

What remains is to understand the phase boundary between the melted and unmelted meson phases as a function of μ_I. We first recall that in the melted phase $\tilde{d}$ is proportional to $\frac{1}{\sqrt{\lambda}}\left(\frac{\mu_I}{T} - \alpha\right)$, for small enough $\tilde{d}$. As depicted in Figure 4.10, in the grand canonical ensemble, the melted meson configuration with small $\tilde{d} \neq 0$ will then have to compete with the $\tilde{d} = 0$ Minkowski embedding as the temperature is decreased. This results in a first order transition between the two phases. It is clear from Figure 4.10 that as the density increases, the transition temperature increases as well (equivalently $\frac{M}{T}$ decreases). The dependence of this transition temperature

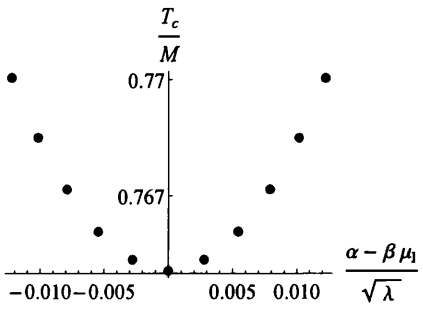

Figure 4.11: The melting transition temperature at different values of μ_I and fixed α.

on the chemical potential determines the shape of the phase boundary in the (μ_I, T) plane. We can numerically obtain the melting transition temperatures $T_c(\mu_I)$ for different values of μ_I (corresponding to different densities $\tilde{d}$ in the melted phase). The result is shown in Figure 4.11. For

$$\alpha = \frac{2\pi r}{N}, \qquad (2r-1)\frac{\pi}{N} \leq \frac{\mu_I}{T} < (2r+1)\frac{\pi}{N}, \qquad r \in \mathbb{Z} \tag{4.52}$$

we find that

$$T_c(\mu_I) - T_0 = K\frac{M}{\lambda}\left(\frac{\mu_I}{T_c(\mu_I)} - \alpha\right)^2 + \ldots, \qquad K \approx 33.5 \tag{4.53}$$

where $T_0 = T_c(0) \approx 0.77M$. We have only kept terms to quadratic order on the right hand side for two reasons: First, since the difference $\frac{\mu_I}{T} - \alpha$ is bounded, higher order terms are suppressed at strong coupling ($\lambda \gg 1$). Secondly, we also have that $\left|\frac{\mu_I}{T} - \alpha\right| \leq \frac{\pi}{N}$, so higher order terms are suppressed by powers of $\frac{1}{N^2}$. At leading order in $\frac{1}{\lambda}$, $T_c(\mu_I)$ may therefore be replaced by T_0 on the right-hand side of (4.53).

The first-order phase boundary between the melted phase at high temperature and the unmelted phase at low temperature has the curvature as shown in Figure 4.12. We find that this phase boundary is given by a set of parabola, centred at $\frac{\mu_I}{T} = \frac{2\pi r}{N}$ ($r \in \mathbb{Z}$). Explicitly, we find

$$\frac{T_c(\mu_I) - T_0}{T_0} = \frac{\kappa}{\lambda}\left(\frac{\mu_I}{T_0} - \frac{2\pi r}{N}\right)^2, \qquad \kappa \approx 43.5 \tag{4.54}$$

Combining this result with the Roberge-Weiss lines at $\mu_I = \mu_{\text{RW}}$ yields an infinite set of points at which three first order transition lines meet. At each of these *triple points*, three phases labelled by distinct values of the Polyakov loop coexist. The location of the triple points in the $\mu_I - T$ plane is given by $(\mu_{\text{RW}}, T_{\text{RW}})$, where

$$\frac{\mu_{\text{RW}}}{T_0} = (2r-1)\frac{\pi}{N}, \qquad \frac{T_{\text{RW}}}{T_0} = 1 + \frac{\kappa}{\lambda}\frac{\pi^2}{N^2}, \tag{4.55}$$

with $r \in \mathbb{Z}$ and $\kappa = \frac{KM}{T} \approx 43.5$. The N-scaling of the formulae may suggest

that these should be subleading effects in the large-N limit and therefore not consistently incorporated in a classical supergravity approximation. However the factors of $\frac{1}{N}$ arise from purely kinematical considerations, namely the symmetry of the theory under shifts $\mu_I \to \mu_I + \frac{2\pi}{N}$. When N is large, the RW transitions are closely spaced, resulting in the N-dependence in the Roberge-Weiss temperature. The curvature of the phase boundary in Figure 4.12 is independent of N, see Eq. (4.54).

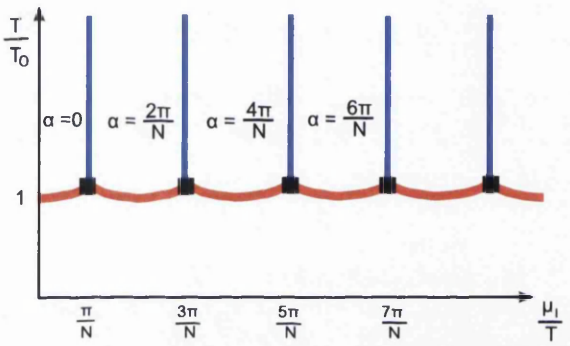

Figure 4.12: Phase diagram in the plane of temperature T and imaginary quark chemical potential μ_I. The blue lines represent the first order Roberge-Weiss transitions in the high-temperature phase. The red line is the line of first-order phase transitions separating the high- and the low-temperature phases. The Roberge-Weiss endpoints, indicated by the black squares, are triple points at $(\mu_{\rm RW}, T_{\rm RW})$. The phase of the Polyakov loop is denoted with α.

4.3.5 Real chemical potential and analytic continuation

For real values of the quark density a rich family of solutions to the DBI equations of motion exists, after making the replacement $F \to iF$ (and setting $B = 0$) in Eq. (4.28). In particular, black hole embeddings, representing melted mesons, exist for all values of the ratio $\frac{M}{T}$ in the canonical ensemble with fixed quark number density. These include low temperature ($M \gg T$) solutions which can be viewed as Minkowski embeddings attached to a spike consisting of strings (quarks) falling into the black hole horizon.

The phase diagram for real chemical potential in the grand canonical ensemble [26,47,117,146] bears little relation to Figure 4.12, either at low or high temperatures. With a real quark chemical potential, there is a single line of phase transitions separating a zero density phase from the dissociated or melted meson phase. For small chemical potential the transition line is first order, while at larger chemical potential the transition is expected to be a continuous one [47, 134, 147], terminating at $\mu = m_q$. In fact it has been argued in [147] that for low temperatures the transition line is actually third order and connects up with the first order line at a tricritical point.

In the context of QCD, the main motivation behind the exploration of the phase diagram as a function of imaginary chemical potential has been to determine the phase structure for real chemical potential, via the use of analytic continuation from imaginary $\mu = i\mu_I$ (with $\mu^2 < 0$) to real μ (with $\mu^2 > 0$) [123–132]. It is therefore natural to ask what aspects of the phase diagram can be captured by analytic continuation in the holographic model we studied here. This is particularly interesting given the qualitative difference in the nature of black hole embeddings and the D7-brane solutions at fixed density. At large real or imaginary chemical potential the phase structures are manifestly different due to the presence of the Roberge-Weiss transitions. However it is expected that the curvature of the meson melting line for imaginary chemical potential, with $\mu^2 < 0$, is directly related to the curvature of the first order transition line for real chemical potential, with $\mu^2 > 0$. Repeating the analysis for real chemical potential we find that the

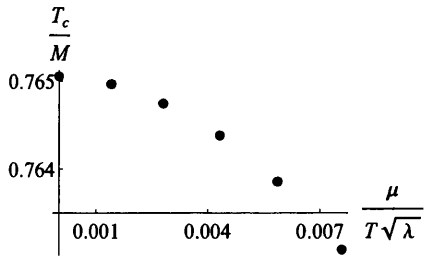

Figure 4.13: The line of first order meson-melting transitions for real chemical potential, $\mu \gtrsim 0$.

curvature of the first order line for $\mu^2 > 0$ is given by (see Figure 4.13)

$$T_c(\mu) - T_0 \approx -33.5 \frac{M}{\lambda} \frac{\mu^2}{T_0^2} \tag{4.56}$$

matching up with our result for imaginary μ. It is reassuring that despite the differences between individual D7-brane probe solutions for $\mu^2 \gtrless 0$, the theory is analytic in μ^2 near $\mu^2 = 0$.

4.4 The Sakai-Sugimoto Model

In this section we will discuss the Sakai-Sugimoto model with an imaginary chemical potential, similarly to the previous section. The background to the Sakai-Sugimoto model was described in section 2.4.

4.4.1 D8 Embedding

Consider the metric for the D8 branes in the background (2.30). We choose the brane to share all coordinates except the x_4 direction where the D8 is pointlike, which we make a function of the radial direction U. The induced metric of the D8 with this choice is

$$\begin{aligned} ds^2_{D8} = &\left(\frac{U}{R}\right)^{3/2} \left(f_T(U) dt_E^2 + \delta_{ij} dx^i dx^j\right) + \\ &+ \left(\left(\frac{R}{U}\right)^{\frac{3}{2}} \frac{1}{f_T(U)} + \left(\frac{U}{R}\right)^{\frac{3}{2}} x_4'^2\right) dU^2 + \left(\frac{R}{U}\right)^{\frac{3}{2}} U^2 d\Omega_4^2 \end{aligned} \tag{4.57}$$

Prime denotes differentiation with respect to U. To incorporate a chemical potential into the gauge theory, on the gravity side we include a worldvolume gauge field on the D8 branes. We also introduce a NS B field into the bulk, dual to the expectation value of the phase of the Polyakov loop in the gauge theory, similarly to the D3/D7 case in the previous section. The only non zero components of these field strengths are F_{tU} and B_{tU}. We can now write

the DBI action of N_f branes

$$S_{\rm DBI} = N_f T_{\rm D8} \int d^8x e^{-\phi} \sqrt{\det\left(g_{ab} + B_{ab} + 2\pi\alpha' F_{ab}\right)} \tag{4.58}$$

$$= \frac{N_f T_{\rm D8} {\rm Vol}(S^4)}{g_s} \int d^4x dU U^4 \sqrt{\frac{R^3}{U^3}\left(1 + \left(B_{tU} + 2\pi\alpha' F_{tU}\right)^2\right) + f_T(U) x_4'^2} \tag{4.59}$$

$T_{\rm D8}$ is the brane tension and we have used that the dilaton is given by

$$e^{\phi} = g_s \left(\frac{U}{R}\right)^{\frac{3}{4}} \tag{4.60}$$

Furthermore, we may set the U components of the gauge potentials to zero with an appropriate choice of gauge, therefore $F_{tU} = -\partial_U A_t = -A'$ and Chern Simons terms do not contribute to the action.

Since the action only depends on derivatives of x_4 and A we have very simple equations of motion that after one integration take the following form. The equation of motion for x_4 is given by

$$\frac{U^4 f_T(U) x_4'}{\sqrt{f_T(U) x_4'^2 + \left(\frac{R}{U}\right)^3 \left(1 + \left(B_{tU} + 2\pi\alpha' F_{tU}\right)^2\right)}} = \frac{k g_s}{N_f T_{\rm D8} {\rm Vol}\left(S^4\right)} = \tilde{k} \tag{4.61}$$

and the equation of motion for F_{tU} is

$$\frac{U R^3 \left(B_{tU} + 2\pi\alpha' F_{tU}\right)}{\sqrt{f_T(U) x_4'^2 + \left(\frac{R}{U}\right)^3 \left(1 + \left(B_{tU} + 2\pi\alpha' F_{tU}\right)^2\right)}} = \frac{d g_s}{2\pi\alpha' N_f T_{\rm D8} {\rm Vol}\left(S^4\right)} = \tilde{d} \tag{4.62}$$

where k and d are constants determined by boundary conditions. As before there are two different types of brane profile allowed by these equations of motion. The first is where the brane extends all the way to the thermal horizon, covering all of the radial direction, and secondly, where the brane turns around meeting a $\overline{\rm D8}$ at some finite radius U_0. In the low temperature phase only the latter solution is allowed, because the x_4 circle in the low temperature geometry shrinks to zero size first while the thermal circle remains

finite sized over the whole range of the radial coordinate. The converse is true in the high temperature case, allowing both types of solution described above. In the Sakai-Sugimoto model these solutions are dual to the chiral symmetric and broken phases in the boundary theory respectively.

It is straightforward to fix the constants above by considering boundary conditions. Consider (4.61) at some point such that $x_4'(U) = 0$. We find

$$\tilde{k} = \mathcal{O}(x_4') \tag{4.63}$$

Therefore $\tilde{k}$ is forced to vanish. We will find a useful constraint on $\tilde{d}$ for this type of embedding later.

Consider now the other type of solution where the brane turns around. There must be some point $U = U_0$ where the slope of $x_4(U)$ diverges so consider $x_4'(U = U_0) \to \infty$. From (4.61) we find

$$\tilde{k} = U_0^4 \sqrt{f_T(U_0)} \tag{4.64}$$

and from equation (4.62)

$$\tilde{d} = \mathcal{O}\left(\frac{1}{x_4'}\right) \tag{4.65}$$

So for this type of embedding, $\tilde{d}$ is forced to vanish[4]. Note that this analysis is analogous to the real chemical potential case studied in [104].

Consider the case where the D8 branes extend all the way to the thermal horizon. From equation (4.62) we can solve for $(B_{tU} + 2\pi\alpha' F_{tU})$ and plug back into (4.61). Doing this we find

$$(B_{tU} + 2\pi\alpha' F_{tU})^2 = \frac{\tilde{d}^2\left(1 + \frac{U^3}{R^3} f_T(U) x_4'^2\right)}{R^3 U^5 - \tilde{d}^2} \tag{4.66}$$

[4]This is strictly $\tilde{d} = \mathcal{O}\left(\frac{F_{Ut}}{x_4'}\right)$ which does not necessarily constrain $\tilde{d}$ to vanish if F_{Ut} diverges. One may assume $U = U(x_4)$ rather than $x_4 = x_4(U)$ as used to derive (4.57) to show that this is not the case and $\tilde{d}$ does indeed vanish for this type of embedding.

and hence

$$\frac{U^4 f_T(U) x_4'}{\sqrt{f_T(U)x_4'^2 + \left(\frac{R}{U}\right)^3 \left(1 + \frac{\tilde{d}^2\left(1+\left(\frac{U}{R}\right)^3 f_T(U) x_4'^2\right)}{U^5 R^3 - \tilde{d}^2}\right)}} = 0 \tag{4.67}$$

One can see that (4.67) admits constant solutions that cover the entire range of the U direction, falling into the horizon at $U = U_T$. Since for these solutions x_4 is arbitrary and any value of x_4 will be have the same action, these solutions must correspond to the phase where chiral symmetry is unbroken and the quarks in the boundary theory are exactly massless. To ensure the reality of $(B_{tU} + 2\pi\alpha' F_{tU})$ to produce an imaginary chemical potential in the gauge theory, and to ensure the reality of x_4 one can see there is a constraint on $\tilde{d}$ from (4.66):

$$\tilde{d}^2 \leq R^3 U_T^5 \tag{4.68}$$

In contrast to the condition derived the previous section, the condition here does not depend on the horizon value of $x_4(U)$. In the D3/D7 case the bound on $\tilde{d}$ depended on the asymptotic value of the slipping mode, or the quark mass in the language of the gauge theory. As described above this type of solution only corresponds to strictly massless quarks.

4.4.2 The Potential

The unbroken chiral symmetry case

Firstly, we note that for all phases of the Sakai-Sugimoto model the Lagrangian quark mass is zero, furthermore in this phase there can be no dynamically generated quark mass as that would break chiral symmetry. As mentioned previously it was shown in [137], the chemical potential is related to the worldvolume gauge field on the gravity side while the expectation value of the Polyakov loop in the theory is related to the NS-NS 2 form. Together we have

$$\alpha - \beta\mu_I = \frac{1}{2\pi\alpha'} \int_{D_2} (B_{tU} + 2\pi\alpha' F_{tU}) \tag{4.69}$$

where the integral is over the thermal cigar. Plugging into this using (4.66) we find an explicit expression for $\alpha - \beta\mu_I$

$$\alpha - \beta\mu_I = \frac{\beta}{2\pi\alpha'}\int_{U_T}^{\infty} dU \frac{\tilde{d}}{\sqrt{U^5 R^3 - \tilde{d}^2}} \tag{4.70}$$

To find the potential we evaluate the (renormalised) action and eliminate $\tilde{d}$ to find S in terms of $\alpha - \beta\mu_I$. In the simple case of black hole embeddings the integrals can be done analytically and we find $\alpha - \beta\mu_I$ is given by a hypergeometric function

$$\begin{aligned}(\alpha - \beta\mu_I) = \frac{d^{\frac{2}{5}}}{2\pi\alpha' T}\Bigg(&\frac{(-1)^{\frac{3}{10}}\Gamma\left(\frac{3}{10}\right)\Gamma\left(\frac{6}{5}\right)}{\sqrt{\pi}R^{\frac{3}{5}}} \\ &- \frac{d^{\frac{3}{5}}U_T\sqrt{1-\frac{R^3U_T^5}{d^2}}\,{}_2F_1\left(\frac{1}{5},\frac{1}{2},\frac{6}{5},\frac{R^3U_T^5}{d^2}\right)}{\sqrt{R^3U_T^5 - d^2}}\Bigg)\end{aligned} \tag{4.71}$$

Plugging into the action (4.59) with the equations of motion and the constraints found for black hole embeddings above we find

$$S = \frac{\sqrt{R^3}N_f T_{\mathrm{D8}}\mathrm{Vol}\left(S^4\right)\mathrm{Vol}\left(\mathbb{R}^3\right)\beta}{g_s}\int_{U_T}^{\infty} dU \frac{U^5}{\sqrt{U^5 - \frac{\tilde{d}^2}{R^3}}} \tag{4.72}$$

Let us relabel the overall constant $\mathcal{A} = \frac{\sqrt{R^3}N_f T_{\mathrm{D8}}\mathrm{Vol}\left(S^4\right)\mathrm{Vol}\left(\mathbb{R}^3\right)\beta}{g_s}$. This integral is divergent, so after regulating we may add a counterterm to cancel the divergence

$$S = \mathcal{A}\int_{U_T}^{\Lambda} dU \frac{U^5}{\sqrt{U^5 - \frac{\tilde{d}^2}{R^3}}} - \mathcal{A}\frac{2\Lambda^{7/2}}{7} \tag{4.73}$$

Evaluating the integral and taking the limit $\Lambda \to \infty$ we find we may write the action exactly in terms of a hypergeometric function,

$$S = \frac{2}{7}\mathcal{A}U_T\sqrt{U_T^5 - \frac{\tilde{d}^2}{R^3}}\left(\frac{(-1)^{\frac{3}{10}}\tilde{d}^{\frac{7}{5}}\Gamma\left(\frac{3}{10}\right)\Gamma\left(\frac{6}{5}\right)}{\sqrt{\pi}R^{\frac{21}{10}}U_T\sqrt{U_T^5 - \frac{\tilde{d}^2}{R^3}}} - 1 + \frac{{}_2F_1\left(\frac{1}{5},\frac{1}{2},\frac{6}{5},\frac{R^3U_T^5}{\tilde{d}^2}\right)}{\sqrt{1-\frac{R^3U_T^5}{\tilde{d}^2}}}\right) \tag{4.74}$$

Using $\tilde{d}$ as a parameter we find figure 4.14. Since the potential is truncated

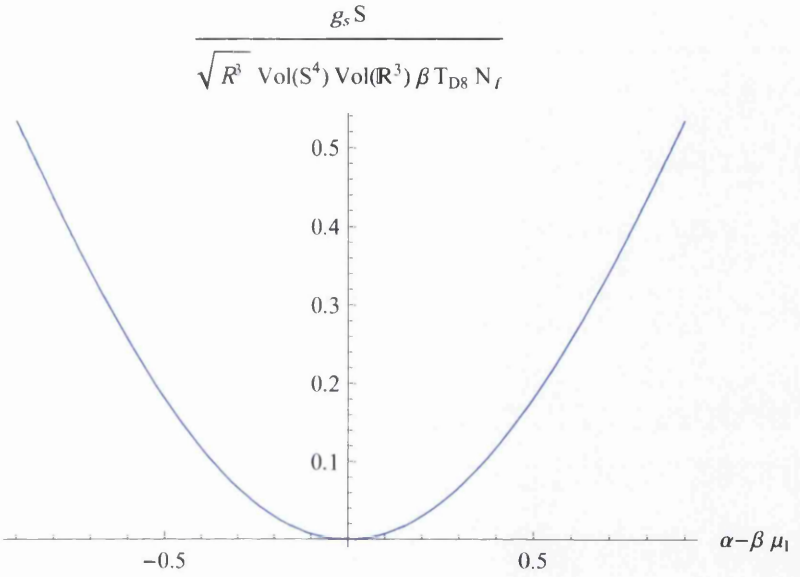

Figure 4.14: The Roberge-Weiss potential as a function of $\alpha - \beta\mu_I$

at order $\frac{1}{N}$, it is instructive to expand these expressions for small $\tilde{d}$ and eliminate to find S in terms of $\alpha - \beta\mu_I$, we find the first order correction to the action and $(\alpha - \beta\mu_I)$ as a function of $\tilde{d}$

$$\alpha - \beta\mu_I \approx \frac{\tilde{d}}{3\pi\alpha' T R^{\frac{3}{2}} U_T^{\frac{3}{2}}} + \mathcal{O}\left(\tilde{d}^3\right) \tag{4.75}$$

$$S \supset \frac{\mathcal{A}\tilde{d}^2}{3R^3 U_T^{\frac{3}{2}}} + \mathcal{O}\left(\tilde{d}^4\right) \tag{4.76}$$

hence

$$S \supset 3\pi^2\alpha'^2\mathcal{A}T^2 U_T^{\frac{3}{2}}(\alpha - \beta\mu_I)^2 + \mathcal{O}\left((\alpha - \beta\mu_I)^4\right) \tag{4.77}$$

We wish to write this expression in terms of field theory quantities. In the high temperature phase the x_4 direction is finite sized over the whole range of the radial coordinate so there is no constraint on it to ensure regularity at the horizon. The size of the x_4 direction is therefore arbitrary and is related

to the Kaluza Klein mass scale simply by

$$\frac{1}{M_{\mathrm{KK}}} = 2\pi R_{x_4} \tag{4.78}$$

The tension of the D8 brane is a dimension 9 object related to the string length by $T_{\mathrm{D8}} = \left((2\pi)^8 l_s^9\right)^{-1}$. We can relate the radius of curvature and the string coupling to gauge theory quantities using the following (from [48])

$$\frac{R^3}{l_s^3} = \pi g_s N, \quad g_s = \frac{g_4^2}{(2\pi)^2 l_s M_{\mathrm{KK}}} \tag{4.79}$$

Where we have used that

$$g_4^2 = \frac{g_5^2}{2\pi R_{x_4}} = M_{\mathrm{KK}} g_5^2 \tag{4.80}$$

Using the relation between the temperature and the position of the horizon (2.31) we find the potential due to flavour degrees of freedom in terms of field theory quantities is

$$V_{\mathrm{eff}} \supset \frac{\lambda N N_f T^4 \mathrm{Vol}\left(\mathbb{R}^3\right)}{1728\pi M_{\mathrm{KK}}} (\alpha - \beta\mu_I)^2 + \mathcal{O}\left((\alpha - \beta\mu_I)^4\right) \tag{4.81}$$

We have used that $\mathrm{Vol}\left(S^4\right) = \frac{\pi^2}{12}$. The potential from the flavours is quadratic, for type IIB the analogous potential due to the adjoint degrees of freedom was periodic from an argument in [40] which we generalised to type IIA in [120]. This was discussed in section 4.3.2.

The broken chiral symmetry case

In the language of the gravity theory this corresponds to Minkowski brane embeddings that turn around at some finite $U_0 > U_T$. In contrast to the previous case, there must be a dynamically generated quark mass in this phase, which is given by

$$m_Q = \frac{1}{2\pi\alpha'} \int_{U_T}^{U_0} dU \sqrt{|g_{tt} g_{UU}|} = \frac{1}{2\pi\alpha'} \left(U_0 - U_T\right) \tag{4.82}$$

Hence, chiral symmetry is no longer a symmetry of the theory. Moreover, as shown previously d must vanish for these solutions. Together with (4.62) this implies that $B_{tU} + 2\pi\alpha' F_{tU} = 0$ and hence the potential does not depend on $\alpha - \beta\mu_I$. Since μ_I is interpreted as $\lim_{U\to\infty}[A(U)]$ we are still able to introduce a chemical potential via the introduction of a constant gauge field, but the physics remains smooth for all values of this chemical potential.

This analysis is also applicable to the low temperature geometry where this type of D8 - $\overline{\text{D8}}$ embedding is the only one allowed. The conclusion is the same and the potential does not depend on $\alpha - \beta\mu_I$. All of this is very similar to the equivalent discussion for the D3/D7 system in the previous section.

4.4.3 The Phase Diagram

At low temperatures the only solutions allowed are Minkowski embeddings so the phase diagram has no phase transitions. Above a certain temperature there is a transition from (2.29) to (2.30) and both types of solution are then allowed. We will compute the phase diagram of the theory at high temperature by considering the difference in the DBI actions of the two types of solution, dual to the grand canonical ensemble in the gauge theory. After applying the conditions for each of the solutions derived above and substituting in using the equations of motion we find

$$S_{\text{Mink}} = \mathcal{C}\int_{U_0}^{\infty} dU U^5 \sqrt{\frac{U^3 f(U)}{U^8 f(U) - U_0^8 f(U_0)}} \tag{4.83}$$

$$S_{\text{BH}} = \mathcal{C}\int_{U_T}^{\infty} dU \frac{U^5}{\sqrt{U^5 - \frac{\tilde{d}^2}{R^3}}} \tag{4.84}$$

$$\mathcal{C} = \frac{\sqrt{R^3} N_f T_{\text{D8}} \text{Vol}(S^4)\,\text{Vol}(\mathbb{R}^3)\,\beta}{g_s} \tag{4.85}$$

hence we define

$$\begin{aligned}\Delta S &= \frac{1}{C}\left(S_{\text{Mink}} - S_{\text{BH}}\right) \\ &= \int_{U_0}^{\infty} dU U^5 \left(\sqrt{\frac{U^3 f(U)}{U^8 f(U) - U_0^8 f(U_0)}} - \frac{1}{\sqrt{U^5 - \frac{\tilde{d}^2}{R^3}}}\right) + \\ &\quad - \int_{U_T}^{U_0} dU \frac{U^5}{\sqrt{U^5 - \frac{\tilde{d}^2}{R^3}}}\end{aligned} \tag{4.86}$$

When $\Delta S = 0$ there is a phase transition. It is worth making some remarks on the method used in [104] to compute the phase diagram of the Sakai-Sugimoto model in the presence of a real chemical potential. The following dimensionless coordinates were used to eliminate U_0 from ΔS

$$u_T = \frac{U_T}{U_0} \qquad u = \frac{U}{U_0} \qquad c^2 = \frac{\tilde{d}^2}{R^3 U_0^5} \tag{4.87}$$

where Wick rotating c would recover the real chemical potential result. In terms of these coordinates we have

$$\begin{aligned}\Delta S_{\text{Dimensionless}} &= \int_1^{\infty} du u^5 \left(\sqrt{\frac{u^3 f(u)}{u^8 f(u) - f(1)}} - \frac{1}{\sqrt{u^5 - c^2}}\right) + \\ &\quad - \int_{u_T}^{1} du \frac{u^5}{\sqrt{u^5 - c^2}}\end{aligned} \tag{4.88}$$

Henceforth we shall refer to the difference in the actions in dimensionless coordinates of [104] as $\Delta S_{\text{Dimensionless}}$, while in the dimensionful coordinates we shall denote it as ΔS. Evaluating (4.88) for $c = 0$ or for zero chemical potential we find figure 4.15. There are two zeros, one of which occurs at approximately $u_T = 0.74$ which corresponds to the $\mu = 0$ limit of the real chemical potential phase transition line. This was originally computed in [48, 49]. The second is at $u_T = 1$ which, when one considers a real chemical potential is lifted and does not contribute to the phase diagram. When we consider an imaginary chemical potential however, this zero persists and would lead to a second phase transition line on the phase diagram. We will

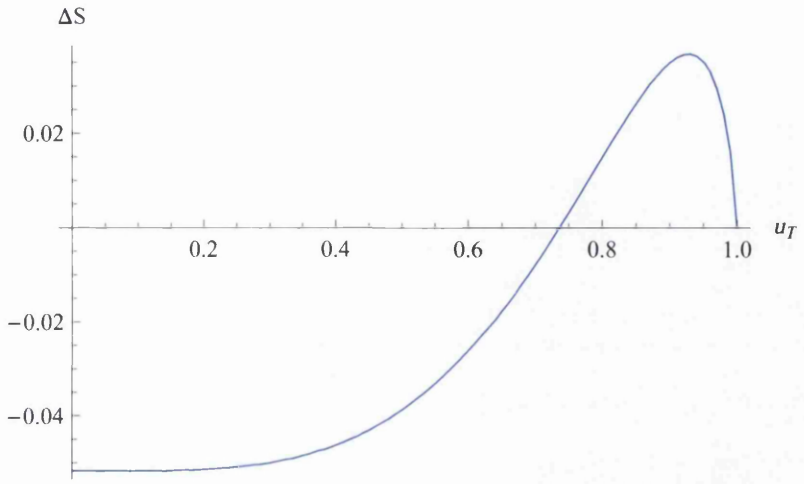

Figure 4.15: The plot of ΔS against $u_T = \frac{U_T}{U_0}$ for zero chemical potential

show that the phase transition line that this zero leads to should not, in fact be present on the phase diagram. Consider the expression relating the dimensionless horizon position and the temperature (from equation (2.31))

$$T = \frac{3}{4\pi}\sqrt{\frac{U_0 u_T}{R^3}} \tag{4.89}$$

The asymptotic separation of the D8 - $\overline{\text{D8}}$ pair is L and is given by

$$\begin{aligned} L &= 2\lim_{U\to\infty} x_4(U) \\ &= 2\int_{U_0}^{\infty} dU x_4'(U) \\ &= 2\sqrt{R^3}\int_{U_0}^{\infty} dU \frac{1}{\sqrt{U^3 f(U)\left(\frac{U^8}{U_0^8}\frac{f(U)}{f(U_0)} - 1\right)}} \\ &= \sqrt{\frac{R^3}{U_0}} F(u_T) \end{aligned} \tag{4.90}$$

where

$$F(u_T) = 2\int_1^{\infty} du \frac{1}{\sqrt{u^3 f(u)\left(u^8 \frac{f(u)}{f(1)} - 1\right)}} \tag{4.91}$$

Note that for black hole embeddings L is arbitrary, so we consider Minkowski embeddings by plugging in for x_4' using (4.61). Using (4.90) to eliminate U_0 from (4.89)

$$TL = 2\sqrt{u_T}F(u_T) \tag{4.92}$$

TL as a function of u_T is not a monotonically increasing function and has a global maximum, it is shown in figure 4.16. Suppose we consider a fixed

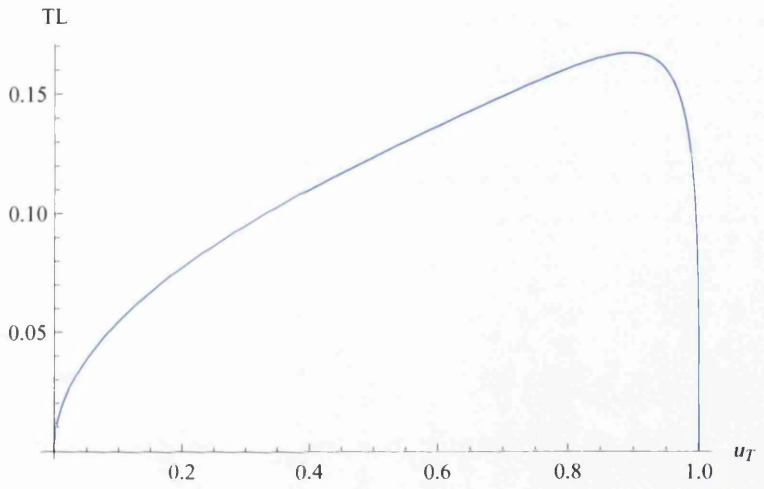

Figure 4.16: TL as a function of u_T

T and L. There are two allowed Minkowski embeddings that have the same value of TL but have different values of u_T. For a fixed u_T however there is only one Minkowski embedding with a particular allowed value of TL. We wish to compute the phase diagram by considering the action for all allowed solutions at each TL and chemical potential (there are three - one black hole embedding and the two Minkowski embeddings), the one that has the lowest action dominates. Using u_T as a parameter to do this is problematic because for each u_T we are only considering one of the Minkowski embeddings allowed at that particular TL. Computing the phase diagram using a parameter that only considers a subset of allowed solutions leads to a phase diagram with a phase transition line that would not appear were we to consider the full set of allowed solutions.

The analysis of $\Delta S_{\text{Dimensionless}}$ has one important consequence however: we note that $\Delta S_{\text{Dimensionless}}$ and the combination TL are functions of u_T only

(at zero chemical potential), therefore the action is a function of TL, rather than T and L individually. Consider now the chemical potential. Rewriting (4.70) using the dimensionless coordinates we have

$$\alpha - \beta\mu_I = \beta U_0 \int_{u_T}^{\infty} du \frac{c}{\sqrt{u^5 - c^2}} \tag{4.93}$$

eliminating U_0 as before we have

$$\frac{L^2}{\beta R^3}(\alpha - \beta\mu_I) = F(u_T) \int_{u_T}^{\infty} du \frac{c}{\sqrt{u^5 - c^2}} \tag{4.94}$$

hence, the combination of the chemical potential and the expectation value of the phase of the Polyakov loop is a function of u_T and c, and vanishes when $c \to 0$. There are two scales on the gravity side (c and u_T) that correspond to two meaningful scales on the gauge theory side, TL and $\frac{L^2}{\beta R^3}(\alpha - \beta\mu_I)$, which we will denote by $\overline{T}$ and $\overline{\mu}$ respectively. We will plot the phase diagram of the model as a function of these two parameters. The phase diagram is computed by finding the zeros of ΔS (4.86) as a function of U_T, $\tilde{d}$ for a fixed U_0 and converting these coordinates to $\overline{T}$ and $\overline{\mu}$. We note that repeating this computation for various values U_0 reproduces the same phase diagram, which is shown in 4.17. The blue line is the first order phase transition line that extends from the phase transition point found in [48, 49] for zero chemical potential. The shaded area of the plot is the area where the chiral symmetry broken phase dominates and the unshaded area is the one where chiral symmetry is restored.

The issue we have noted regarding the use of the dimensionless coordinates to study the phase structure of the model was not problematic for real chemical potential. We will now show why this was the case. Consider $\Delta S_{\text{Dimensionless}}$ for the theory when $\overline{\mu}$ is small. Expanding in powers of c and similarly expanding equation (4.94) we may capture the leading behaviour

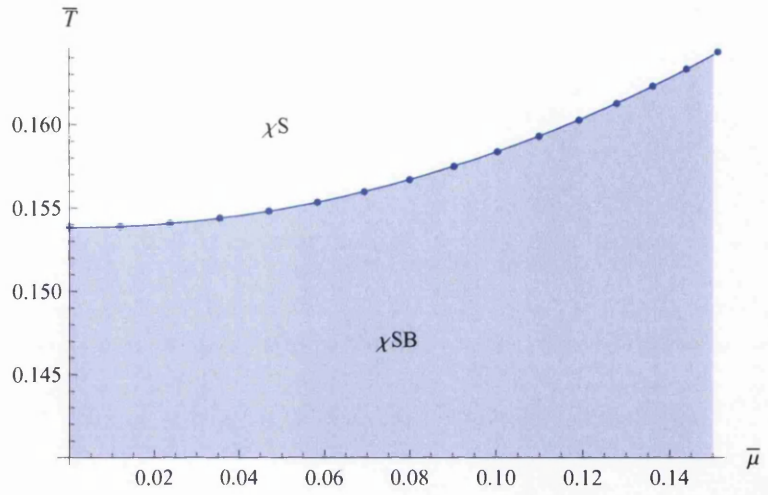

Figure 4.17: The phase diagram of the Sakai-Sugimoto model with an imaginary chemical potential as a function of the dimensionless temperature and chemical potential.

of $\Delta S_{\text{Dimensionless}}$ as a function of $\overline{\mu}$

$$\begin{aligned}\Delta S_{\text{Dimensionless}} &\approx \Delta S_{\text{Dimensionless}}\big|_{c=0} - \frac{9\overline{\mu}^2}{52F\left(u_T\right)^2\sqrt{u_T^7}} + \mathcal{O}\left(\overline{\mu}^4\right) \\ &\approx \Delta S_{\text{Dimensionless}}\big|_{c=0} - \frac{9\overline{\mu}^2}{52\overline{T}^2\sqrt{u_T^5}} + \mathcal{O}\left(\overline{\mu}^4\right) \end{aligned} \tag{4.95}$$

where we have used (4.92) to exchange $F\left(u_T\right)$ for $\overline{T}$. $\Delta S_{\text{Dimensionless}}\big|_{c=0}$ must be evaluated numerically and is shown in figure 4.15. The factors of u_T in the denominator of the above expression are problematic at first sight, however, we note that the limited range of u_T from (4.68) implies $u_T^5 \geq c^2$ so for a fixed value of $c > 0$, u_T must be strictly greater than zero and the first correction term never diverges. When u_T is close to 1, $\Delta S_{\text{Dimensionless}}\big|_{c=0}$ is small and positive. For an imaginary chemical potential the first correction term that appears at order $\overline{\mu}^2$ is negative leading to the second zero of $\Delta S_{\text{Dimensionless}}$. Were we to Wick rotate $\overline{\mu}$ so that we are considering the theory with a real chemical potential the sign of this correction term would be positive, so $\Delta S_{\text{Dimensionless}}$ does not vanish when u_T is close to 1 for a finite but small real $\overline{\mu}$.

Performing a similar expansion for small $\tilde{d}$ on ΔS (4.86) is also instructive. Using an expansion of (4.70) to eliminate $\tilde{d}$ and (2.31) to eliminate U_T we find

$$\Delta S \approx \Delta S|_{\tilde{d}=0} - \frac{64}{9}(\alpha - \beta\mu_I)^2 \pi^5 R^{\frac{9}{2}} T^5 \alpha'^2 + \mathcal{O}\left((\alpha - \beta\mu_I)^4\right) \tag{4.96}$$

We could in principle restore the dimensionful coefficient and rewrite ΔS using field theory quantities, however it is not very enlightening to do so. It is important to note that the first correction term does not depend on U_0 and the equations relating T to U_T and $(\alpha - \beta\mu_I)$ to $\tilde{d}$ contain no dependence on U_0 so the above expression for ΔS contains no hidden factors of U_0. Therefore the system must be well behaved when U_0 approaches U_T, which when one considers the model using the dimensionless coordinates discussed above corresponds to the $u_T \to 1$ regime. This analysis also shows the action depends on the square of the chemical potential, ensuring the analyticity of the phase diagram as a function of $(\alpha - \beta\mu_I)^2$.

In summary, when comparing the actions of the two different types of embedding it is important to work in a coordinate system where there is a one to one correspondence between the position of a horizon and a temperature scale.

In the low temperature phase when $\overline{T} < \overline{T}_d$ where $\overline{T}_d$ is the deconfinement temperature chiral symmetry is broken and the glue in the theory is confined. Above the deconfinement temperature in the chiral symmetry broken phase the glue is deconfined and the theory contains mesons. In the chiral symmetry restored phase the mesons melt and the fundamental degrees of freedom in the theory are quarks and gluons. The quarks are also massless due to the chiral symmetry restoration. Including the Roberge-Weiss lines the phase diagram of the theory is given in figure 4.18. The equation of the phase transition line is

$$\overline{T} = 0.154 + 0.447\overline{\mu}^2 + \mathcal{O}\left(\overline{\mu}^4\right) \tag{4.97}$$

The equation for $\overline{T}$ behaves as expected, ie, is a function of even powers of $\overline{\mu}$.

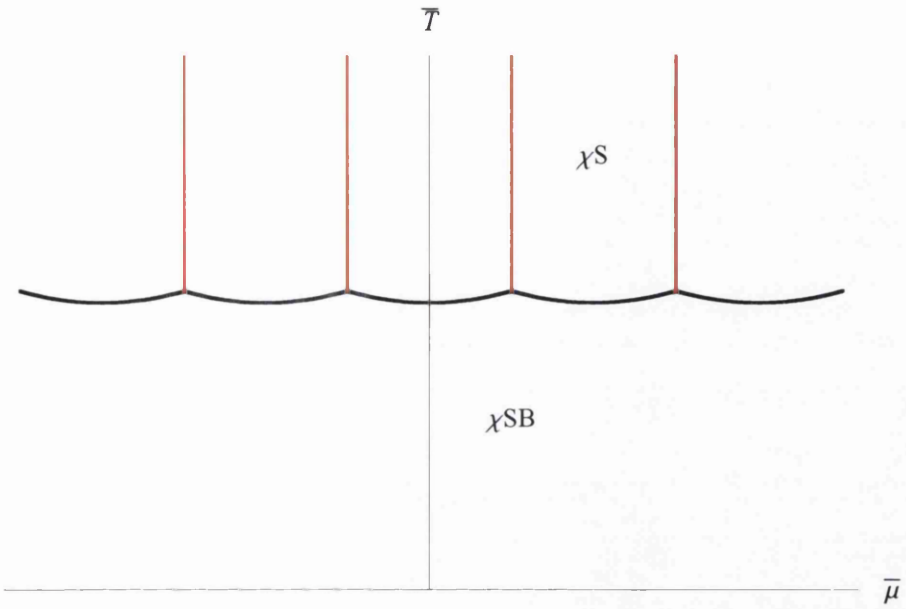

Figure 4.18: The phase diagram of the Sakai-Sugimoto model with an imaginary chemical potential. The black line extends from the line found for the real chemical potential case. The red lines are the Roberge-Weiss lines which appear in the chiral symmetry restored phase. Since the equation of the phase transition line is a function of $\overline{\mu}^2$ the second derivative of the phase transition line is strictly positive so even though the Roberge-Weiss lines appear at order $\frac{1}{N}$ the chiral symmetry breaking transition does show curvature between the Roberge-Weiss lines.

4.4.4 Pressure due to Flavours

We will compute the pressure holographically by studying the DBI action as a function of temperature. From basic thermodynamics

$$F = TdS - PdV + \mu dN_q \tag{4.98}$$

The pressure is given by

$$P = -\frac{\partial F}{\partial V} \tag{4.99}$$

holographically, the DBI action is dual to the free energy density in the grand canonical ensemble, therefore it is also related to the pressure. The

DBI action is

$$S_{\text{DBI}} = \int dU d\tau d^3x d\Omega_4 \mathcal{L}_{\text{DBI}} \tag{4.100}$$

The integrals over the field theory directions contribute a volume of $\mathbb{R}^3$ and a factor of β, because $\mathcal{L}_{\text{DBI}}$ is not a function of these directions. One may go from the energy density to the pressure by dividing through by these factors or we may directly compute the pressure by evaluating

$$P = -\int dU d\Omega_4 \mathcal{L}_{\text{DBI}} \tag{4.101}$$

Black Hole Embeddings - Zero Density

When the density is zero the pressure takes a simple form

$$P_{\text{BH}} = -\mathcal{N} \int_{U_T}^{\infty} dU U^{\frac{5}{2}} \tag{4.102}$$

we have relabelled the overall constant in front of the pressure as

$$\mathcal{N} = \frac{\pi^2 \sqrt{R^3} N_f T_{\text{D8}}}{12 g_s} \tag{4.103}$$

Regulating the integral and adding a counterterm to cancel the divergence as $\Lambda \to \infty$ we have

$$P_{\text{BH}} = -\lim_{\Lambda \to \infty} \mathcal{N} \left(\frac{2U^{\frac{7}{2}}}{7} \Big|_{U_T}^{\Lambda} - \frac{2\Lambda^{\frac{7}{2}}}{7} \right) \tag{4.104}$$

Hence

$$P_{\text{BH}} = \frac{2}{7} \mathcal{N} U_T^{\frac{7}{2}} \tag{4.105}$$

Using the expression for the temperature given in (2.31) we can show

$$P_{\text{BH}} = \frac{2^4}{7} \frac{(2\pi)^9 T_{\text{D8}} N_f}{3^8 g_s} R^{12} T^7 \tag{4.106}$$

Using the expressions given in section 4.4.2 we find the pressure in terms of field theory quantities is

$$P_{\rm BH} = \frac{\lambda^3}{7.3^8}\frac{N_f N}{2\pi}T^4\left(\frac{T}{M_{\rm KK}}\right)^3 \tag{4.107}$$

where $\lambda = g_4^2 N$. This expression is quite surprising, even though the pressure is given by T^4 multiplied by a dimensionless function as we expect from dimensional analysis, the overall dependence of the pressure on the temperature is T^7.

Non Zero Density

Expanding $P_{\rm BH}$ for small $\tilde{d}$ we have

$$P_{\rm BH} = \mathcal{N}\int_{U_T}^{\infty} dU\left(U^{5/2} + \frac{\tilde{d}^2}{2R^3U^{5/2}} + \mathcal{O}\left(\tilde{d}^4\right)\right) \tag{4.108}$$

Evaluating the integral as before, showing only the first order correction for non zero d

$$P_{\rm BH} \supset -\mathcal{N}\left(\frac{3^2\tilde{d}^2}{(4\pi)^3 R^{\frac{15}{2}}T^3} + \mathcal{O}\left(\tilde{d}^4\right)\right) \tag{4.109}$$

For small density we can expand the expression for the chemical potential (assuming the phase of the Polyakov loop vanishes)

$$\mu_I = -\frac{1}{2\pi\alpha'}\int_{U_T}^{\infty} dU\frac{\tilde{d}}{\sqrt{U^5R^3 - \tilde{d}^2}} \tag{4.110}$$

$$\Rightarrow d \approx \frac{8\pi^5\left(2\pi\alpha'\right)^2 N_f T_{\rm D8}}{3^3 g_s}R^6T^3\mu_I + \mathcal{O}\left(\mu_I^3\right) \tag{4.111}$$

where we have restored the correct dimensionality of the density. In terms of field theory quantities, the density in terms of the chemical potential is

$$d \approx \frac{N_f N}{2\pi}\frac{T^3\lambda\mu_I}{2^4 3^3 M_{\rm KK}} + \mathcal{O}\left(\mu_I^3\right) \tag{4.112}$$

The first order correction depends on the square of the chemical potential and it is

$$-\frac{N_f N}{2\pi}\frac{\lambda}{2^5 3^3}\frac{T^3\mu^2}{M_{\rm KK}}+\mathcal{O}\left(\mu^4\right) \tag{4.113}$$

Together, the leading order behaviour of the pressure is

$$P=\frac{1}{3^3}\frac{N_f N}{2\pi}T^4\left(\frac{\lambda^3}{7.3^5}\left(\frac{T}{M_{\rm KK}}\right)^3-\frac{\lambda}{2^5}\frac{\mu^2}{TM_{\rm KK}}+\mathcal{O}\left(\mu^4\right)\right) \tag{4.114}$$

Since the pressure is a mass dimension 4 object, the expression for the pressure will always be proportional to T^4 multiplied by a dimensionless function of the scales in the problem, in this case T, μ_I and $M_{\rm KK}$. An expected feature of the expression for the pressure is that the leading order term dominates when the temperature is very large but, as commented previously, the pressure computed here does not correlate with what is known in QCD. The action for the black hole embeddings can be evaluated exactly in terms of a hypergeometric function, and it is

$$\begin{aligned}P=&\frac{N_f N\lambda^3}{7.2^2 3^8\pi^{\frac{5}{2}}(\mathcal{T}-1)\mathcal{T}^{\frac{7}{10}}}\left(\frac{T}{M_{\rm KK}}\right)^3 T^4\Bigg((-1)^{\frac{3}{10}}(\mathcal{T}-1)\Gamma\left(\frac{3}{10}\right)\Gamma\left(\frac{6}{5}\right)\\&-\sqrt{\pi}\sqrt{\mathcal{T}-1}\mathcal{T}^{\frac{6}{5}}+\sqrt{\pi}(\mathcal{T}-1)^{\frac{3}{2}}\mathcal{T}^{\frac{1}{5}}{}_2F_1\left(\frac{7}{10},1,\frac{6}{5},\mathcal{T}\right)\Bigg)\end{aligned} \tag{4.115}$$

where

$$\mathcal{T}=\frac{N_f^2 N^2}{(2\pi)^2}\frac{\lambda^4}{2^4 3^{12}}\frac{T^{10}}{M_{\rm KK}^4 d^2} \tag{4.116}$$

Since this formalism captures the strong coupling behaviour of the field theory expanding for large 't Hooft coupling is a natural thing to do

$$P\approx T^4\left(\frac{N_f N}{2\pi}\frac{\lambda^3}{7.3^8}\frac{T^3}{M_{\rm KK}^3}-\frac{2\pi}{N_f N}\frac{6^3}{7\lambda}\frac{d^2 M_{\rm KK}}{T^7}+\mathcal{O}\left(\frac{1}{\lambda^5}\right)\right) \tag{4.117}$$

When one substitutes in for small d in terms of μ_I using (4.112) the same result as for the small density expansion is obtained (4.114).

Minkowski Embeddings

The integral over the radial direction for the action of Minkowski embeddings cannot be evaluated in closed form. The pressure for the Minkowski embeddings is

$$P_{\text{Mink}} = -\mathcal{N}\int_{U_0}^{\infty} dU U^5 \sqrt{\frac{U^3 f(U)}{U^8 f(U) - U_0^8 f(U_0)}} \tag{4.118}$$

Rewriting:

$$P_{\text{Mink}} = -\mathcal{N}\int_{U_0}^{\infty} dU \frac{U^{\frac{5}{2}}}{\sqrt{1 - \frac{U_0 f(U_0)}{U f(U)}}} \tag{4.119}$$

Replacing U_0 using

$$2\pi\alpha' m_q = M = U_0 - U_T \tag{4.120}$$

and expanding in powers of M (note, since the lower limit of integration is a function of M we expand the integrand, evaluate the integral and then expand the result. The first order correction only receives contributions from the first order of the expansion of the integrand, while the corrections at order M^2 contain contributions from higher orders of the expansion of the integrand.)

In the zero mass limit the pressure for Minkowski embeddings captures the same behaviour of the chiral symmetry restored phase so we choose to only consider the terms proportional to M as the leading behaviour. To $\mathcal{O}(M^2)$ we have

$$\begin{aligned} P_{\text{Mink}} = -\mathcal{N}\int_{U_0}^{\infty} dU \Bigg(& \frac{3U_T^7 M}{2U^{5/2}\left(U^3 - U_T^3\right)} + \\ & + \frac{9U_T^6\left(8U^8 - 8U^5 U_T^3 + 3U_T^8\right)M^2}{8U^{15/2}\left(U^3 - U_T^3\right)^2} + \mathcal{O}\left(M^3\right) \Bigg) \end{aligned} \tag{4.121}$$

Once we have performed the integral the leading behaviour of the pressure

is

$$P_{\text{Mink}} = -\frac{\mathcal{N}}{20} M U_T^{5/2} \left(5 \log \left(3.2^4 \left(\frac{U_T}{M} \right)^2 \right) + 5\sqrt{3}\pi - 12 \right) \tag{4.122}$$

using the above expressions to rewrite in terms of field theory quantities we have

$$P_{\text{Mink}} = -\frac{\lambda^2}{5.2^4 3^6} \frac{N_f N}{2\pi} T^4 \frac{m_q T}{M_{\text{KK}}^2} \left(5 \log \left(\frac{64\lambda^2}{27} \frac{T^4}{m_q^2 M_{\text{KK}}^2} \right) + 5\sqrt{3}\pi - 12 \right) \tag{4.123}$$

therefore the leading behaviour is proportional to $T^5 \frac{m_q}{M_{\text{KK}}^2} \log \left(\frac{T^4}{m_q^2 M_{\text{KK}}^2} \right)$.

Hadron Resonance Gas Model

Since the results we have here are for a system which contains bound states of quarks and strong coupling it is natural to compare to the hadron resonance gas model of QCD [148]. This is a model of non interacting hadronic and mesonic resonances, which is a good model of QCD at low temperatures since the quarks are confined and are no longer the physical degrees of freedom of the theory. The pressure contribution of a single particle in this model is given by

$$\beta^4 P_i = \frac{g_i}{2\pi^2} \sum_{k=1}^{\infty} (-\eta)^{k+1} \frac{(\beta m_i)^2}{k^2} K_2 (k\beta m_i) \tag{4.124}$$

β is the inverse temperature, g_i is a degeneracy factor and $\eta = 1$ for bosons and -1 for fermions. K_2 is a modified Bessel function of the second kind. Assuming the mass is small we have

$$\beta^4 P_i = \frac{g_i}{2\pi^2} \sum_{k=1}^{\infty} \left(\frac{2(-\eta)^{1+k}}{k^4} + \frac{\beta^2 (-\eta)^k \eta m_i^2}{2k^2} + \mathcal{O}\left(m^4\right) \right) \tag{4.125}$$

evaluating the sum

$$\beta^4 P_i = \frac{\eta g_i}{2\pi^2} \left(-2\text{Li}_4 (-\eta) + \frac{m_i^2 \beta^2}{2} \text{Li}_2 (-\eta) + \mathcal{O}\left(m_i^4\right) \right) \tag{4.126}$$

Note that Li is a polylogarithm function that contributes a numerical factor when we plug in for η. Note that the first order correction to the pressure for non zero quark mass is

$$P \sim T^4 \frac{m^2}{T^2} \tag{4.127}$$

While we note that the Sakai-Sugimoto is very different from QCD, being 5 dimensional and having a large number of colours etc., the pressure from the hadron resonance gas model exhibits very different behaviour to that found in the Sakai-Sugimoto model above.

4.5 Defect Theories

The work of section 4.3 showed that when one considers $\mathcal{N} = 4$ super Yang-Mills theory with quenched $\mathcal{N} = 2$ flavours at strong coupling, dual to type IIB supergravity on $AdS_5 \times S^5$ with probe D7 branes, in the presence of an imaginary chemical potential the resulting phase diagram contains only first order phase transition lines. Therefore, the points where the Roberge-Weiss lines meet the deconfinement transition are triple points. It would be interesting to find a model where the deconfinement line is not of the first order and one way that could possibly be the case is in a defect theory. This type of background was discussed in a very general way in [134], but we limit ourselves to the background that comes from the backreaction of D3 branes in type IIB supergravity. To include flavours we put N_f D$(7-2k)$ branes into the $AdS_5 \times S^5$ background. k is the number of directions in which the flavour sector does not extend but the colour sector does and is the codimension of the intersection of the branes. We take $k = 1$ ($k = 2$) representing a bulk theory containing N_f D5 (D3-$\overline{\text{D3}}$) probe branes in the geometry that results from N D3 branes where $N \to \infty$. This bulk theory corresponds to a field theory where the fundamental matter lives on a $2+1$ $(1+1)$ dimensional submanifold of the $3+1$ dimensional boundary. The adjoint fields live in the full $3+1$ dimensions of the boundary. $k = 0$ would correspond to having no defect, ie the D3 /D7 system. In order for the theory to retain $\mathcal{N} = 2$ supersymmetry, the brane must cover $3-k$ spatial dimensions of the bound-

ary and $3-k$ directions of the S^5 in addition to the time direction and the radial direction. This type of theory has been discussed extensively in the literature. See for example [149–152].

The metric corresponding to the high temperature phase of $\mathcal{N}=4$ super Yang-Mills having Wick rotated to Euclidean signature is

$$ds^2 = \left(\frac{r}{R}\right)^2 \left(h(r)d\tau^2 + \delta_{ij}dx^i dx^j\right) + \left(\frac{R}{r}\right)^2 \left(\frac{dr^2}{h(r)} + r^2 d\Omega_5^2\right) \tag{4.128}$$

with

$$h(r) = 1 - \left(\frac{r_h}{r}\right)^4 \tag{4.129}$$

Rescaling the radial coordinate using

$$\frac{d\sigma}{\sigma} = \frac{dr}{r\sqrt{h(r)}} \tag{4.130}$$

leads to the metric

$$ds^2 = \left(\frac{\sigma}{R}\right)^2 h_+(\sigma) \left(\left(\frac{h_-(\sigma)}{h_+(\sigma)}\right)^2 d\tau^2 + \delta_{ij}dx^i dx^j\right) + \left(\frac{R}{\sigma}\right)^2 \left(d\sigma^2 + \sigma^2 d\Omega_5^2\right) \tag{4.131}$$

where i and j run from 1 to 3 and

$$h_\pm(\sigma) = 1 \pm \left(\frac{\sigma_h}{\sigma}\right)^4 \tag{4.132}$$

For convenience we choose to rewrite the metric of the transverse coordinates as

$$d\sigma^2 + \sigma^2 d\Omega_5^2 = d\rho^2 + dy^2 + \rho^2 d\Omega_{3-k}^2 + y^2 d\Omega_{1+k}^2 \tag{4.133}$$

The Hawking temperature in this coordinate system is given by

$$T = \frac{\sqrt{2}}{\pi R}\frac{\sigma_h}{R} \tag{4.134}$$

Assuming that the position of the brane in the y direction is a function of

the radial coordinate only, the induced metric on the brane is given by

$$ds^2_{\mathrm{D}(7-2k)} = \left(\frac{\sigma}{R}\right)^2 h_+(\sigma)\left(\left(\frac{h_-(\sigma)}{h_+(\sigma)}\right)^2 d\tau^2 + \delta_{\tilde{i}\tilde{j}}dx^{\tilde{i}}dx^{\tilde{j}}\right) + \\ + \left(\frac{R}{\sigma}\right)^2 \left(\left(1+y'(\rho)^2\right)d\rho^2 + \rho^2 d\Omega^2_{3-k}\right) \tag{4.135}$$

where $\tilde{i}$ and $\tilde{j}$ run from 1 to $3-k$ and $\sigma^2 = \rho^2 + y^2$. One may now write the DBI action for the D$(7-2k)$ brane and solve the resulting equations of motion to get the profile of the brane, from which we can compute the free energy in the field theory. We note that in the case of field theories dual to D3 brane geometries the resulting boundary theory is always conformal so the equation of motion for the dilaton is solved by a constant for all of the defect theories we consider.

4.5.1 Brane Embedding

From the induced metric of a D$(7-2k)$ brane (4.135) we can write the DBI action of N_f branes including a worldvolume gauge field living on them in the same way as for the models considered above

$$S_{\mathrm{D}(7-2k)} = T_k N_f \beta V_k \mathrm{Vol(Defect)} \int d\rho \rho^{3-k} h_+^{\frac{3-k}{2}} \sqrt{\frac{h_-^2}{h_+}\left(1+y'^2\right) + \left(B+2\pi\alpha' F\right)^2} \tag{4.136}$$

Note that T_k is the tension of the branes and β is the inverse temperature. V_k is the volume of an S^{3-k}. Since the action only depends on the derivative of the gauge potential and not the gauge potential itself there is an integral of motion

$$\frac{\partial \mathcal{L}}{\partial F} = c_F \Rightarrow \frac{c_F}{2\pi\alpha' T_k N_f V_k} = \tilde{c}_F = \frac{\left(B+2\pi\alpha' F\right)\rho^{3-k} h_+^{\frac{3-k}{2}}}{\sqrt{\frac{h_-^2}{h_+}\left(1+y'^2\right) + \left(B+2\pi\alpha' F\right)^2}} \tag{4.137}$$

hence

$$\left(B+2\pi\alpha' F\right)^2 = \frac{h_-^2}{h_+}\frac{\tilde{c}_F^2\left(1+y'^2\right)}{\rho^{2(3-k)}h_+^{3-k} - \tilde{c}_F^2} \tag{4.138}$$

The other equation of motion is

$$\frac{\partial}{\partial\rho}\left[\rho^{3-k}\frac{3-k}{2}h_+^{\frac{5-k}{2}}\frac{\partial h_+}{\partial\rho}\mathcal{G}\left(y',y,\rho\right)+\frac{h_-h_+^{\frac{7-k}{2}}}{2}\frac{1+y'^2}{\mathcal{G}\left(y',y,\rho\right)}\left(\frac{\frac{\partial h_-}{\partial\rho}h_+-h_-\frac{\partial h_+}{\partial\rho}}{h_+^2}\right)\right]=\frac{2y'\rho^{3-k}h_+^{\frac{3-k}{2}}}{\mathcal{G}\left(y',y,\rho\right)} \tag{4.139}$$

with

$$\mathcal{G}\left(y',y,\rho\right)=\sqrt{\frac{h_-^2}{h_+^2}\left(1+y'^2\right)+\left(B+2\pi\alpha' F\right)^2} \tag{4.140}$$

We find solutions for the embedding function $y(\rho)$ by using equation (4.138) to eliminate $(B+2\pi\alpha' F)$ from (4.139) and solving numerically. As before for Minkowski embeddings, one can show it is not possible to turn on a non constant gauge field A however all chemical potentials are accessible via the asymptotic value of a constant gauge field. This means that the action, which only depends upon the derivative of A does not depend on the chemical potential for Minkowski embeddings. Furthermore, for black hole embeddings there is a constraint on $\tilde{c}_F$ that comes from (4.138). To ensure the reality of $(B+2\pi\alpha' F)$ and hence to ensure the chemical potential is purely imaginary we must have

$$\tilde{c}_F < 2^{\frac{3-k}{2}}\rho_h^{3-k} \tag{4.141}$$

Since we expect there to be Roberge-Weiss lines at $\mu_I \sim \frac{1}{N}$ exploring the behaviour of the theory for small $\tilde{c}_F$ is sufficient.

Once solutions are found we evaluate the renormalised DBI action[5], dual to the grand canonical ensemble in the gauge theory and observe the transition between the two types of solution. The chemical potential is the asymptotic value of the worldvolume gauge field on the flavour branes, while the expectation value of the phase of the Polyakov loop is similarly related to

[5]The counterterm that exists for all defect theories is $S_{ct1} = -TN_f\beta\text{Vol}(S^{3-k})\text{Vol}(\text{Defect})\frac{\Lambda^{4-k}}{4-k}$. In the case of $k=2$ defects there is an additional counterterm which we will describe below

the NS - NS B field, as before.

$$\alpha - \beta\mu_I = \int_{D_2} (B + 2\pi\alpha' F) = \tilde{c}_F \beta \int_{\rho_h}^{\infty} d\rho \frac{h_-}{h_+} \sqrt{\frac{(1+y'^2)}{\rho^{2(3-k)} h_+^{3-k} - \tilde{c}_F^2}} \quad (4.142)$$

Consider the theory when the chemical potential is small. Expanding (4.138) in powers of $\tilde{c}_F$ and integrating we find

$$\alpha - \beta\mu_I \approx \Psi \tilde{c}_F + \mathcal{O}\left(\tilde{c}_F^3\right) \quad (4.143)$$

where

$$\Psi = \beta \int_{\rho_h}^{\infty} d\rho \sqrt{1+y'^2} \rho^{k-3} h_- h_+^{\frac{k}{2}-2} \quad (4.144)$$

Ψ of course depends on the brane embedding but crucially does not depend on $\tilde{c}_F$. We may invert equation (4.143) and substitute into the DBI action (4.136). We find

$$S_{\mathrm{D}(7-2k)} = T N_f \beta \mathrm{Vol}(S^{3-k}) \mathrm{Vol}(\mathrm{Defect}) \int d\rho \sqrt{1+y'^2} \rho^{3-k} h_- h_+^{\frac{3-k}{2}} \times$$
$$\times \left(1 + \frac{\Psi^2}{2\rho^{2(3-k)} h_+^{3-k}} (\alpha - \beta\mu_I)^2 + \mathcal{O}\left(\alpha - \beta\mu_I\right)^4\right) \quad (4.145)$$

This shows that when $\alpha - \beta\mu_I$ is small the first order correction to the grand canonical ensemble is quadratic in the chemical potential, as expected.

4.5.2 The $k = 1$ Case

A codimension $k = 1$ defect means that the glue sector of the theory exists in the full $3+1$ dimensions of the boundary while the fundamental fermionic degrees of freedom live on a $2+1$ dimensional subsurface. For a codimension 1 defect in the limit of zero chemical potential the phase transition between Minkowski and black hole embeddings is of first order as shown in figure 4.19. One can immediately see the characteristic swallowtail shape of the first order phase transition in the grand canonical ensemble for all values of $\tilde{c}_F$ and therefore for all chemical potentials. In [134] it was shown that there is a first order phase transition below some critical value of the chemical

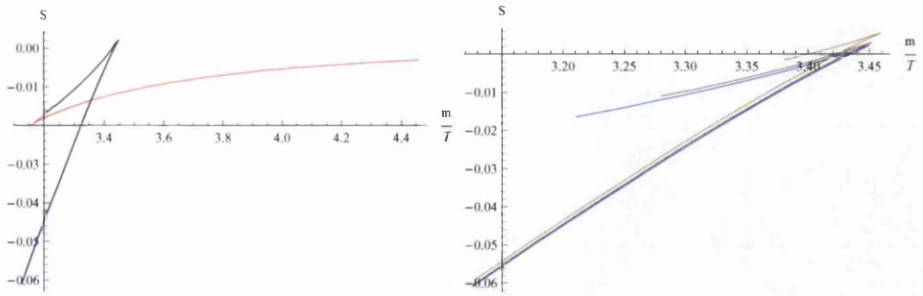

Figure 4.19: For $k = 1$: Left; The action as a function of $\frac{m}{T}$ for $\tilde{c}_F = 0$, both Minkowski and black hole embeddings. Right; The action as a function of $\frac{m}{T}$ for various $\tilde{c}_F$, for black hole embeddings only.

potential, above which the transition becomes of the second order. In the imaginary chemical potential case the phase transition is always of the first order because the Roberge-Weiss lines appear at order $\frac{1}{N}$ so only the small imaginary chemical potential behaviour of the phase diagram is accessible.

One can compute the phase diagram of the theory by examining the point at which the single line from the Minkowski embeddings intersects the lines that arise from the black hole embeddings. For non zero $\tilde{c}_F$ there is no longer a Minkowski embedding allowed, so the point where the black hole embeddings for some c_F intersect the Minkowski embedding line for $\tilde{c}_F = 0$ is taken to be the position of the phase transition. Recall that one may turn on an arbitrary chemical potential in the Minkowski embeddings by turning on a constant time component of the worldvolume gauge field on flavour branes which does not contribute to the DBI action. Therefore, Non zero chemical potentials are accessible in the Minkowski phase, while non zero $\tilde{c}_F$ is not.

When we compute the phase diagram we find figure 4.20. For small μ_I we the phase transition line is given by

$$\frac{T}{m} = 0.298 + 0.273\left(\alpha - \beta\mu_I\right)^2 + \mathcal{O}\left(\alpha - \beta\mu_I\right)^4 \tag{4.146}$$

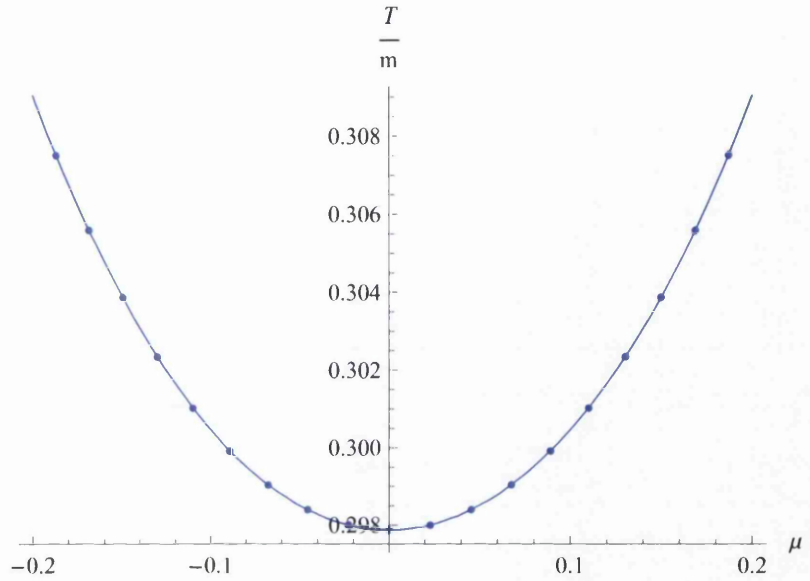

Figure 4.20: The first order meson melting transition line in a codimension 1 defect theory with imaginary chemical potential.

4.5.3 The $k = 2$ Case

In this setup the fundamental fermions live in a $1+1$ dimensional subspace of the boundary. The gravity theory is quite different in this case because the embedding function diverges logarithmically at the boundary, which implies by (4.138) that the worldvolume gauge field diverges logarithmically at the boundary as well. We still interpret the constant value of the asymptotic embedding function as the quark mass and constant value of the asymptotic worldvolume gauge field as the chemical potential. This means the leading order contribution both of our bulk fields at the boundary is no longer the quark mass and chemical potential in the case of the embedding function and worldvolume gauge field respectively, but the logarithmic term, the coefficient of which is related to the vacuum expectation value of the quark bilinear, and the integral of motion that was defined in (4.137).

$$\lim_{\rho\to\infty} y(\rho) \approx m + c\log\rho + \ldots \qquad \lim_{\rho\to\infty} A_t(\rho) \approx \mu + \tilde{c}_F \log\rho + \ldots \tag{4.147}$$

One may show that, as a result of the logarithmic divergences of the embedding function and the worldvolume gauge field, the action requires an additional logarithmic counterterm to renormalise it correctly. The additional counterterm is

$$S_{ct2} = -\frac{1}{2} T N_f \beta \mathrm{Vol}(S^{3-k}) \mathrm{Vol}(\mathrm{Defect}) \left(c^2 + \tilde{c}_F^2\right) \log \Lambda \tag{4.148}$$

When we compute the renormalised action as a function of $\frac{m}{T}$ we find a very similar graph to those found before (see figure 4.21). The discontinuity in

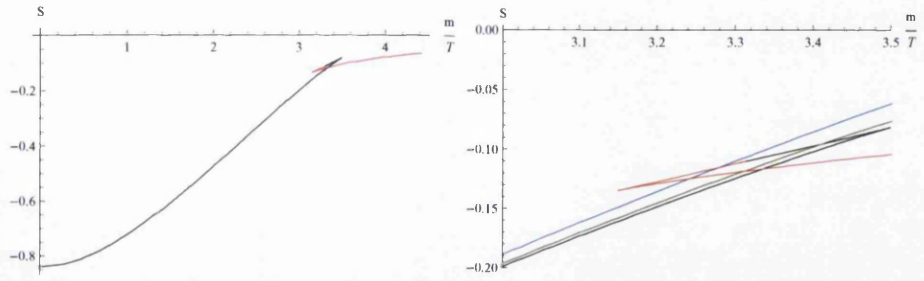

Figure 4.21: The DBI action as a function of $\frac{m}{T}$. On the left is the Minkowski (red) and black hole (black) embedding for $\tilde{c}_F = 0$. On the right is a zoomed in version also including black hole embeddings with non zero $\tilde{c}_F$ (green and blue lines).

the grand canonical ensemble is clearly first order, and when we compute the position of the first order phase transition we find figure 4.22.

$$\frac{T}{m} = 0.2997 + 0.0037 \left(\alpha - \beta\mu_I\right)^2 + \mathcal{O}\left(\alpha - \beta\mu_I\right)^4 \tag{4.149}$$

The phase diagram for codimension 2 systems in μ^2 is still not fully known. It was found in [134] that there is a second order phase transition meeting the deconfinement transition so there must be a point at some positive μ^2 where the phase transition becomes first order, since we have shown the phase diagram to be analytic in μ^2 for μ^2 close to zero.

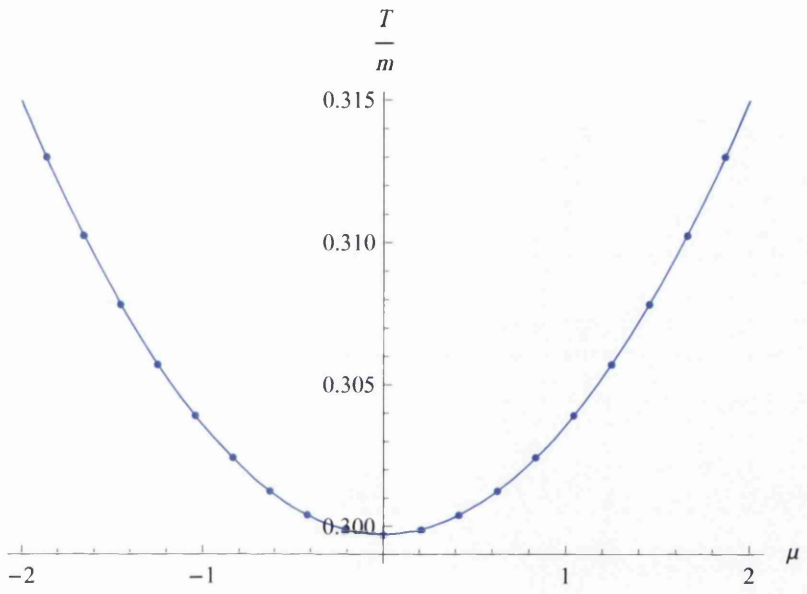

Figure 4.22: The meson melting phase transition line of $k = 2$ defect theory in the $\left(\mu_I, \frac{T}{m}\right)$ plane.

4.5.4 Pressure due to Flavours for Zero Quark Mass

Similarly to the Sakai-Sugimoto case, the pressure is computed by integrating over the bulk directions not on the boundary.

$$P = -\int d\rho d\Omega_{3-k} \mathcal{L}_{\text{DBI}}$$

$$P = -N_f T_k \int d\rho d\Omega_{3-k} \rho^{3-k} h_+^{\frac{3-k}{2}} \sqrt{\frac{h_-^2}{h_+}\left(1 + y'^2\right) + \left(B + 2\pi\alpha' F\right)^2} \tag{4.150}$$

Dimensional analysis tells us that $[P] = 4 - k$ which is expected because the flavours exist only on the defect so the pressure should have the dimension of $-\left[\beta \,\text{Vol}\,(\text{Defect})\right] = 4 - k$. Taking the quarks to be massless simplifies things considerably, because this condition implies $y' = y = 0$

$$P = -N_f T_k V_k \int_{\rho_h}^{\infty} d\rho \rho^{3-k} \left(1 + \frac{\sigma_h^4}{\rho^4}\right)^{\frac{3-k}{2}} \sqrt{\frac{\left(\rho^4 - \sigma_h^4\right)^2}{\rho^4\left(\rho^4 + \sigma_h^4\right)} + \left(B + 2\pi\alpha' F\right)^2} \tag{4.151}$$

Using the integral of motion (4.137) to eliminate $(B + 2\pi\alpha' F)$ from the pressure we find

$$P = -N_f T_k V_k \int_{\rho_h}^{\infty} d\rho \rho^{1-k} \left(1 + \frac{\sigma_h^4}{\rho^4}\right)^{\frac{3-k}{2}} \frac{(\rho^8 - \sigma_h^8)}{\sqrt{(\rho^4 + \sigma_h^4)^3 - \tilde{c}_F^2 \rho^{6+2k} \left(1 + \frac{\sigma_h^4}{\rho^4}\right)^k}} \tag{4.152}$$

We cannot do this integral analytically, so we expand in powers of the density c_F which, when we restore the correct factors of the brane tension and α' has dimension $3 - k$, as we expect. The leading contribution to the pressure is

$$P = -\int_{\rho_h}^{\infty} d\rho \frac{N_f T_k V_k \rho^{1-k} \left(1 + \frac{\sigma_h^4}{\rho^4}\right)^{\frac{3-k}{2}} (\rho^8 - \sigma_h^8)}{(\rho^4 + \sigma_h^4)^{\frac{3}{2}}} \tag{4.153}$$

Which, after integration and renormalisation is

$$P = \frac{2^{\frac{3}{2}+\frac{1-k}{2}} N_f T_k V_k \sigma_h^{4-k}}{4 - k} \tag{4.154}$$

We can translate this into field theory quantities using (4.134) and the following relations

$$T_k = \frac{1}{(2\pi)^{7-2k} l_s^{8-2k}}, \quad \frac{R^4}{l_s^4} = \lambda \tag{4.155}$$

The volume of a $3 - k$ sphere is given by

$$V_k = \frac{\pi^{\frac{3}{2}-\frac{k}{2}}}{\Gamma\left(\frac{5}{2} - \frac{k}{2}\right)} \tag{4.156}$$

therefore the leading contribution to the pressure is given by

$$P = \frac{2^{2k-7} N_f \pi^{-\frac{3-k}{2}+k-3} \lambda^{\frac{1}{4}(8-2k)} T^{4-k}}{(4 - k)\Gamma\left(1 + \frac{3-k}{2}\right)} \tag{4.157}$$

The only dimensionful scale in the problem when the chemical potential is zero is the temperature, so the leading order expression for the pressure must be some function of the dimensionless field theory parameters times

T^{4-k}. This is exactly what we see above. The first order correction when the chemical potential is non zero is

$$-\frac{2^{\frac{1+k}{2}-\frac{5}{2}}c_F^2\sigma_h^{k-2}}{(2\pi\alpha')^2(k-2)N_fT_kV_k} \tag{4.158}$$

Replacing with field theory quantities as before, the pressure is

$$\frac{4^{2-k}\pi^{\frac{3}{2}-\frac{k}{2}}\lambda^{\frac{k}{2}-1}\Gamma\left(\frac{5}{2}-\frac{k}{2}\right)}{(k-2)N_f}c_F^2T^{k-2} \tag{4.159}$$

The factor of $k-2$ in the denominator is potentially worrisome, however we shall see that when we rewrite the correction in terms of the chemical potential rather than the density this factor cancels and the expression is well behaved for all values of k we consider. Using the expansion (4.143), with the additional condition that the quarks are massless and we find

$$c_F \approx \frac{2^{2k-5}(k-2)}{\Gamma\left(\frac{5}{2}-\frac{k}{2}\right)}N_f\pi^{\frac{1}{2}(k-3)}T^{2-k}\lambda^{1-\frac{k}{2}}\mu_I + \mathcal{O}\left(\mu_I^3\right) \tag{4.160}$$

Therefore the first order correction to the pressure is

$$\frac{4^{k-3}(k-2)N_f\pi^{\frac{1}{2}(k-3)}\lambda^{1-\frac{k}{2}}}{\Gamma\left(\frac{5}{2}-\frac{k}{2}\right)}T^{2-k}\mu^2 \tag{4.161}$$

and the pressure for small density is

$$P = \frac{2^{2k-7}N_f\pi^{\frac{1}{2}(k-3)}\lambda^{2-\frac{k}{2}}}{\Gamma\left(\frac{5}{2}-\frac{k}{2}\right)}T^{4-k}\left(\frac{1}{(4-k)}+\frac{2(k-2)}{\lambda}\frac{\mu^2}{T^2}+\mathcal{O}\left(\frac{\mu^4}{T^4}\right)\right) \tag{4.162}$$

Of course, one may obtain the pressure due to flavours for the gauge theory dual to the D3-D7 system simply be setting $k=0$ in the expressions given above. We note that when $k=2$ the first order correction to the pressure vanishes. It would be interesting to see whether the leading order expression for the pressure is exact or corrections come in at higher order in the expansion.

4.6 Discussion

In this chapter we studied three holographic theories, the D3/D7 system, the Sakai-Sugimoto model and the D3/D($7-2k$) defect systems in the presence of an imaginary chemical potential.

All of these holographic models exhibit a first order transition as a result of the presence of flavours in the theory at high temperature. The models in type IIB, namely the D3/D7 system and the D3/D($7-2k$) defect systems display meson melting transition while the Sakai-Sugimoto model has a chiral symmetry restoration transition. The first-order lines join a set of first-order Roberge-Weiss transitions at fixed $\mu_I = \mu_{\rm RW}$ in the high-temperature phase at a series of triple points in the (μ_I, T) plane and we have determined the location of these triple points and the curvature of the phase boundaries.

In the case of the codimension k defect theories, one may compare the phase diagrams and we note the following; The phase diagram is always of the form

$$\frac{T}{m} = T_0(k) + T_2(k)\left(\alpha - \beta\mu_I\right)^2 + \ldots \tag{4.163}$$

where the coefficients depend on the detail of the defect. We have shown that T_0 is always of the same order, but T_2 changes significantly between models. Indeed, we note that $T_2(k+1)$ is approximately 100 times smaller than $T_2(k)$, which means the meson melting transition line is flatter the higher the codimension of the defect. This observation is also valid for the case when $k = 0$, or the D3/D7 system.

When we compute the pressure for small density the defect theories yield what would be expected from dimensional analysis and symmetry arguments - pressure is proportional to T^{4-k} multiplied by a function of $\frac{\mu^2}{T^2}$. The Sakai Sugimoto model on the other hand does not behave as expected, since the pressure goes like T^7 at leading order.

An important and non trivial result of this work is we have shown that these models are all analytic in μ^2 when μ^2 is small as is to be hoped since we expect these models to be invariant under charge conjugation symmetry, or equivalently the transformation $\mu \to -\mu$.

Recently, it has been demonstrated in QCD that the Roberge-Weiss end-

points are triple points for two [131] or three [126] degenerate light or heavy flavours, and second order endpoints in the 3d Ising universality class for intermediate quark masses. It would be extremely interesting to find a holographic model where the triple points turn into second order endpoints, as the quark mass m_q is varied. This could potentially be realized in models incorporating backreaction of flavours.

Chapter 5

Discussion and Conclusion

To briefly conclude this thesis, in chapter 3 we have computed the two point correlation functions of the scalar glueball operator and the R-charge current on $dS_3 \times S^1$. There is a $\mathbb{Z}_N$ invariant phase dual to topological AdS black hole in which we have computed the correlation functions exactly and there is a $\mathbb{Z}_N$ broken phase, dual to the AdS bubble of nothing in which we have calculated the scalar glueball correlation function in the WKB approximation as it is not possible to calculate it exactly in this background. The correlation functions imply the $\mathbb{Z}_N$ broken phase is a low temperature hadronized phase since there are poles on the real axis of the glueball correlation function, indicating stable bound states exist. The $\mathbb{Z}_N$ invariant phase is therefore the high temperature plasma phase, although the R-charge correlator does not seem to exhibit diffusive properties because the rate of de Sitter expansion and the temperature are of the same order.

In chapter 4 we have computed the phase diagrams of three holographic theories. We have found that, in addition to the first order Roberge-Weiss lines that appear at high temperature at fixed μ_I, there is a first order transition in the background dual to the high temperature phase of the gauge theory as a result of the presence of flavours. This phase transition has some non trivial profile in the (μ_I, T) plane which we have computed for each of the models under consideration. Furthermore, we have calculated the pressure due to the flavours. The type IIB models behave as one would expect from

dimensional analysis considerations, but the Sakai-Sugimoto model exhibits unusual temperature dependence that has yet to be explained.

Chapter 6

Appendix

Appendix A: Strongly Coupled $\mathcal{N} = 4$ SYM on $dS_3 \times S^1$

A.1 Nonvanishing S^1 momentum

We provide here, the steps in the calculation leading to the boundary action for fluctuations which are homogeneous on the spatial slices of dS_3 but with momentum along the spatial S^1. The equations of motion (3.66),(3.67) can be solved in terms of hypergeometric functions

$$\mathcal{F}'_n = C_\tau(\nu,\bar{n})\,(1-z)^{-\frac{i(\nu-i)}{2}}\,{}_2F_1\left(\frac{1}{2}+\frac{i}{2}(\bar{n}-\nu),\frac{1}{2}-\frac{i}{2}(\bar{n}+\nu)\,;1-i\nu\,;1-z\right) \tag{6.1}$$

Here C_τ is a frequency dependent constant, to be determined by the boundary values of the fields. Near the boundary of AdS space, the solution approaches

$$\begin{aligned}\mathcal{F}'_n\big|_{z\to 0} = -\ C_\tau\ &\frac{\Gamma(1-i\nu)}{\Gamma\left(\frac{1}{2}+\frac{i}{2}(\bar{n}-\nu)\right)\Gamma\left(\frac{1}{2}-\frac{i}{2}(\bar{n}+\nu)\right)}\times \\ &\times\left(2\gamma_E+\log z+\psi\left(\frac{1}{2}+\frac{i}{2}(\bar{n}-\nu)\right)+\psi\left(\frac{1}{2}-\frac{i}{2}(\bar{n}+\nu)\right)\right)\end{aligned} \tag{6.2}$$

Imposing the boundary conditions at $z \to 0$

$$\lim_{\epsilon\to 0}\mathcal{F}_n(\nu,\epsilon) = \mathcal{F}^0_n(\nu), \qquad \lim_{\epsilon\to 0}\mathcal{G}_n(\nu,\epsilon) = \mathcal{G}^0_n(\nu) \tag{6.3}$$

from (3.64) we find that

$$C_\tau(\nu,\bar{n}) = -\frac{\Gamma\left(\frac{1}{2}+\frac{i}{2}(\bar{n}-\nu)\right)\Gamma\left(\frac{1}{2}-\frac{i}{2}(\bar{n}+\nu)\right)}{4\Gamma(1-i\nu)}\times \\ \times\left(\bar{n}^2\mathcal{F}_n^0(\nu)-\frac{R}{r_\chi}\bar{n}(\nu-i)\mathcal{G}_n^0(\nu)\right) \tag{6.4}$$

With the normalization fixed in terms of the boundary values of the relevant fields we have that

$$\mathcal{F}_n'(\nu,\epsilon) = \frac{1}{4}\left(\bar{n}^2\mathcal{F}_n^0-\frac{R}{r_\chi}\bar{n}(\nu-i)\mathcal{G}_n^0\right)\times \\ \times\left(2\gamma_E+\log\epsilon+\psi\left(\frac{1}{2}+\frac{i}{2}(\bar{n}-\nu)\right)+\psi\left(\frac{1}{2}-\frac{i}{2}(\bar{n}+\nu)\right)\right) \tag{6.5}$$

From (3.63) we also obtain

$$\mathcal{G}_n'(\nu,\epsilon) = \frac{r_\chi}{R}\frac{\nu+i}{\bar{n}}\mathcal{F}_n'(\nu,\epsilon) \tag{6.6}$$

We can now plug these solutions into the boundary action to obtain the retarded R-current correlators. Following identical steps for the normalizable (in time) modes, we have

$$\mathcal{F}_n^{\mathrm{N}\prime}(\epsilon) = \frac{1}{4}\bar{n}^2\mathcal{F}_n^{\mathrm{N}0}\left(2\gamma_E+\log\epsilon+\psi\left(1+\frac{i}{2}\bar{n}\right)+\psi\left(1-\frac{i}{2}\bar{n}\right)\right) \tag{6.7}$$

The induced boundary action for bulk Maxwell fields has the form

$$S\big|_{z=\epsilon} = \frac{4\pi}{g_{SG}^2}\sum_n\frac{1}{2\pi}\times \\ \times\left(\int_{-\infty}^{\infty}\frac{d\nu}{2\pi}\left(r_\chi\mathcal{F}_{-n}^0(-\nu)\,\mathcal{F}_n'(\nu)\big|_{z=\epsilon}-\frac{R^2}{r_\chi}\mathcal{G}_{-n}^0(-\nu)\mathcal{G}_n'(\nu)\big|_{z=\epsilon}\right)+ \right. \\ \left. +r_\chi\mathcal{F}_{-n}^{\mathrm{N}0}\mathcal{F}_n^{\mathrm{N}\prime}\big|_{z=\epsilon}\right) \tag{6.8}$$

where $g_{SG}^2 = \frac{16\pi^2 R}{N^2}$. The complete real time retarded correlation functions for the R-currents, can now be accessed readily. First we define the boundary

values of our gauge fields as

$$A_{\chi,\tau}(\epsilon,\tau,\chi) \equiv \sum_n \frac{e^{in\chi}}{2\pi} A^n_{\chi,\tau}(\tau) \tag{6.9}$$

so that

$$\mathcal{G}^0_n(-\nu) = \int_{-\infty}^{\infty} A^n_\chi(\tau)\, \mathcal{T}_\chi(\nu,\tau) \cosh^2\tau \tag{6.10}$$

and similarly

$$\mathcal{F}^0_n(-\nu) = \int_{-\infty}^{\infty} A^n_\tau(\tau)\, \mathcal{T}_\tau(\nu,\tau) \cosh^2\tau, \qquad \mathcal{F}^{\mathrm{N}0}_n = \int_{-\infty}^{\infty} A^n_\tau(\tau)\, \mathcal{T}^{\mathrm{N}}_\tau(\tau) \cosh^2\tau \tag{6.11}$$

Putting these ingredients together, we find that the boundary action is

$$\begin{aligned}
S\big|_{z=\epsilon} &= \frac{N^2}{4\pi R} \sum_n \frac{1}{2\pi} \int_{-\infty}^{\infty} d\tau \cosh^2\tau \int_{-\infty}^{\infty} d\tau' \cosh^2\tau' \\
&\left[\int_{-\infty}^{\infty} \frac{d\nu}{2\pi} \left(2\gamma_E + \log\epsilon + \psi\left(\frac{1}{2} + \frac{i}{2}(\bar{n}-\nu)\right) + \psi\left(\frac{1}{2} - \frac{i}{2}(\bar{n}+\nu)\right)\right) \times \right. \\
&\times \Big(A^{-n}_\tau(\tau) A^n_\tau(\tau') \frac{\bar{n}^2}{4} r_\chi \mathcal{T}_\tau(\nu,\tau) \mathcal{T}_\tau(-\nu,\tau') - A^{-n}_\tau(\tau) A^n_\chi(\tau') R \frac{\bar{n}}{4}(\nu - i) \times \\
&\times \mathcal{T}_\tau(\nu,\tau) \mathcal{T}_\chi(-\nu,\tau') - A^{-n}_\chi(\tau) A^n_\tau(\tau') R \frac{\bar{n}}{4}(\nu + i) \mathcal{T}_\chi(\nu,\tau) \mathcal{T}_\tau(-\nu,\tau') + \\
&+ A^{-n}_\chi(\tau) A^n_\chi(\tau') \frac{R^2}{r_\chi} \frac{1}{4}(\nu^2+1) \mathcal{T}_\chi(\nu,\tau) \mathcal{T}_\chi(-\nu,\tau') \Big) + r_\chi A^{-n}_\tau(\tau) A^n_\tau(\tau') \times \\
&\left. \times \frac{\bar{n}^2}{4} \mathcal{T}^{\mathrm{N}}(\tau) \mathcal{T}^{\mathrm{N}}(\tau') \left(2\gamma_E + \log\epsilon + \psi\left(1 + \frac{i}{2}\bar{n}\right) + \psi\left(1 - \frac{i}{2}\bar{n}\right)\right)\right]
\end{aligned} \tag{6.12}$$

A.2 Nonzero momentum along the spatial slices of dS_3

Below we fill in the steps in the derivation of the boundary action for the Maxwell fields in the bulk. The asymptotic form of the radial dependence of the bulk potential $\mathcal{F}'_\ell$, can be determined from (3.89)

$$F_\ell\big|_{z\to 0} = C_\ell(\nu)\,(C_1(\nu) + C_2(\nu)\log z) \tag{6.13}$$

where

$$C_1 = -\frac{2\gamma_E + \psi\left(1 - \frac{i\nu}{2}\right) + \psi\left(-\frac{i\nu}{2}\right)}{\Gamma\left(1 - \frac{i\nu}{2}\right)\Gamma\left(-\frac{i\nu}{2}\right)} \tag{6.14}$$

$$C_2 = -\frac{1}{\Gamma\left(1 - \frac{i\nu}{2}\right)\Gamma\left(-\frac{i\nu}{2}\right)} \tag{6.15}$$

We can solve for C_ℓ in terms of the boundary values of the gauge potentials, using the bulk equation of motion (3.81) for $\mathcal{F}'_\ell$ near the boundary which yields

$$4\int_{-\infty}^{\infty}\frac{d\nu}{2\pi}\Gamma(1+i\nu)P_\ell^{-i\nu}(\tanh\tau)C_\ell(\nu)C_2(\nu) = \ell(\ell+1)\left(\mathcal{F}^0_\ell(\tau) - \partial_\tau\mathcal{G}^0_\ell(\tau)\right) \tag{6.16}$$

Note that the other equation of motion (3.80) for $\mathcal{G}'_\ell$, just yields the time derivative of this condition, so that we have only one equation to determine the coefficient C_ℓ. This equation can be solved if we recall that the associated Legendre functions are mutually orthogonal[1]

$$\int_{-\infty}^{\infty} d\tau P_\ell^{i\nu}(\tanh\tau)P_\ell^{-i\nu'}(\tanh\tau) = \frac{\delta(\nu-\nu')}{\Gamma(1-i\nu)\Gamma(1+i\nu)} \tag{6.17}$$

Thus, we have

$$C_\ell = \frac{\ell(\ell+1)}{4C_2}\Gamma(1-i\nu)\int_{-\infty}^{\infty} d\tau'\left(\mathcal{F}^0_\ell(\tau') - \partial_{\tau'}\mathcal{G}^0_\ell(\tau')\right)P_\ell^{i\nu}(\tanh\tau') \tag{6.18}$$

[1]The orthogonality of these functions for purely imaginary order follows from the fact that they are eigenfunctions of the Schrödinger equation in the sech^2 potential, $\left(-\frac{d^2}{d\tau^2} - \frac{\ell(\ell+1)}{\cosh^2\tau}\right)P_\ell^{i\nu}(\tanh\tau) = \nu^2 P_\ell^{i\nu}(\tanh\tau)$. In particular for $\nu \in \mathbb{R}$, these are scattering states and are delta-function normalizable, and the eigenfunctions corresponding to two different eigenvalues are orthogonal as usual.

from which we obtain the solution

$$\cosh^2\tau\mathcal{F}'_\ell(\epsilon,\tau) = \frac{\ell(\ell+1)}{4}\int_{-\infty}^{\infty} d\tau' \left(\mathcal{F}^0_\ell(\tau') - \partial_{\tau'}\mathcal{G}^0_\ell(\tau')\right) \times$$
$$\times \left[\int_{-\infty}^{\infty} \frac{d\nu}{2\pi}\frac{\pi\nu}{\sinh\pi\nu} P_\ell^{-i\nu}(\tanh\tau)P_\ell^{i\nu}(\tanh\tau')\times\right.$$
$$\times \left(\log\epsilon + 2\gamma_E + \psi\left(-\frac{i\nu}{2}\right) + \psi\left(1-\frac{i\nu}{2}\right)\right) +$$
$$+\sum_{m=1}^{\ell} m\frac{(\ell-m)!}{(\ell+m)!}P_\ell^m(\tanh\tau)P_\ell^m(\tanh\tau')\times$$
$$\left.\times \left(\log\epsilon + 2\gamma_E + \psi\left(\frac{m}{2}\right) + \psi\left(1+\frac{m}{2}\right)\right)\right] \tag{6.19}$$

Plugging these back into the expression for the boundary action (3.92), we obtain the generating functional for two point correlators of R-currents.

A.3 WKB matching conditions for $\nu > \tilde{r}_h$

Near the turning point $u = u_c$ corresponding to $\rho = \sqrt{1+\nu^2}$, since we are well away from any extrema, we can assume that

$$\mathcal{V}(\nu,u) = \kappa(u_c - u) + \dots, \qquad u \to u_c \tag{6.20}$$

In this region where the potential is basically linear, the exact solution in terms of Airy functions is

$$\Psi\big|_{u\to u_c} = A_+\frac{2\sqrt{\pi}}{\kappa^{1/6}}\mathrm{Ai}\left(\kappa^{1/3}(u_c-u)\right) + A_-\frac{\sqrt{\pi}}{\kappa^{1/6}}\mathrm{Bi}\left(\kappa^{1/3}(u_c-u)\right) \tag{6.21}$$

The normalizations and constants of integration have been chosen carefully so that the exact solution near the turning point, in terms of Airy functions, matches the WKB solution (3.119) in Region I ($u < u_c$) away from the turning point. Now, we can continue the solution (6.21) into Region II ($u > u_c$). For $u > u_c$, where the WKB solution (3.123) should be valid, the Airy

functions have the asymptotic form

$$\Psi\big|_{u>u_c} \approx 2A_+ \frac{\sin\left(\frac{2}{3}\sqrt{\kappa}(u-u_c)^{\frac{3}{2}}+\frac{\pi}{4}\right)}{\kappa^{\frac{1}{4}}(u-u_c)^{\frac{1}{4}}} + A_- \frac{\cos\left(\frac{2}{3}\sqrt{\kappa}(u-u_c)^{\frac{3}{2}}+\frac{\pi}{4}\right)}{\kappa^{\frac{1}{4}}(u-u_c)^{\frac{1}{4}}} \tag{6.22}$$

Comparison with (3.123) near the turning point then implies

$$B_+ = e^{i\frac{\pi}{4}}\left(\frac{1}{2}A_- - iA_+\right), \quad B_- = e^{-i\frac{\pi}{4}}\left(\frac{1}{2}A_- + iA_+\right) \tag{6.23}$$

There is yet another condition that emergies from the behaviour of the solutions near the second "turning point", $\rho \to \sqrt{1+\tilde{r}_h^2}$ or $u \to \infty$ where the space ends. In this region we have

$$\frac{du}{d\rho}\Big|_{\rho\to\sqrt{1+\tilde{r}_h^2}} \approx -\frac{\sqrt{1+\tilde{r}_h^2}}{2(2\tilde{r}_h^2+1)(\rho-\sqrt{1+\tilde{r}_h^2})} \tag{6.24}$$

so that

$$\rho - \sqrt{1+\tilde{r}_h^2} \approx 2\sqrt{1+\tilde{r}_h^2}\exp\left(-2\frac{(1+2\tilde{r}_h^2)}{\sqrt{1+\tilde{r}_h^2}}\,u + \frac{\tilde{r}_h}{\sqrt{1+\tilde{r}_h^2}}\cot^{-1}\left(\frac{\sqrt{1+\tilde{r}_h^2}}{\tilde{r}_h}\right)\right) \tag{6.25}$$

It follows then that, as a function of u, the high frequency potential decays exponentially,

$$\mathcal{V}(\nu,u)\big|_{u\to\infty} \approx (mR)^2\left(1-\frac{\nu^2}{\tilde{r}_h^2}\right)\exp\left(-2\frac{(1+2\tilde{r}_h^2)}{\sqrt{1+\tilde{r}_h^2}}u + \text{constants}\right) \tag{6.26}$$

Note that for $\nu > \tilde{r}_h$, the potential approaches zero from below. Let us define constants A and B, in terms of which the potential is simply

$$\tilde{V}_0(\nu,u)\big|_{u\to\infty} \approx -Ae^{-Bu} \tag{6.27}$$

where A and B can be read off easily from the expressions above. The Schrödinger equation with an exponentially decaying potential is solved ex-

actly by Bessel functions:

$$-\Psi''(u) - Ae^{-Bu}\Psi(u) = 0, \tag{6.28}$$

$$\Psi = C_1\, J_0\left(2\frac{\sqrt{A}}{B}\, e^{-\frac{Bu}{2}}\right) + C_2\, Y_0\left(2\frac{\sqrt{A}}{B}\, e^{-\frac{Bu}{2}}\right) \tag{6.29}$$

Recall that we are looking for a zero energy eigenfunction of the Schrödinger problem. This means that for a potential that vanishes at infinity, the corresponding (normalizable) wavefunction can only be zero. This is an important difference to the black hole case where the wave functions are infalling plane waves at the horizon. Requiring that the wave function Ψ vanish or approach a constant as $u \to \infty$ then eliminates the term proportional to Y_0. Hence, in the exponentially decaying region

$$\Psi(u) \propto J_0\left(2\frac{\sqrt{A}}{B}\, e^{-Bu/2}\right) \tag{6.30}$$

The WKB approximation should match onto the Bessel function for large values of the argument of the Bessel function. Using the standard asymptotic expansion for Bessel functions

$$J_0(x)\big|_{x\gg 1} \simeq \frac{\cos(x)}{\sqrt{\pi x}} + \frac{\sin(x)}{\sqrt{\pi x}} \tag{6.31}$$

From this we can deduce a relationship between the constants B_+ and B_- in (3.123). To make this precise we define the integral

$$\mathcal{S}_{II}(u) = \int_{\infty}^{u} \sqrt{|\mathcal{V}(\nu,u)|}du. = -mR\int_{\tilde{r}_h}^{\rho^2-1} dx\sqrt{\frac{x^2-\nu^2}{(x^2-\tilde{r}_h^2)(x^2+1+\tilde{r}_h^2)}} \tag{6.32}$$

where

$$\mathcal{S}_{II}(u(\rho)) = i\,\frac{mR}{\sqrt{1+2\tilde{r}_h^2}}\left[\nu\left(F\left(\sin^{-1}\sqrt{\frac{1}{a}\frac{\rho^2+\tilde{r}_h^2}{\rho^2-1}},k\right)-\frac{1}{\sqrt{k}}\,K\left(\frac{1}{k}\right)\right)+\right.$$
$$\left.\frac{1}{\nu}(1+\tilde{r}_h^2)\left(\Pi\left(a;\sin^{-1}\sqrt{\frac{1}{a}\frac{\rho^2+\tilde{r}_h^2}{\rho^2-1}}\middle|k\right)-\frac{1}{\sqrt{k}}\Pi\left(b\middle|\frac{1}{k}\right)\right)\right], \tag{6.33}$$

$$a=\frac{\nu^2+1+\tilde{r}_h^2}{\nu^2};\qquad b=\frac{1+2\tilde{r}_h^2}{\tilde{r}_h^2}\;;\qquad k=\frac{a}{b} \tag{6.34}$$

Then the WKB solution in Region II is

$$\Psi_{\text{WKB}}=\frac{1}{|\mathcal{V}|^{1/4}}\left(B_+\,e^{i\mathcal{S}_{II}(u)-i\mathcal{S}_{II}(u_c)}+B_-e^{-i\mathcal{S}_{II}(u)+i\mathcal{S}_{II}(u_c)}\right) \tag{6.35}$$

For large u,

$$\mathcal{S}_{II}(u)\big|_{u\gg 1}\approx\int_\infty^u\sqrt{A}e^{-\frac{Bu}{2}}=-2\frac{\sqrt{A}}{B}e^{-\frac{Bu}{2}} \tag{6.36}$$

Using this result and comparing (6.35) to the asymptotics of the Bessel function (6.31), we find

$$\frac{B_+}{B_-}=ie^{2i\mathcal{S}_{II}(u_c)} \tag{6.37}$$

The final ingredient consists in determining A_+ and A_-. To this end we first define

$$\mathcal{S}_I(u)=\int^u\sqrt{\mathcal{V}(\nu,u)}\,du \tag{6.38}$$

which then gives us

$$\begin{aligned}
&\mathcal{S}_I(u(\rho)) = \\
&\frac{mR}{\sqrt{1+2\tilde{r}_h^2}}\left[\nu F\left(\sin^{-1}\left(\sqrt{\frac{1}{a}\frac{\rho^2+\tilde{r}_h^2}{\rho^2-1}}\right),k\right)+\right. \\
&\left.+\frac{1}{\nu}(1+\tilde{r}_h^2)\Pi\left(a;\sin^{-1}\left(\sqrt{\frac{1}{a}\frac{\rho^2+\tilde{r}_h^2}{\rho^2-1}}\right)\middle|k\right)\right] \qquad (6.39)\\
&a=\frac{\nu^2+1+\tilde{r}_h^2}{\nu^2}; \qquad b=\frac{1+2\tilde{r}_h^2}{\tilde{r}_h^2}\ ; \qquad k=\frac{a}{b}
\end{aligned}$$

Near the boundary $u \to 0$ or equivalently $\rho \to \infty$, we find

$$\begin{aligned}
&\Psi_{\text{WKB}} \approx A_-\frac{1}{\sqrt{mR}}\,\rho^{mR-\frac{1}{2}}\,e^{i\pi\frac{mR}{2}}\left(\frac{4}{1+\tilde{r}_h^2}\right)^{\frac{mR}{4}}\nu^{-\frac{mR}{2}}\times \\
&\exp\left[\frac{mR}{\sqrt{1+2\tilde{r}_h^2}}\left(\nu(F\left(\csc^{-1}\sqrt{a},k\right)-K(k))-\frac{1}{\nu}(1+\tilde{r}_h^2)\Pi(a|k)\right)\right] \\
&+A_+\frac{1}{\sqrt{mR}}\,\rho^{-mR-\frac{1}{2}}\,e^{-\frac{i\pi mR}{2}}\left(\frac{4}{1+\tilde{r}_h^2}\right)^{-\frac{mR}{4}}\nu^{\frac{mR}{2}}\times \\
&\exp\left[-\frac{mR}{\sqrt{1+2\tilde{r}_h^2}}\left(\nu(F\left(\csc^{-1}\sqrt{a},k\right)-K(k))-\frac{1}{\nu}(1+\tilde{r}_h^2)\Pi(a|k)\right)\right]
\end{aligned} \qquad (6.40)$$

Combining (6.23) and (6.37) we obtain

$$A_+ = -A_-\frac{1}{2}\tan\left(\mathcal{S}_{II}(u_c)\right) \qquad (6.41)$$

A.4 WKB matching for $|\nu| < \tilde{r}_h$

When $|\nu| < \tilde{r}_h$, the potential energy $\mathcal{V}(\nu, u)$ is a monotonic function of u which exponentially vanishes as $u \to \infty$. Now, the potential has effectively only one turning point and the wave function has no region where it propagates. The WKB solution (3.119) in Region I should smoothly match onto

the exact solution of

$$-\psi''(u) + Ae^{-Bu}\psi(u) = 0\,, \qquad A, B > 0 \tag{6.42}$$

The solutions to these are the modified Bessel's functions. Enforcing regular behaviour as $u \to \infty$ picks out

$$\psi(u) \propto I_0\left(2\frac{\sqrt{A}}{B}e^{-\frac{Bu}{2}}\right) \tag{6.43}$$

The WKB approximation for $I_0(x)$ is valid when $x \gg 1$,

$$I_0(x)\big|_{x\gg 1} \simeq \frac{1}{2\sqrt{2\pi x}}\left(e^x + ie^{-x}\right) \tag{6.44}$$

We write the WKB solution to the wave equation in the bubble of nothing background as

$$\Psi_{\mathrm{WKB}}(\nu, u) = A_+\frac{1}{\mathcal{V}^{\frac{1}{4}}}\exp\left(\int_\infty^u \sqrt{\mathcal{V}}du\right) + A_-\frac{1}{\mathcal{V}^{\frac{1}{4}}}\exp\left(-\int_\infty^u \sqrt{\mathcal{V}}du\right) \tag{6.45}$$

Comparison with the modified Bessel function implies

$$A_+ = iA_- \tag{6.46}$$

Near the boundary $u \to 0$, which is equivalent to $\rho \to \infty$, we have

$$\Psi_{\text{WKB}} \approx A_- \frac{1}{\sqrt{mR}} \rho^{mR-\frac{1}{2}} e^{\frac{i\pi mR}{2}} \left(\frac{4}{1+\tilde{r}_h^2}\right)^{\frac{mR}{4}} \nu^{-\frac{mR}{2}} \times$$
$$\exp\left[\frac{mR}{\sqrt{1+2\tilde{r}_h^2}}\left(\nu\left(F\left(\csc^{-1}\sqrt{a},k\right) - \frac{1}{\sqrt{k}}K\left(\frac{1}{k}\right)\right) + \right.\right.$$
$$\left.\left. - \frac{1}{\nu}(1+\tilde{r}_h^2)\frac{1}{\sqrt{k}}\Pi\left(a\middle|\frac{1}{k}\right)\right)\right] +$$
$$+ A_+ \frac{1}{\sqrt{mR}} \rho^{-mR-\frac{1}{2}} e^{-\frac{i\pi mR}{2}} \left(\frac{4}{1+\tilde{r}_h^2}\right)^{-\frac{mR}{4}} \nu^{\frac{mR}{2}} \times$$
$$\exp\left[-\frac{mR}{\sqrt{1+2\tilde{r}_h^2}}\left(\nu\left(F\left(\csc^{-1}\sqrt{a},k\right) - \frac{1}{\sqrt{k}}K\left(\frac{1}{k}\right)\right) + \right.\right.$$
$$\left.\left. - \frac{1}{\nu}(1+\tilde{r}_h^2)\frac{1}{\sqrt{k}}\Pi\left(a\middle|\frac{1}{k}\right)\right)\right] \qquad (6.47)$$

Bibliography

[1] M. E. Peskin and D. V. Schroeder, *An Introduction To Quantum Field Theory (Frontiers in Physics).* Westview Press, 1995.

[2] K. G. Wilson, *Confinement of quarks*, *Phys. Rev. D* **10** (Oct, 1974) 2445–2459.

[3] I. Montvay and G. Munster, *Quantum fields on a lattice.* 1994. Cambridge, UK: Univ. Pr. (1994) 491 p. (Cambridge monographs on mathematical physics).

[4] C. DeTar and U. M. Heller, *QCD Thermodynamics from the Lattice*, *Eur. Phys. J.* **A41** (2009) 405–437, [arXiv:0905.2949].

[5] G. Veneziano, *Construction of a crossing - symmetric, Regge behaved amplitude for linearly rising trajectories*, *Nuovo. Cim.* **A57** (1968) 190–197.

[6] L. Susskind, *Dual symmetric theory of hadrons. 1*, *Nuovo Cim.* **A69** (1970) 457–496.

[7] J. Scherk and J. H. Schwarz, *Dual Models for Nonhadrons*, *Nucl. Phys.* **B81** (1974) 118–144.

[8] T. Yoneya, *Connection of Dual Models to Electrodynamics and Gravidynamics*, *Prog. Theor. Phys.* **51** (1974) 1907–1920.

[9] Y. Nambu, *Lectures at the copenhagen summer symposium*, *Unpublished* (1970).

[10] T. Goto, *Relativistic quantum mechanics of one-dimensional mechanical continuum and subsidiary condition of dual resonance model*, *Prog. Theor. Phys.* **46** (1971) 1560–1569.

[11] F. Gliozzi, J. Scherk, and D. I. Olive, *Supergravity and the Spinor Dual Model*, *Phys. Lett.* **B65** (1976) 282.

[12] J. Dai, R. G. Leigh, and J. Polchinski, *New Connections Between String Theories*, *Mod. Phys. Lett.* **A4** (1989) 2073–2083.

[13] P. Horava, *Background Duality of Open String Models*, *Phys. Lett.* **B231** (1989) 251.

[14] M. Nakahara, *Geometry, Topology and Physics, Second Edition (Graduate Student Series in Physics)*. Taylor & Francis, 2 ed., June, 2003.

[15] O. Aharony, S. S. Gubser, J. M. Maldacena, H. Ooguri, and Y. Oz, *Large N field theories, string theory and gravity*, *Phys. Rept.* **323** (2000) 183–386, [hep-th/9905111].

[16] J. M. Maldacena, *The large N limit of superconformal field theories and supergravity*, *Adv. Theor. Math. Phys.* **2** (1998) 231–252, [hep-th/9711200].

[17] M. F. Sohnius and P. C. West, *Conformal invariance in $n = 4$ supersymmetric yang-mills theory*, *Physics Letters B* **100** (1981), no. 3 245–250.

[18] S. Mandelstam, *Light-cone superspace and the ultraviolet finiteness of the $\mathcal{N} = 4$ model*, *Nuclear Physics B* **213** (1983), no. 1 149–168.

[19] N. Seiberg, *Supersymmetry and Nonperturbative beta Functions*, *Phys. Lett.* **B206** (1988) 75.

[20] E. Witten, *Anti-de Sitter space and holography*, *Adv. Theor. Math. Phys.* **2** (1998) 253–291, [hep-th/9802150].

[21] S. S. Gubser, I. R. Klebanov, and A. M. Polyakov, *Gauge theory correlators from non-critical string theory*, *Phys. Lett.* **B428** (1998) 105–114, [hep-th/9802109].

[22] A. Nunez and A. O. Starinets, *AdS/CFT correspondence, quasinormal modes, and thermal correlators in N = 4 SYM*, *Phys. Rev.* **D67** (2003) 124013, [hep-th/0302026].

[23] E. Witten, *Anti-de Sitter space, thermal phase transition, and confinement in gauge theories*, *Adv. Theor. Math. Phys.* **2** (1998) 505–532, [hep-th/9803131].

[24] L. Alvarez-Gaume, C. Gomez, H. Liu, and S. Wadia, *Finite temperature effective action, AdS(5) black holes, and 1/N expansion*, *Phys. Rev.* **D71** (2005) 124023, [hep-th/0502227].

[25] J. Erdmenger, N. Evans, I. Kirsch, and E. Threlfall, *Mesons in Gauge/Gravity Duals - A Review*, *Eur. Phys. J.* **A35** (2008) 81–133, [arXiv:0711.4467].

[26] D. Mateos, S. Matsuura, R. C. Myers, and R. M. Thomson, *Holographic phase transitions at finite chemical potential*, *JHEP* **11** (2007) 085, [arXiv:0709.1225].

[27] M. Ishihara, K. Ghoroku, and A. Nakamura, *D3/D7 holographic gauge theory and chemical potential*, *Int. J. Mod. Phys.* **A23** (2008) 2251–2252.

[28] D. Yamada and L. G. Yaffe, *Phase diagram of N = 4 super-Yang-Mills theory with R- symmetry chemical potentials*, *JHEP* **09** (2006) 027, [hep-th/0602074].

[29] A. Karch, A. O'Bannon, and E. Thompson, *The Stress-Energy Tensor of Flavor Fields from AdS/CFT*, *JHEP* **04** (2009) 021, [arXiv:0812.3629].

[30] A. Karch and A. O'Bannon, *Metallic AdS/CFT*, *JHEP* **09** (2007) 024, [arXiv:0705.3870].

[31] A. O'Bannon, *Hall Conductivity of Flavor Fields from AdS/CFT*, *Phys. Rev.* **D76** (2007) 086007, [arXiv:0708.1994].

[32] S. A. Hartnoll, *Lectures on holographic methods for condensed matter physics*, *Class. Quant. Grav.* **26** (2009) 224002, [arXiv:0903.3246].

[33] T. Sakai and S. Sugimoto, *Low energy hadron physics in holographic QCD*, *Prog. Theor. Phys.* **113** (2005) 843–882, [hep-th/0412141].

[34] J. M. Maldacena and C. Nunez, *Towards the large N limit of pure N = 1 super Yang Mills*, *Phys. Rev. Lett.* **86** (2001) 588–591, [hep-th/0008001].

[35] I. R. Klebanov and M. J. Strassler, *Supergravity and a confining gauge theory: Duality cascades and chiSB-resolution of naked singularities*, *JHEP* **08** (2000) 052, [hep-th/0007191].

[36] I. R. Klebanov and E. Witten, *Superconformal field theory on threebranes at a Calabi-Yau singularity*, *Nucl. Phys.* **B536** (1998) 199–218, [hep-th/9807080].

[37] J. Polchinski, *String theory. Vol. 1: An introduction to the bosonic string*, . Cambridge, UK: Univ. Pr. (1998) 402 p.

[38] J. Polchinski, *String theory. Vol. 2: Superstring theory and beyond*, . Cambridge, UK: Univ. Pr. (1998) 531 p.

[39] K. Becker, M. Becker, and J. H. Schwarz, *String theory and M-theory: A modern introduction*, . Cambridge, UK: Cambridge Univ. Pr. (2007) 739 p.

[40] O. Aharony and E. Witten, *Anti-de Sitter space and the center of the gauge group*, *JHEP* **11** (1998) 018, [hep-th/9807205].

[41] E. D'Hoker, D. Z. Freedman, and W. Skiba, *Field theory tests for correlators in the AdS/CFT correspondence*, *Phys. Rev.* **D59** (1999) 045008, [hep-th/9807098].

[42] S. Lee, S. Minwalla, M. Rangamani, and N. Seiberg, *Three-point functions of chiral operators in D = 4, N = 4 SYM at large N*, *Adv. Theor. Math. Phys.* **2** (1998) 697–718, [hep-th/9806074].

[43] S. W. Hawking and D. N. Page, *Thermodynamics of Black Holes in anti-De Sitter Space*, *Commun. Math. Phys.* **87** (1983) 577.

[44] S. W. Hawking, *Particle Creation by Black Holes*, *Commun. Math. Phys.* **43** (1975) 199–220.

[45] O. Aharony, J. Marsano, S. Minwalla, K. Papadodimas, and M. Van Raamsdonk, *A first order deconfinement transition in large N Yang- Mills theory on a small 3-sphere*, *Phys. Rev.* **D71** (2005) 125018, [hep-th/0502149].

[46] A. Karch and E. Katz, *Adding flavor to AdS/CFT*, *JHEP* **06** (2002) 043, [hep-th/0205236].

[47] A. Karch and A. O'Bannon, *Holographic Thermodynamics at Finite Baryon Density: Some Exact Results*, *JHEP* **11** (2007) 074, [arXiv:0709.0570].

[48] O. Aharony, J. Sonnenschein, and S. Yankielowicz, *A holographic model of deconfinement and chiral symmetry restoration*, *Annals Phys.* **322** (2007) 1420–1443, [hep-th/0604161].

[49] A. Parnachev and D. A. Sahakyan, *Chiral phase transition from string theory*, *Phys. Rev. Lett.* **97** (2006) 111601, [hep-th/0604173].

[50] E. Antonyan, J. A. Harvey, S. Jensen, and D. Kutasov, *NJL and QCD from string theory*, hep-th/0604017.

[51] V. Balasubramanian, P. Kraus, and A. E. Lawrence, *Bulk vs. boundary dynamics in anti-de Sitter spacetime*, *Phys. Rev.* **D59** (1999) 046003, [hep-th/9805171].

[52] V. Balasubramanian, P. Kraus, A. E. Lawrence, and S. P. Trivedi, *Holographic probes of anti-de Sitter space-times*, *Phys. Rev.* **D59** (1999) 104021, [hep-th/9808017].

[53] D. T. Son and A. O. Starinets, *Minkowski-space correlators in AdS/CFT correspondence: Recipe and applications*, *JHEP* **09** (2002) 042, [hep-th/0205051].

[54] C. P. Herzog, A. Karch, P. Kovtun, C. Kozcaz, and L. G. Yaffe, *Energy loss of a heavy quark moving through $N = 4$ supersymmetric Yang-Mills plasma*, *JHEP* **07** (2006) 013, [hep-th/0605158].

[55] S. A. Hartnoll, C. P. Herzog, and G. T. Horowitz, *Building a Holographic Superconductor*, *Phys. Rev. Lett.* **101** (2008) 031601, [arXiv:0803.3295].

[56] D. T. Son and A. O. Starinets, *Viscosity, Black Holes, and Quantum Field Theory*, *Ann. Rev. Nucl. Part. Sci.* **57** (2007) 95–118, [arXiv:0704.0240].

[57] S. Bhattacharyya, V. E. Hubeny, S. Minwalla, and M. Rangamani, *Nonlinear Fluid Dynamics from Gravity*, *JHEP* **02** (2008) 045, [arXiv:0712.2456].

[58] C. P. Herzog and D. T. Son, *Schwinger-Keldysh propagators from AdS/CFT correspondence*, *JHEP* **03** (2003) 046, [hep-th/0212072].

[59] K. Skenderis and B. C. van Rees, *Real-time gauge/gravity duality*, *Phys. Rev. Lett.* **101** (2008) 081601, [arXiv:0805.0150].

[60] N. D. Birrell and P. C. W. Davies, *Quantum Fields in Curved Space*. Cambridge, Uk: Univ. Pr. (1982) 340p.

[61] R. M. Wald, *Quantum field theory in curved space-time and black hole thermodynamics*. 1995.

[62] G. W. Gibbons and S. W. Hawking, *Cosmological Event Horizons, Thermodynamics, and Particle Creation*, *Phys. Rev.* **D15** (1977) 2738–2751.

[63] R. Stanley and T. J. Hollowood, *Graviton Propagation and Vacuum Polarization in Curved Space*, arXiv:1106.4675.

[64] T. J. Hollowood and G. M. Shore, *'Superluminal' Photon Propagation in QED in Curved Spacetime is Dispersive and Causal*, arXiv:1006.1238.

[65] T. J. Hollowood and G. M. Shore, *The Effect of Gravitational Tidal Forces on Vacuum Polarization: How to Undress a Photon*, *Phys. Lett.* **B691** (2010) 279–284, [arXiv:1006.0145].

[66] J. A. Hutasoit, S. P. Kumar, and J. Rafferty, *Real time response on dS_3: the Topological AdS Black Hole and the Bubble*, *JHEP* **04** (2009) 063, [arXiv:0902.1658].

[67] D. Birmingham and M. Rinaldi, *Bubbles in anti-de Sitter space*, *Phys. Lett.* **B544** (2002) 316–320, [hep-th/0205246].

[68] V. Balasubramanian and S. F. Ross, *The dual of nothing*, *Phys. Rev.* **D66** (2002) 086002, [hep-th/0205290].

[69] R.-G. Cai, *Constant curvature black hole and dual field theory*, *Phys. Lett.* **B544** (2002) 176–182, [hep-th/0206223].

[70] S. F. Ross and G. Titchener, *Time-dependent spacetimes in AdS/CFT: Bubble and black hole*, *JHEP* **0502** (2005) 021, [hep-th/0411128].

[71] V. Balasubramanian, K. Larjo, and J. Simon, *Much ado about nothing*, *Class.Quant.Grav.* **22** (2005) 4149–4170, [hep-th/0502111].

[72] O. Aharony, M. Fabinger, G. T. Horowitz, and E. Silverstein, *Clean time-dependent string backgrounds from bubble baths*, *JHEP* **07** (2002) 007, [hep-th/0204158].

[73] E. Witten, *Instability of the Kaluza-Klein Vacuum*, *Nucl. Phys.* **B195** (1982) 481.

[74] R. C. Myers and M. J. Perry, *Black Holes in Higher Dimensional Space-Times*, *Ann. Phys.* **172** (1986) 304.

[75] F. Dowker, J. P. Gauntlett, G. W. Gibbons, and G. T. Horowitz, *The Decay of magnetic fields in Kaluza-Klein theory*, *Phys. Rev.* **D52** (1995) 6929–6940, [hep-th/9507143].

[76] D. Astefanesei and G. C. Jones, *S-branes and (anti-)bubbles in (A)dS space*, *JHEP* **06** (2005) 037, [hep-th/0502162].

[77] R. Emparan, *AdS/CFT duals of topological black holes and the entropy of zero-energy states*, *JHEP* **06** (1999) 036, [hep-th/9906040].

[78] J. Alsup and G. Siopsis, *Low-lying quasinormal modes of topological AdS black holes and hydrodynamics*, *Phys. Rev.* **D78** (2008) 086001, [arXiv:0805.0287].

[79] G. Koutsoumbas, E. Papantonopoulos, and G. Siopsis, *Discontinuities in Scalar Perturbations of Topological Black Holes*, *Class. Quant. Grav.* **26** (2009) 105004, [arXiv:0806.1452].

[80] G. Koutsoumbas, E. Papantonopoulos, and G. Siopsis, *Shear Viscosity and Chern-Simons Diffusion Rate from Hyperbolic Horizons*, *Phys. Lett.* **B677** (2009) 74–78, [arXiv:0809.3388].

[81] M. Banados, *Constant curvature black holes*, *Phys. Rev.* **D57** (1998) 1068–1072, [gr-qc/9703040].

[82] M. Banados, A. Gomberoff, and C. Martinez, *Anti-de Sitter space and black holes*, *Class. Quant. Grav.* **15** (1998) 3575–3598, [hep-th/9805087].

[83] M. Banados, M. Henneaux, C. Teitelboim, and J. Zanelli, *Geometry of the (2+1) black hole*, *Phys. Rev.* **D48** (1993) 1506–1525, [gr-qc/9302012].

[84] M. Banados, C. Teitelboim, and J. Zanelli, *The Black hole in three-dimensional space-time*, *Phys. Rev. Lett.* **69** (1992) 1849–1851, [hep-th/9204099].

[85] K. Skenderis and B. C. van Rees, *Real-time gauge/gravity duality: Prescription, Renormalization and Examples*, *JHEP* **05** (2009) 085, [arXiv:0812.2909].

[86] G. Policastro, D. T. Son, and A. O. Starinets, *From AdS/CFT correspondence to hydrodynamics*, *JHEP* **09** (2002) 043, [hep-th/0205052].

[87] E. Mottola, *Particle Creation in de Sitter Space*, *Phys. Rev.* **D31** (1985) 754.

[88] M. Spradlin, A. Strominger, and A. Volovich, *Les Houches lectures on de Sitter space*, hep-th/0110007.

[89] J. A. Hutasoit, *Vacuum Ambiguity in de Sitter Space at Strong Coupling*, *JHEP* **02** (2010) 026, [arXiv:0910.5509].

[90] S. A. Hartnoll and S. Prem Kumar, *AdS black holes and thermal Yang-Mills correlators*, *JHEP* **12** (2005) 036, [hep-th/0508092].

[91] J. Bros, H. Epstein, and U. Moschella, *Particle decays and stability on the de Sitter universe*, *Annales Henri Poincare* **11** (2010) 611–658, [arXiv:0812.3513].

[92] J. Bros, H. Epstein, M. Gaudin, U. Moschella, and V. Pasquier, *Triangular invariants, three-point functions and particle stability on the de Sitter universe*, *Commun. Math. Phys.* **295** (2010) 261–288, [arXiv:0901.4223].

[93] D. Boyanovsky, R. Holman, and S. Prem Kumar, *Inflaton decay in De Sitter spacetime*, *Phys. Rev.* **D56** (1997) 1958–1972, [hep-ph/9606208].

[94] L. Fidkowski, V. Hubeny, M. Kleban, and S. Shenker, *The black hole singularity in AdS/CFT*, *JHEP* **02** (2004) 014, [hep-th/0306170].

[95] G. Festuccia and H. Liu, *Excursions beyond the horizon: Black hole singularities in Yang-Mills theories. I*, *JHEP* **04** (2006) 044, [hep-th/0506202].

[96] M. Abramowitz and I. Stegun, *Handbook of Mathematical Functions.* Dover, New York, fifth ed., 1964.

[97] C. Csaki, H. Ooguri, Y. Oz, and J. Terning, *Glueball mass spectrum from supergravity*, *JHEP* **01** (1999) 017, [hep-th/9806021].

[98] *Wolfram functions*, Aug., 2011.

[99] D. Marolf, M. Rangamani, and M. Van Raamsdonk, *Holographic models of de Sitter QFTs*, *Class. Quant. Grav.* **28** (2011) 105015, [arXiv:1007.3996].

[100] J. Maldacena, *Vacuum decay into Anti de Sitter space*, arXiv:1012.0274.

[101] M. Li and Y. Pang, *Holographic de Sitter Universe*, *JHEP* **07** (2011) 053, [arXiv:1105.0038].

[102] J. Blackman, M. B. McDermott, and M. Van Raamsdonk, *Acceleration-Induced Deconfinement Transitions in de Sitter Spacetime*, arXiv:1105.0440.

[103] J. Erdmenger, K. Ghoroku, and R. Meyer, *Holographic (De)confinement Transitions in Cosmological Backgrounds*, *Phys. Rev.* **D84** (2011) 026004, [arXiv:1105.1776].

[104] N. Horigome and Y. Tanii, *Holographic chiral phase transition with chemical potential*, *JHEP* **01** (2007) 072, [hep-th/0608198].

[105] O. Aharony, K. Peeters, J. Sonnenschein, and M. Zamaklar, *Rho meson condensation at finite isospin chemical potential in a holographic model for QCD*, *JHEP* **02** (2008) 071, [arXiv:0709.3948].

[106] A. Parnachev, *Holographic QCD with Isospin Chemical Potential*, *JHEP* **02** (2008) 062, [arXiv:0708.3170].

[107] D. Mateos, R. C. Myers, and R. M. Thomson, *Thermodynamics of the brane*, *JHEP* **05** (2007) 067, [hep-th/0701132].

[108] S. S. Gubser, *Thermodynamics of spinning D3-branes*, *Nucl. Phys.* **B551** (1999) 667–684, [hep-th/9810225].

[109] A. Chamblin, R. Emparan, C. V. Johnson, and R. C. Myers, *Charged AdS black holes and catastrophic holography*, *Phys. Rev.* **D60** (1999) 064018, [hep-th/9902170].

[110] M. Cvetic and S. S. Gubser, *Phases of R-charged black holes, spinning branes and strongly coupled gauge theories*, *JHEP* **04** (1999) 024, [hep-th/9902195].

[111] J. Babington, J. Erdmenger, N. J. Evans, Z. Guralnik, and I. Kirsch, *Chiral symmetry breaking and pions in non-supersymmetric gauge / gravity duals*, *Phys. Rev.* **D69** (2004) 066007, [hep-th/0306018].

[112] I. Kirsch, *Generalizations of the AdS/CFT correspondence*, *Fortsch. Phys.* **52** (2004) 727–826, [hep-th/0406274].

[113] T. Albash, V. G. Filev, C. V. Johnson, and A. Kundu, *A topology-changing phase transition and the dynamics of flavour*, *Phys. Rev.* **D77** (2008) 066004, [hep-th/0605088].

[114] A. Karch and A. O'Bannon, *Chiral transition of $N = 4$ super Yang-Mills with flavor on a 3-sphere*, *Phys. Rev.* **D74** (2006) 085033, [hep-th/0605120].

[115] K. Ghoroku, T. Sakaguchi, N. Uekusa, and M. Yahiro, *Flavor quark at high temperature from a holographic model*, *Phys. Rev.* **D71** (2005) 106002, [hep-th/0502088].

[116] D. Mateos, R. C. Myers, and R. M. Thomson, *Holographic phase transitions with fundamental matter*, *Phys. Rev. Lett.* **97** (2006) 091601, [hep-th/0605046].

[117] K. Ghoroku, M. Ishihara, and A. Nakamura, *D3/D7 holographic Gauge theory and Chemical potential*, *Phys. Rev.* **D76** (2007) 124006, [arXiv:0708.3706].

[118] A. O'Bannon, *Holographic Thermodynamics and Transport of Flavor Fields*, arXiv:0808.1115.

[119] F. Bigazzi, A. L. Cotrone, J. Mas, D. Mayerson, and J. Tarrio, *D3-D7 Quark-Gluon Plasmas at Finite Baryon Density*, *JHEP* **04** (2011) 060, [arXiv:1101.3560].

[120] H.-U. Yee, *Fate of Z(N) domain wall in hot holographic QCD*, *JHEP* **04** (2009) 029, [arXiv:0901.0705].

[121] A. Roberge and N. Weiss, *Gauge Theories With Imaginary Chemical Potential and the Phases of QCD*, *Nucl. Phys.* **B275** (1986) 734.

[122] P. de Forcrand, *Simulating QCD at finite density*, *PoS* **LAT2009** (2009) 010, [arXiv:1005.0539].

[123] P. de Forcrand and O. Philipsen, *The QCD phase diagram for small densities from imaginary chemical potential*, *Nucl. Phys.* **B642** (2002) 290–306, [hep-lat/0205016].

[124] P. de Forcrand and O. Philipsen, *The QCD Phase Diagram for Three Degenerate Flavors and Small Baryon Density*, *Nucl. Phys.* **B673** (2003) 170–186, [hep-lat/0307020].

[125] P. de Forcrand and O. Philipsen, *The chiral critical line of $N_f = 2 + 1$ QCD at zero and non- zero baryon density*, *JHEP* **01** (2007) 077, [hep-lat/0607017].

[126] P. de Forcrand and O. Philipsen, *Constraining the QCD phase diagram by tricritical lines at imaginary chemical potential*, arXiv:1004.3144.

[127] M. D'Elia and M.-P. Lombardo, *Finite density QCD via imaginary chemical potential*, *Phys. Rev.* **D67** (2003) 014505, [hep-lat/0209146].

[128] M. D'Elia and M. P. Lombardo, *QCD thermodynamics from an imaginary mu(B): Results on the four flavor lattice model*, *Phys. Rev.* **D70** (2004) 074509, [hep-lat/0406012].

[129] M. D'Elia, F. Di Renzo, and M. P. Lombardo, *The strongly interacting Quark Gluon Plasma, and the critical behaviour of QCD at imaginary chemical potential*, *Phys. Rev.* **D76** (2007) 114509, [arXiv:0705.3814].

[130] M. D'Elia and F. Sanfilippo, *Thermodynamics of two flavor QCD from imaginary chemical potentials*, *Phys. Rev.* **D80** (2009) 014502, [arXiv:0904.1400].

[131] M. D'Elia and F. Sanfilippo, *The order of the Roberge-Weiss endpoint (finite size transition) in QCD*, *Phys. Rev.* **D80** (2009) 111501, [arXiv:0909.0254].

[132] P. Cea, L. Cosmai, M. D'Elia, and A. Papa, *The phase diagram of QCD with four degenerate quarks*, *Phys. Rev.* **D81** (2010) 094502, [arXiv:1004.0184].

[133] A. Karch and L. Randall, *Open and closed string interpretation of SUSY CFT's on branes with boundaries*, *JHEP* **06** (2001) 063, [hep-th/0105132].

[134] P. Benincasa, *Universality of Holographic Phase Transitions and Holographic Quantum Liquids*, arXiv:0911.0075.

[135] N. Weiss, *The Effective Potential for the Order Parameter of Gauge Theories at Finite Temperature*, *Phys. Rev.* **D24** (1981) 475.

[136] N. Weiss, *The Wilson Line in Finite Temperature Gauge Theories*, *Phys. Rev.* **D25** (1982) 2667.

[137] G. Aarts, S. P. Kumar, and J. Rafferty, *Holographic Roberge-Weiss Transitions*, *JHEP* **07** (2010) 056, [arXiv:1005.2947].

[138] J. M. Maldacena, *Wilson loops in large N field theories*, *Phys. Rev. Lett.* **80** (1998) 4859–4862, [hep-th/9803002].

[139] S.-J. Rey and J.-T. Yee, *Macroscopic strings as heavy quarks in large N gauge theory and anti-de Sitter supergravity*, *Eur. Phys. J.* **C22** (2001) 379–394, [hep-th/9803001].

[140] S. Kobayashi, D. Mateos, S. Matsuura, R. C. Myers, and R. M. Thomson, *Holographic phase transitions at finite baryon density*, *JHEP* **02** (2007) 016, [hep-th/0611099].

[141] C. Fefferman and C. R. Graham, *Conformal Invariants*, *Elie Cartan et les Mathematiques d'aurjourd'hui (Asterique)* **95** (1985).

[142] A. Karch, A. O'Bannon, and K. Skenderis, *Holographic renormalization of probe D-branes in AdS/CFT*, *JHEP* **04** (2006) 015, [hep-th/0512125].

[143] R. C. Myers, A. O. Starinets, and R. M. Thomson, *Holographic spectral functions and diffusion constants for fundamental matter*, *JHEP* **11** (2007) 091, [arXiv:0706.0162].

[144] C. Hoyos-Badajoz, K. Landsteiner, and S. Montero, *Holographic Meson Melting*, *JHEP* **04** (2007) 031, [hep-th/0612169].

[145] M. Kruczenski, D. Mateos, R. C. Myers, and D. J. Winters, *Meson spectroscopy in AdS/CFT with flavour*, *JHEP* **07** (2003) 049, [hep-th/0304032].

[146] S. Nakamura, Y. Seo, S.-J. Sin, and K. P. Yogendran, *Baryon-charge Chemical Potential in AdS/CFT*, *Prog. Theor. Phys.* **120** (2008) 51–76, [arXiv:0708.2818].

[147] T. Faulkner and H. Liu, *Condensed matter physics of a strongly coupled gauge theory with quarks: some novel features of the phase diagram*, arXiv:0812.4278.

[148] F. Karsch, K. Redlich, and A. Tawfik, *Hadron resonance mass spectrum and lattice QCD thermodynamics*, *Eur. Phys. J.* **C29** (2003) 549–556, [hep-ph/0303108].

[149] O. DeWolfe, D. Z. Freedman, and H. Ooguri, *Holography and defect conformal field theories*, *Phys. Rev.* **D66** (2002) 025009, [hep-th/0111135].

[150] R. C. Myers and M. C. Wapler, *Transport Properties of Holographic Defects*, *JHEP* **12** (2008) 115, [arXiv:0811.0480].

[151] M. C. Wapler, *Holographic Experiments on Defects*, *Int. J. Mod. Phys.* **A25** (2010) 4397–4473, [arXiv:0909.1698].

[152] L.-Y. Hung and A. Sinha, *Holographic quantum liquids in 1+1 dimensions*, *JHEP* **01** (2010) 114, [arXiv:0909.3526].